Terms and Conditions of Use of Digitised Theses from Trinity College Library Dublin

Copyright statement

All material supplied by Trinity College Library is protected by copyright (under the Copyright and Related Rights Act, 2000 as amended) and other relevant Intellectual Property Rights. By accessing and using a Digitised Thesis from Trinity College Library you acknowledge that all Intellectual Property Rights in any Works supplied are the sole and exclusive property of the copyright and/or other IPR holder. Specific copyright holders may not be explicitly identified. Use of materials from other sources within a thesis should not be construed as a claim over them.

A non-exclusive, non-transferable licence is hereby granted to those using or reproducing, in whole or in part, the material for valid purposes, providing the copyright owners are acknowledged using the normal conventions. Where specific permission to use material is required, this is identified and such permission must be sought from the copyright holder or agency cited.

Liability statement

By using a Digitised Thesis, I accept that Trinity College Dublin bears no legal responsibility for the accuracy, legality or comprehensiveness of materials contained within the thesis, and that Trinity College Dublin accepts no liability for indirect, consequential, or incidental, damages or losses arising from use of the thesis for whatever reason. Information located in a thesis may be subject to specific use constraints, details of which may not be explicitly described. It is the responsibility of potential and actual users to be aware of such constraints and to abide by them. By making use of material from a digitised thesis, you accept these copyright and disclaimer provisions. Where it is brought to the attention of Trinity College Library that there may be a breach of copyright or other restraint, it is the policy to withdraw or take down access to a thesis while the issue is being resolved.

Access Agreement

By using a Digitised Thesis from Trinity College Library you are bound by the following Terms & Conditions. Please read them carefully.

I have read and I understand the following statement: All material supplied via a Digitised Thesis from Trinity College Library is protected by copyright and other intellectual property rights, and duplication or sale of all or part of any of a thesis is not permitted, except that material may be duplicated by you for your research use or for educational purposes in electronic or print form providing the copyright owners are acknowledged using the normal conventions. You must obtain permission for any other use. Electronic or print copies may not be offered, whether for sale or otherwise to anyone. This copy has been supplied on the understanding that it is copyright material and that no quotation from the thesis may be published without proper acknowledgement.

An Investigation into the physiological expression and function of mitochondrial uncoupling protein 1 in thymus.

A dissertation submitted to Trinity College Dublin
for the degree of Doctor of Philosophy
April 2011
By

Alison Elizabeth Adams B.A. (Mod)

School of Biochemistry & Immunology
University of Dublin
Trinity College

Declaration

I certify that none of the work in this thesis has been submitted for an degree or diploma at this, or any other university and that all of the work described in this thesis is entirely my own. I give permission for the library to lend or copy this thesis upon request.

Summary

Our study confirms the presence of mitochondrial uncoupling protein 1 in thymus. Using laser scanning confocal microscopy, we showed the constitutive expression of UCP 1 in pure thymocytes. Using a primary peptide antibody specific to UCP 1, and secondary fluorescently labelled antibody, we were able to demonstrate that UCP 1 is associated with mitochondria in thymoctes from wild-type mice but not thymocytes from UCP 1 knock-out mice. We are the first lab to demonstrate UCP 1 expression in cells other than brown adipocytes. We also show UCP 1 in thymocytes isolated from rat. As there was data refuting the existence of UCP 1 in thymus/thymocytes, we addressed discrepancies in these studies. We demonstrate that the antibody raised to full length UCP 1 protein appears to be non-specific to UCP 1, as it detects protein in wild-type and UCP 1 knock-out mice thymocyte mitochondria. We also show that CIDEA, a soluble protein with a suggested role in regulating UCP 1 function, is equally abundant in thymocytes from wild-type and UCP 1 knock-out mice. The absence of UCP 1 does not effect native expression of CIDEA in thymocytes. Our study also shows the novel finding that UCP 1 in the thymus has a shorter half-life than UCP 1 in brown adipose tissue mitochondria.

In our endeavours to understand the role of mitochondrial uncoupling protein 1 in thymocyte function, we compared cell profiles in thymus and spleen of wild-type mice with those of UCP 1 knock-out mice. We demonstrate that spleen cell numbers were reduced ~ 3 fold in UCP 1 knock –out mice compared to wild-type mice. Using flow cytometry, we show that there is a halving of CD8 thymocytes in thymus with a significant incremental increase in DP in the thymus of UCP 1 knock-out mice compared to wild-type mice. These data were mirrored by ~ halving of CD8 thymocytes, and a doubling of DP cells in the spleen of UCP 1 knock-out mice compared to wild-type mice. We also show that thymocytes from UCP 1 knock-out mice have a decreased apoptotic potential and higher ATP levels compared to wild-

type controls. We conclude that constitutively expressed UCP 1 may play a role in determining T-cell selection in mice.

The study presented has shown the novel finding of an increase in UCP 1 protein expression after activation and proliferation of T cells in the thymus using LPS and PHA. We have also shown that LPS or PHA treatment of mice has no effect on UCP 1 expression in brown adipose tissue. Lack of UCP 1 results in (a) a doubling of the proportion of CD4 & CD8 cells concomitant with a halving of the proportion of DP cells following PHA treatment, and (b) an increase in the proportion of CD4 and a reduction in the proportion of DP cells following LPS treatment. We have shown that lack of UCP 1 leads to a tripling of the absolute cell numbers of CD4 and CD8 cells after PHA treatment. We have also shown that lack of UCP 1 has no effect on oxygen consumption or proton leak after LPS or PHA treatment, despite the increase in UCP 1 protein. This suggests UCP 1 may play a non-thermogenic role in the thymus. We also show the novel finding of UCP 1 in activated murine neutrophils.

Acknowledgements

So its 2010, the year EVERYONE got married and I finished (hopefully) a PhD. Not sure yet which is the biggest joke. I actually can't believe I'm at this point, I'm a child!! Anyways I have a lot of people to thank for helping me.....

Firstly I'd like to thank my supervisor, Richie, for his help and guidance. I know we've had our ups and downs but I know ultimately you just want the best for us. Thanks for your support & especially for introducing me to the "inner bioenergetics circle" – I'll never forget those conferences!!

Dr. Carroll, what can I stay?! Thanks a million for getting me into the lab. And then leaving the first chance you got. Seriously though...you're a star, and have never said no to me, no matter what I have asked of you. Except for that time I asked for your lanacane cream (the one for chaffing). I love you and you better not forget me!!

Kiki LaRue, you have really shown your true colours in the last few weeks....and I can now confirm that you are officially a Legend!! You should really be getting two PhD's. You might actually beat Eamon to the title of smartest person I know. You know I'm here if you ever change you mind.

Lars, you'll be happy now you'll never have to listen to david guetta, usher, Enrique, gaga, pitbull, flo rida, Alexandra or Justin bieber again!! Sorry for forcing it all on you- now you can listen to opera music til your heart's content. Thanks for all the motivational talks and career guidance. I'll probably be coming in to you with something baked every week!! Stephen Quinn, thanks for all the laughs. One minute around you and I'm in stiches, and not because you bust my lip. I promise 2011 will be the year of brownies for you. And no not "those" sort.

Kiva, thanks for always checking up on me and giving me the motivation to go on....powerplate in 2011?? To everyone in BRU, thanks for all your help with everything, especially Ciaran. MP & Miriam, the most obliging secretaries ever, thanks for all your help with menial stuff, I know your door is always open. To everyone in the prep-room, Ronnie, Maura, Roisin, Olga & Brian (storree bud??) , thanks for never saying no to me & humouring me by laughing at my stories!! Thanks to all the technical staff, Liam, Noel& Liam (after 5 years in this department I finally know who is who), Dave & Kyran, and everyone else in the department!!

To the boys & girl in the molecular design lab, Danny, Trev, Paul, Laura & especially Chris, thanks for all the laughs over the years. Chris, thanks for checking up on me in the last few weeks, and for bringing me coffee, and for the constant unintentional laughs from your clothes/hair. Glynis, thanks for recipes and demonstrating and for telling me about up and coming baking threats in biochem. Thanks to my constant stream of visitors to the lab, especially Clare (you should be a story teller) and Kristine (your optimistic view on science is infectious).

Eamon, what can I say. I'm sorry for all those late night emails when I was stressing out (they were not spam...nom nom spam!!). I'm so glad we got to spend some time together in the lab, short but very sweet....umm sweets!! I'm proud to be

your fatty. Can't wait to see you over xmas so can can compare who is now the most obese, not morbidly obese but super obese. I know inside you have a heart of gold, you just don't want to show people (or they can't see it through the rolls of fat) x

Wu, you've been a rock, I know you would have done anything to help me, even constantly meeting me in Lemon (I know how much you hate that place), before you dashed off to pick up an asos package. Or ten.

Arlene, I actually can't put into words how much I love you, but I'm gonna try. You have always been there, and tried to understand what I've been doing, and you were always at the end of the phone when I needed you, especially during the last few months when things were tough. But when I'm finished this- I'll have nothing to moan about....what will I do?? xx

Miss Burke, sorry about the lack of contact in the last few months I promise I'll make it up you, in cinnamon buns & Diep take-away.....love from the turkey girl.

Orlagh Kelly. Quite possibly the best thing to come out of my time in trinity. I never thought I'd meet someone who actually has the same thought process as me. Thanks for everything over the last few years, you are actually one of the kindest most generous people I know.....sorry if I've been hard work for the last few months!! Can't wait for 2011, and for plenty of dancing, and scones, and Chinese. (food).

To my family, thanks for all the support and you'll be delighted I'm finally finished college!!! And I'm not a teacher. So Mark, hopefully you will be able to tell people you have a doctor as a sister. You should know you are way too smart for your age. And definitely too funny. Emma, you're the next one to finish college-hurry up so your life can start!! Keith, for a douche, you're not too bad to live with. Thanks for the grannies smiths. "You got galas- I don't want them!! What do you mean I'm moody?? "But seriously you are extremely generous and thoughtful; it'll be a lucky guy ~~girl who~~ who gets you.

Financial Support from Science Foundation Ireland is acknowledged.

Table of Contents

Chapter 2 Materials and methods

Abbreviations:

ADP	Adenosine 5'-diphosphate
APC	Antigen Presenting Cell
ATP	Adenosine 5'-triphosphate
BAT	Brown Adipose Tissue
B_{MAX}	Maximal Binding Capacity
BSA	Bovine Serum Albumin
CD	Cluster of Differentiation
CD4SP	CD 4 single positive
CD8SP	CD8 single positive
CIDEA	Cell death-inducing DFFA-like effector a
CL-	Chloride ion
cAPK	cAMP-dependant protein kinase
CREB	cAMP-response-element-binding-protein
Da	Dalton
DC	Dendritic Cell
DNA	Deoxyribonucleic Acid
DNP	2,4-dinitrophenol
DIT	Diet induced thermogenesis
DP	Double positive
DN	Double negative
ETC	Electron Transport Chain
FA	Fatty Acid
FACS	Florescence Activated Cell Sorter
FAD^+	Flavin adenine dinucleotide oxidised form
$FADH_2$	Flavin adenine dinucleotide reduced form
FCCP	*p*- carbonylcyanide trifluoromethoxyphenylhydrazone
FFA	Free Fatty Acid

FCS	Fetal Calf Serum
HCL	Hydrochloric Acid
kb	kilobase
K_D	Equilibrium Dissociation Constant
LS-MS/MS	Liquid chromatography/ tandem mass spectrometry
LPS	Lipopolysaccharide
MAPK	Mitogen-activated protein (MAP) kinases
MHC	Major Histocompatibility Complex
NAD^+	Nicotinamide adenine dinucleotide oxidized form
NADH	Nicotinamide adenine dinucleotide reduced form
NE	noradrenaline
NK	Natural Killer
Δp	Proton electrochemical gradient
ΔpH	pH gradient across the mitochondrial inner membrane
PA	Palmitic Acid
PBS	Phosphate buffered saline
PCR	Polymerase Chain Reaction
PDVF	Polyvinylidene Fluoride
PHA	Phytohaemaglutinin
PI	Propidium iodide
PPAR	Peroxisome proliferation activating receptors
PRR	Pattern recognition receptor
ROS	Reactive Oxygen Species
RT	Room Temperature
RNA	Ribonuclease
SDS-PAGE	sodium dodecyl sulfate polyacrylamide gel electrophoresis
T_3	triiodothyronine
TCR	T cell receptor
TEC	thymic epithelial cell

TLR	Toll-like receptor
TRE's	Thyroid hormone response elements
T_{reg}	Regulatory T cells
UCP	Uncoupling protein
V	Volt
v/v	volume per unit volume
w/v	weight per unit volume
WAT	White Adipose Tissue

Chapter 1

Introduction

Chapter One
Introduction

[1.1] Mitochondria

In cell biology a mitochondrion is a membrane-enclosed organelle found in most eukaryotic cells (Henze & Martin, 2003). Mitochondria are sometimes described as "cellular power plants," because they convert food molecules into energy in the form of ATP via the process of oxidative phosphorylation. A schematic representation of a eukaryotic cell is shown in figure 1.1. A typical eukaryotic liver cell contains about 2,000 mitochondria, which occupy roughly one fifth of its total volume (Voet *et al.*, 2006) Mitochondria contain DNA that is independent of the DNA located in the cell nucleus.

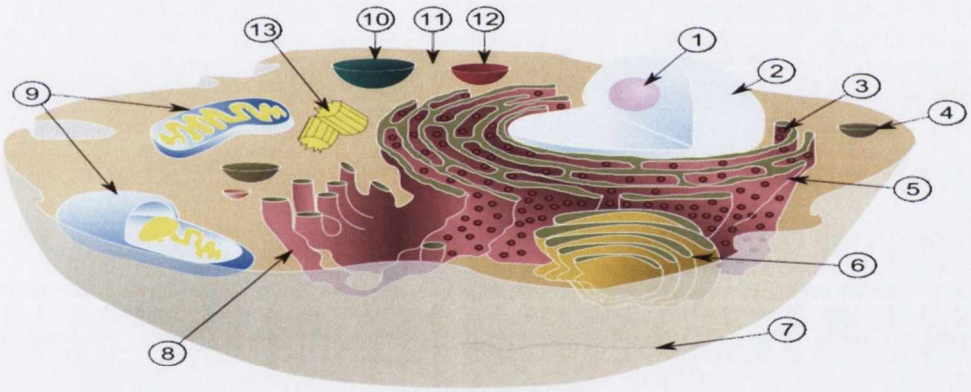

1. Nucleolus
2. Nucleus
3. Ribosome
4. Vesicle
5. Rough Endoplasmic Reticulum
6. Golgi apparatus
7. Cytoskeleton
8. Smooth Endoplasmic Reticulum
9. **Mitochondria**
10. Vacuole
11. Cytoplasm
12. Lysosome
13. Centriole

Figure 1.1 Schematic Representation of a cell showing mitochondria [9] (www.wikipedia.org/wiki/Image:Biological_cell.svg)

[1.2] Mitochondria structure

Mitochondria have inner and outer membranes composed of phospholipid bilayers and proteins (figure 1.2). The two membranes, however, have different properties. As a result of this double membraned organization, there are 5 distinct compartments within mitochondria. There is the outer membrane, the intermembrane space (the space between the inner and outer membranes), the inner membrane, the cristae space (formed by infoldings of the inner membrane), and the matrix (space within the inner membrane). Mitochondria range in size from 1 to 10 μm. Mitochondrial matrix volume ranges from 0.6-1μl/mg mitochondrial protein.

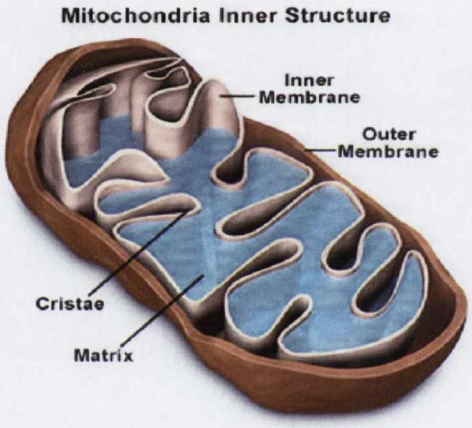

Figure 1.2 Simplified structure of a typical mitochondrion (picture: **www.cartage.org)**

[1.3] Energy Conversion and Oxidative Phosphorylation

Oxidative phosphorylation is the terminal process of cellular respiration in eukaryotes. During oxidative phosphorylation electrons are transferred from NADH or $FADH_2$ - created in glycolysis, fatty acid metabolism and the Krebs's cycle- to molecular oxygen, via a series of protein complexes located in the inner mitochondrial membrane (figure

1.3). Protons are pumped from the mitochondrial matrix into the intermembrane space as a result of this flow of electrons, generating a pH gradient and a transmembrane electrical potential across the membrane, producing a form of potential energy which is referred to as a proton-motive force (Δp). This potential energy is harnessed by ATP synthase. Protons are allowed to flow back into the matrix and the following reaction is catalyzed:

$$ADP^{3+} + H^{+} + P_i \longleftrightarrow ATP^{4-} + H_2O$$

The synthase functions almost as a mechanical motor, with each NADH molecule contributing enough proton motive force to generate 2.5 ATP. Each $FADH_2$ molecule is worth 1.5 ATP. All together, the 10 NADH and 2 $FADH_2$ molecules produced via the complete oxidation of glucose account for 23 of the 30 total ATP energy carrier molecules.

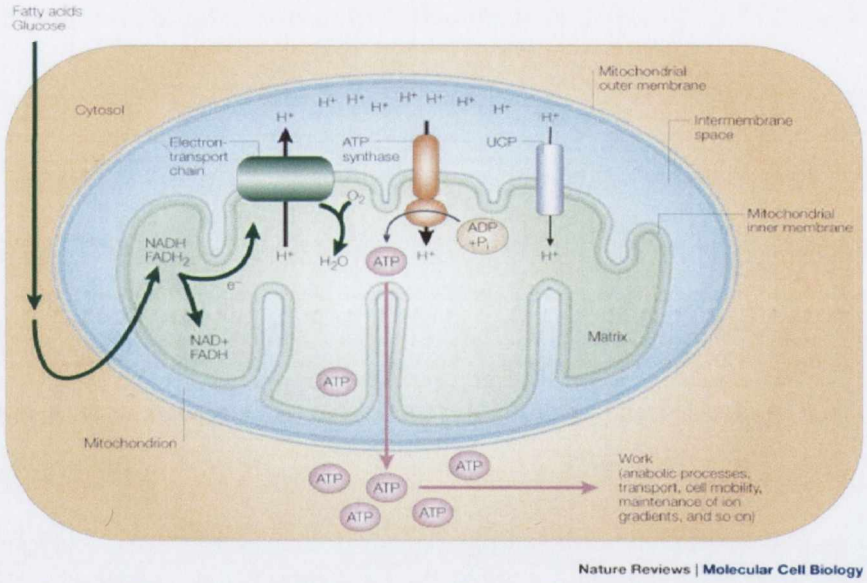

Figure 1.3 *Substrate oxidation and oxidative phosphorylation in mammalian cells.* ***[Krauss et al., 2005]***

[1.4] Proton leak

There are three types of proton leak across the mitochondrial inner membrane:

(1) Basal Proton Leak

(2) Artificially induced Proton Leak

(3) Protein-mediated Proton Leak

[1.4.1] Basal Proton Leak

There are three types of proton gradient leak. The first is known as ubiquitous or basal proton leak, which occurs in all mitochondria. Its mechanism is not fully understood, but it is believed to be a non-enzymic diffusion process of protons back into the mitochondrial matrix. This type of proton leak displays a non-linear (non-ohmic) dependence on its driving force, Δp, such that leak is maximal in state 4 respiring mitochondria (i.e. in absence of ADP) and minimal in state 3 respiring mitochondria (i.e. presence of ADP) (Nicholls & Rial, 1974). Proton leak accounts for approximately 25% of resting oxygen consumption of the whole animal due to mitochondrial processes. Therefore, it is clear that proton leak is a major contributor to basal metabolism. (Porter, 2001)

[1.4.2] Artificially induced Proton Leak

One of the most notable early successes of the chemiosmotic theory was its explanation of the action of uncoupling agents. Uncoupling agents abolish the link between oxidation and phosphorylation, allowing electron transport to proceed without coupled ATP synthesis (Brand, 2000). Over the years, many compounds including 2,4-dinitrophenol (DNP) and Carbonyl cyanide-*p*-trifluoromethoxyphenylhydrazone (FCCP) have been found to "uncouple" oxidative phosphorylation. DNP and FCCP are lipophilic weak acids that can cross the mitochondrial inner membrane in either a protonated or deprotonated state. This sets up a catalytic cycle that dissipates Δp and so allows substrate oxidation to proceed without providing the driving force for coupled ATP synthesis (Brand, 2000). In fact, uncoupling of mitochondria has been shown to reduce body fat in humans. The artificial uncoupler 2,4-dinitrophenol (DNP) had been used for this purpose for many years (Parascandola, 1974). DNP was introduced as an anti-obesity drug in the 1930's and used with some considerable success, though reports of

side effects (cataracts) and even some deaths from overdose, led to it being removed from the market by the U.S. Food and Drug administration (F.D.A) in 1938 (Parascandola, 1974).

[1.4.3] Protein-mediated Proton Leak

In addition to diffusion mediated natural "proton leak", it is widely known that the mitochondrial inner membrane of the brown adipocyte contain an uncoupling protein (UCP; originally called thermogenin) that can supercede the " diffusion mediated basal or natural proton leak" again enabling dissipation of the proton gradient independently of ATP utilization, thus enabling fuel to be oxidized for direct production of heat in thermoregulation (Nicholls & Locke, 1984) . Recent research has shown that there are other members of the UCP family, namely UCP 2 and UCP 3. Hence UCP in BAT has been renamed UCP 1 (Fleury *et al.,* 1997). UCP 1, when activated, catalyzes rapid proton leak across the mitochondrial membrane, leading to non-shivering thermogenesis (Nicholls & Locke, 1984)

[1.5] Brown Adipose Tissue and UCP1

Much non-shivering thermogenesis (also called metabolic thermogenesis) in small mammals is achieved in the brown adipose tissue (BAT) (Ricquier & Bouillaud, 2000). The thermogenic function of BAT was demonstrated in the early 1960s when several research groups reported that BAT produces heat, in particular under conditions requiring extra heat production, such as cold exposure, birth or arousal from hibernation as reviewed by Ricquier & Bouillaud, 2000.

BAT is a major site of cold and diet-induced thermogenesis (DIT) (Rothwell & Stock, 1979). BAT is found in almost all small mammals and in the newborn of larger mammals, such as humans. BAT is found in characteristic deposits scattered in specific areas of the body. The major deposits being interscapular, perirenal, cervical and auxiliary regions, in the surrounding of the thymus and thryoid, associated with the rib cage and within the thoracic cavity and the abdominal cavity (Néchad, 1986). The topology of BAT is such

that, upon activation of brown adipocytes, heat is quickly cleared through large vessels which convey it to the thoracic spinal cord, heart, thoracic structures, brain and kidneys (Ricquier & Bouillaud, 2000). BAT consists of brown adipocytes, which are morphologically and functionally distinct from white adipocytes. Brown adipocytes contain droplets of triglycerides, a central nucleus and numerous mitochondria which are characterised by a highly developed mitochondrial inner membrane (Ricquier & Bouillaud, 2000).

Given the specific role of BAT in nonshivering thermogenesis, it has always seemed logical that brown adipocytes are equipped with a mechanism that induces uncoupling of respiration in their mitochondria. Using photo-affinity labelling experiments, the protein responsible for this uncoupling was identified as thermogenin (now known as UCP 1) (Heaton *et al.,* 1978)

UCP 1, cloned in 1985 (Bouillaud *et al.,* 1985) and called UCP until 1997, was thought to be exclusively expressed in the brown adipocytes (Cannon *et al.*, 1982). UCP 1 is the key molecule in the thermogenic function of brown adipose tissue (BAT). UCP 1 is a 32 kDa protein, located in the inner membrane of BAT mitochondria, where it functions as both a proton conductor and chloride ion (Cl^-) channel (Huang & Klingenberg, 1996) .The thermogenic role of this protein is due to its capacity to dissipate Δp (Nicholls & Locke, 1984). Consequently, more fuel is oxidized and the liberated energy is dissipated as heat instead of being captured in ATP.

Newborn mammals that lack fur, such as humans, as well as hibernating animals and rodents contain brown BAT that contributes to both the maintenance of body temperature in a cold environment through non shivering thermogenesis and the control of body weight through the regulatory part of diet-induced thermogenesis (Rothwell & Stock, 1979). It has been shown that during cold acclimation, the capacity of BAT to produce heat is determined by the UCP1 content of their mitochondria (Hansen & Knudsen, 1986). Active BAT accounts for approximately 50% of heat production in non-shivering thermogenesis in the cold acclimated rat but only accounts up to 1% of the body mass of a rat (Foster, 1986). It was generally accepted that in humans, BAT is

rapidly lost (after a few years) and that adult humans do not possess more than vestigial amounts of brown adipose tissue, some contrary evidence has been largely ignored (Nibblelink *et al.*, 2001). However, since 2002, unrelated pieces of research within nuclear medicine have produced convincing evidence of the presence of active brown adipose tissue in human adults (Nedergaard *et al.*, 2007). This suggests that classical adaptive thermogenesis, mediated by UCP 1, can also be activated in the human adult. These results indicate that brown adipose tissue is indeed present and active in (at least a significant fraction of) adult humans and it may thus be considered to be an organ of physiological and pharmaceutical importance even in adults (Nedergaard *et al.*, 2007).

[1.6] Biochemistry of UCP 1

[1.6.1] Structure

UCP 1 has been successfully purified from BAT mitochondria (Lin & Klingenberg, 1980). The primary structure of UCP 1 has also been elucidated by *N*- terminal sequencing (Aquila *et al.,* 1985).

UCP 1 is a 32 kDa monomer of 306 amino acids, the functional unit maybe a homodimer. UCP 1 is proposed to contain 6 transmembrane helices with both C and N termini protruding to the cytosolic side (figure 1.6, Klingenberg *et al.,* 1999). UCP 1's amino acid sequence is highly homologous to that of several ubiquitous mitochondrial inner-membrane carriers, including the ADP/ATP carrier, the phosphate carrier and the oxoglutarate carrier (Klaus *et al.,* 1991). As a member of the mitochondrial carrier family, the structure can be divided into 3 similar repeat domains of about 100 residues, each containing 2 transmembrane helices (Palou *et al.*, 1998).

Within each domain, two helices are separated on the matrix side by an approximately 40 residue long hydrophilic stretch. UCP 1 from hamster contains 28 positively and 19 negatively charged residues, resulting in excess of nine positive charges (Klingenberg *et al.,* 1999), with most of the charges localized in the hydrophilic matrix region. Many charges occur at conserved repeats in each domain. The aspartate 27 is located at the

same position of a lysine characteristic for all ADP/ATP carriers. In the third domain, the first helix is limited by histine (H214) instead of lysine, which is unique for UCP 1. In the matrix region, a well conserved motif KXR is found in all three domains, which is characteristic for the mitochondrial carrier family. Other charged residues are partially conserved in this highly charged region. The His pair HLH (145-147) is found only in UCP 1 (Klingenberg *et al.,* 1999). The overall protein structure consists of about 50% α-helix, 30% β-structure, 15% β-turns and 7% random (Palou *et al.*, 1998).

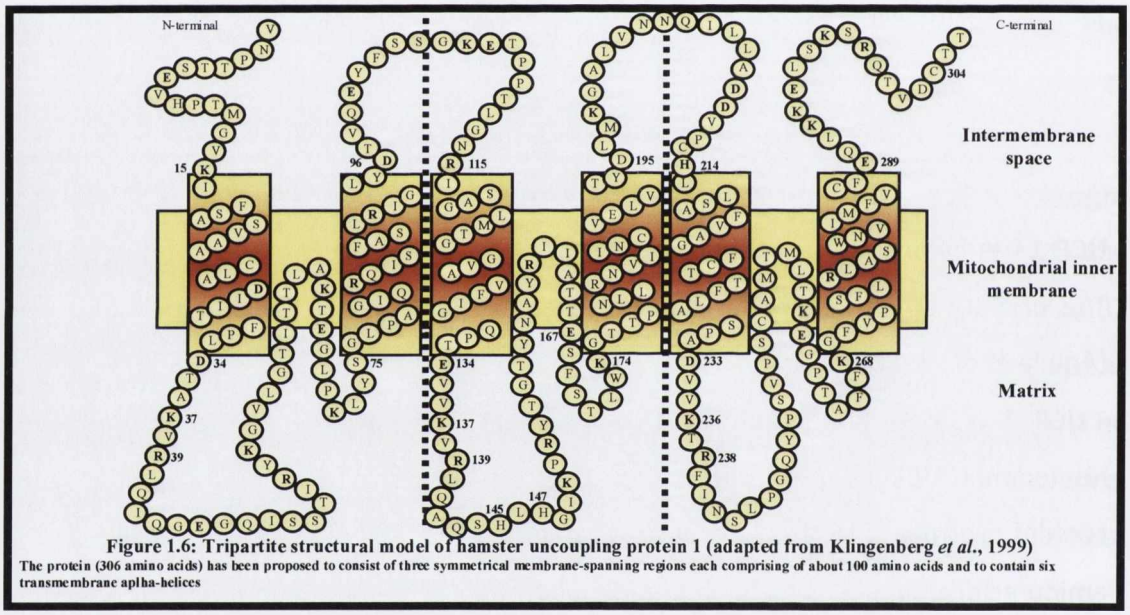

Figure 1.6: Tripartite structural model of hamster uncoupling protein 1 (adapted from Klingenberg *et al.*, 1999)
The protein (306 amino acids) has been proposed to consist of three symmetrical membrane-spanning regions each comprising of about 100 amino acids and to contain six transmembrane alpha-helices

[1.6.2] Synthesis and Degradation of UCP 1

Thermogenesis in BAT is activated in response to cold exposure, chronic overeating, free fatty acids and β_3-adrengic receptors (Ricquier & Bouillaud, 1986). The concentration of fatty acids in BAT is controlled by the hormone noradrenalin (NA).

Noradrenalin plays an important role in brown adipocytes, promoting UCP 1 activity (UCP activation) and differentiation (UCP synthesis) (Cannon *et al.,* 1996). The major adrenoreceptor mediating the effects of NA in mature BAT cells is β_3-adrenoreceptor, which is mainly expressed in white and brown adipocytes.

Upon cold-exposure, NA is released from sympathetic terminals and binds to its cell surface receptor. The NA-receptor complex stimulates adenylate cyclase to synthesize cAMP, thereby causing cAMP levels to rise. cAMP binding allosterically activates cAMP-dependant protein kinase (cAPK). cAPK phosphorylates hormone sensitive triacylglycerol lipase, thereby activating thermogenesis. Finally, the activated lipase hydrolyzes triacylglyerols to yield the free fatty acids that open the proton channel. Free fatty acids overcome the purine nucleotide (GDP) block of the proton channel formed by the uncoupling protein, allowing protons to enter mitochondria uncoupled from ATP synthesis.

Another key downstream target of cAPK is CREBP (cAMP-response-element-binding-protein) which stimulates transcription of the UCP 1 gene (Silva & Rabelo, 1997). The UCP gene is mainly regulated at the transcriptional level (figure 1.6.2). Besides NA, another activator of UCP transcription is triiodothyronine (T_3), which acts in connection with NA, since NA stimulation markedly increases thryoxine deiodinase activity of brown adipocytes, thus allowing high intracellular generation of T_3 from thyroxine. T_3 stimulates UCP 1 gene expression via thryoid hormone response elements (TRE's) (Silva & Rabelo, 1997). Retinoic acid, the natural active form of vitamin A, has been shown to stimulate UCP 1 gene transcription (Larose *et al.*, 1996). Retinoic acid and vitamin D receptors bind to the specific response elements in the genes as heterodimers with other receptors, most commonly with the so-called RXR-receptors. It is also known that activators of peroxisome proliferation activating receptors (PPAR), such as pioglitazone cause UCP 1 gene expression (Sears *et al.*, 1996). Sears *et al.,* (1996) have shown that PPARγ-RXR heterodimers are necessary for cAMP-mediated stimulation of the UCP 1 gene.

Concerning UCP 1 degradation, it has been suggested that a post-translational regulatory mechanism exists which ensures the rapid degradation of newly synthesized molecules when the physiological stimulation ceases (Bonet *et al.*, 1995).

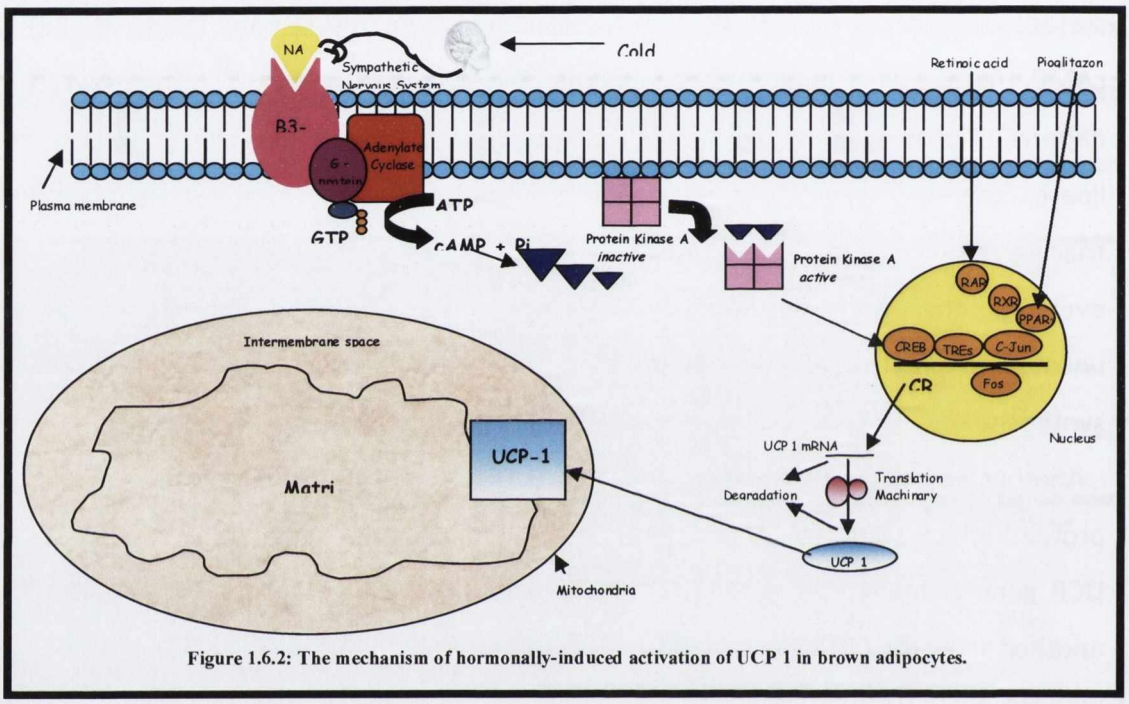

Figure 1.6.2: The mechanism of hormonally-induced activation of UCP 1 in brown adipocytes.

10

[1.6.3] Regulation of UCP 1

[1.6.3a] Purine Nucleotide Inhibition

UCP 1 is inhibited by purine nucleotides and stimulated by free fatty acids (Nicholls and Rial, 1974). Purine nucleotides consist of a purine base, a sugar moiety and one or more phosphate groups. Common derivatives of purine are adenine and guanine, which are both found in DNA and RNA. The nitrogen atom-9 of the purine is covalently attached to what is known as carbon-1' of the sugar in a glycosidic linkage. Synthesis of purine nucleotides is completed when one or more phosphates are joined to the sugar via an ester linkage.

The purine nucleotide binding site on UCP 1 has been well characterized (Heaton *et al.*, 1978). Nucleotides only bind from the cytosolic side of UCP 1. UCP 1 has a high affinity for both tri- and di-nucleoside phosphates but a lower affinity for mono-nucleoside phosphates (Klingenberg, 1988). The phosphate groups are known to interact with three arginine residues on helices 2,4 and 6 whereas the sugar base moiety reacts with the matrix part of UCP 1, which connects helices 5 and 6 (Porter, 2001). Purine nucleotide binding to UCP 1 is believed to induce a conformational change in UCP 1, which is responsible for its inhibitory activity. Specifically , the α-phosphate of purine nucleotides bind to arginine residue number 276, which induces a conformational change in UCP 1, which is believed to occlude the fatty acid binding site (Klingenberg & Huang, 1999)

Purine nucleotide inhibition is an important regulatory mechanism of UCP 1. Inhibition of UCP 1 activity is necessary to restore coupledness to BAT mitochondria. Therefore this means that respiratory activity is coupled to ATP synthesis. Purine nucleotide inhibition of UCP 1 activity can occur in the absence of thermogenesis or during thermogenesis when ATP utilisation of the cell exceeds ATP synthesis via oxidative phosphorylation. It is known that sensitivity of UCP 1 to different nucleotides varies, but its overall sensitivity to purine nucleotides is greatly increased following induction of UCP1 activity by cold-exposure. Purine nucleotide inhibition of UCP 1 activity is also pH dependant with sensitivity declining as the pH becomes greater than approximately 7.2 (Huang & Klingenberg, 1995). This is due to an essential glutamic acid residue at position number 190 within the fourth helix of UCP1.

[1.6.3b] Activation by Long Chain Fatty Acids

UCP 1 is activated by free fatty acids and by long chain fatty-acyl CoA esters (Nicholls & Rial, 1974). It has been found that a fatty-acid chain length of at least ten carbons is required to activate UCP 1 uncoupling activity (Klingenberg & Huang, 1999). Unsaturated fatty-acids (i.e. contain at least one double bond between two carbon

atoms) are known to be good activators of UCP 1 catalyzed proton conductance (e.g. oleic acid (C_{18}) (Klingenberg & Echtay, 2001). As well as this, some well known physiological fatty-acid analogues such as retinoic acid are good activators of UCP 1 induced proton transport. This has been reported by Rial *et al.*, (1999) in BAT and yeast mitochondria expressing UCP 1.

Although purine nucleotide inhibition of UCP 1 is well understood, the mechanism of fatty-acid activation of UCP 1 activity remains controversial. There are two general models of fatty-acid stimulation of uncoupling activity in UCP 1; the fatty-acid protonophore model (Garlid *et al.,* 1996) and the proton buffering model (Winkler & Klingenberg, 1994).

[1.6.3b (i)] Protonophore model

In the Garlid model, it is known that protonated fatty-acids can naturally diffuse (i.e. flip-flop) across the lipid bilayer of the mitochondrial inner membrane. It can then release a proton into the mitochondrial matrix. Unlike classical uncoupler (e.g. FCCP), deprotonated fatty-acids cannot diffuse back across the mitochondrial inner membrane easily, due to the presence of a localized negative charge. Therefore, according to the Garlid model, in order for free fatty-acids to act as uncouplers, their negatively charged deprotonated form must be transported catalytically across the membrane via UCP 1. As it is known that UCP 1 is a member of a subfamily belonging to the mitochondrial anion carrier family, which includes the ADP/ATP carrier, UCP 1 can therefore transport anions (Garlid *et al.,* 1998).

Therefore, the uncoupling activity of UCP 1 may be due to fatty-acid cycling across the mitochondrial inner membrane, it is the deprotoned anionic form driven from the matrix into the intermembrane space by UCP 1. This model would explain the known uncoupling activity of other mitochondrial anion carriers in the mitochondrial inner membrane, especially the ADP/ATP carrier, which has been observed *in vitro* (Talbot *et al,* 2004). The physiological significance, if any, of this uncoupling activity by mitochondrial anion carriers *in vivo* is uncertain. In this model, free fatty-acids are

obligatory for the dissipation of the Δp across the mitochondrial inner membrane, as they are the source of the proton. Furthermore, cycling of the anionic fatty-acid via UCP 1 from the matrix back to the intermembrane space where it can be reprotonated only occurs at high membrane potential. High membrane potential only occurs at the state 4 rate of respiration. Therefore this model explains how fatty acids may activate UCP 1 uncoupling activity during state 4 respiration.

[1.6.3b (ii)] Proton buffering model

However, in the second model (i.e. the proton buffering model), it is hypothesized that UCP 1 mediates a specific pathway for proton transport. This transport may occur in the absence of fatty acids (Ricquier & Bouillaud, 1986), where the role of fatty acids is to make proton transport by UCP 1 more efficient. According to this model, intramembrane fatty –acids insert their head groups into the proton transport pathway and provide buffering sites to assist proton translocation via UCP 1. Therefore, in this model, fatty-acids do not provide the source of proton to UCP1 but instead, is believed to provide an essential free carboxyl head group, which activates the proton transport activity of UCP 1, making it more efficient. (Winkler & Klingenberg, 1994). This model would explain why uncoupling activity is much higher in BAT mitochondria than in other tissues which are devoid of UCP 1 yet still contain members of the mitochondrial family of anion carriers. Instead of UCP 1 mediating uncoupling via fatty acid cycling, similar to other mitochondrial anion carriers, UCP 1 uncouples mitochondria in its own unique way by catalyzing the direct transport of protons across the membrane with fatty-acids acting as buffering co-factors of UCP 1 catalysed proton transport.

[1.7] UCP 1 Protein Expression

Up to recently, UCP 1 has only ever been associated with BAT mitochondria. No significant quantities of UCP 1 were detected in immunological studies of liver, heart, epididymal white fat, parametrial white fat of thigh muscle-even from cold acclimated

animals (Ricquier & Bouillaud, 1986). A study by Nibbelink *et al.* (2001) showed that UCP 1 is expressed in uterine longitudinal smooth muscle cells, but this has since been disproven (Rousset *et al.*, 2003) Commercial and in-house anti-UCP 1 peptide antibodies have been successful in determining factors affecting UCP 1's protein expression. It has been shown that cold-acclimation induces an increase in UCP 1 protein expression in BAT mitochondria isolated from rats (Nicholls & Rial, 1999). By contrast, starvation has been shown to decrease UCP 1 protein expression in BAT mitochondria (Nedergaard *et al.*, 2001). In addition, certain dietary regimes such as cafeteria diets, high-fat diets and high-sucrose diets have been shown to increase UCP 1 protein content in BAT (Nedergaard *et al.*, 2001).

[1.7.1] UCP 1-Exclusive to BAT?

In 2005, Carroll *et al.* showed that rat and mouse thymi contains mitochondrial UCP 1. Their evidence was strong and multilayered. Firstly RT-PCR detected RNA transcripts for UCP 1 in whole thymus and thymocytes. Secondly, peptide antibodies specific for UCP 1 detected UCP 1 protein in thymus mitochondria of wild-type but not UCP 1 knock-out mice. Immunodetection of UCP 1 protein was also evident with other polyclonal anti-UCP 1 peptide antibodies. Thirdly radiolabelled-GDP binding to mitochondria from thymus resulted in equivalent $B_{MAX\ and}$ K_D values to those observed in BAT mitochondria. Similarly a palmitate activatable /GDP-inhibitable oxygen consumption rate was observed in thymus mitochondria. UCP 1 from rat thymus was also purified and identified by mass spectrometry. Finally the reconstitution of thymus UCP 1 into phospholipid vesicles catalyses a fatty acid dependant GDP-inhibitable proton leak (Breen *et al.*, 2006). UCP 1 is not thought to play a role in thermogenesis in the thymus (Brennan *et al.*, 2006) as cold acclimation results in an 8-fold decrease in oxygen consumption by thymocytes. However, the identification of UCP 1 in the thymus has been challenged by Frontini *et al.*, (2007). Frontini believes that UCP 1 in the thymus is due to contamination from surrounding BAT. However BAT is visibly distinguishable

from the translucent white thymus and is easily removed. Recently there are reports of UCP 1 in skin and skin derived cells (Mori et al., 2008)

[1.8] The novel uncoupling proteins- UCP 2 and UCP 3

Since the discovery of UCP1 in the 1970s, other mitochondrial proteins have been discovered. These new uncoupling proteins share high sequence homology with UCP1. These proteins are not confined to BAT and are distributed throughout the body in various tissues in both humans and rodents (Boss et al., 1997b; Fleury et al., 1997; Gong et al., 1997; Vidal-Puig et al., 1997).

Screening of a skeletal muscle library using cDNA as a probe led to the discovery of Uncoupling protein 2 (UCP2) (Fleury et al., 1997). Further analysis revealed that this novel uncoupling protein shared 59% homology with UCP1 and had an approximate molecular mass of 30kDa. Many studies have shown that UCP2 mRNA expression is widespread in tissues including WAT, BAT, skeletal muscle, heart, placenta, brain, stomach, kidney, lung, mycocytes, lymphocytes, macrophages and the Kupffer cells of liver (Boss et al., 1997a; Fleury et al., 1997; Gimeno et al., 1997; Gong et al., 1997;Krauss et al., 2002; Larrouy et al., 1997; Pecqueur et al., 2001; Ricquier and Bouillaud, 2000; Rousset et al., 2003). However UCP2 protein expression is only found in mouse and rat spleen, lung, stomach, kidney, thymus, WAT, pancreatic islets and macrophages (Echtay and Brand, 2001; Krauss et al., 2002; Pecqueur et al., 2001; Ricquier and Bouillaud, 2000; Zhang et al., 2001). UCP2 mRNA and protein levels have been shown to increase under various physiological states including cold exposure, 48 hours starvation (Boss et al., 1997a) and leptin administration (Zhou et al., 1997 Pecqueur et al., 2001).

A third uncoupling protein was found in skeletal muscle which was termed uncoupling protein 3 (UCP3). Like the other two uncoupling proteins UCP 3 was found to be a mitochondrial inner membrane protein. It was initially cloned by Boss *et al* (1997) and shortly thereafter by Vidal-Puig *et al* (1997) and Gong *et al* (1997). Existing as two

isoforms in humans, the long form ($UCP3_L$) and the short form ($UCP3_S$), it differs from UCP1 and UCP2 which have no known isomers. Along with the other uncoupling proteins and mitochondrial carriers, UCP3 has six transmembrane domains (Boss et al, 1997). However the $UCP3_S$ lacks the sixth potential transmembrane region and putative nucleotide binding site which is implicated in the control of UCP activity. UCP3 mRNA is expressed in skeletal muscle of humans (Vidal-Puig et al., 1997). Rodents express UCP3 in skeletal muscle, BAT, spleen and thymus (Carroll and Porter, 2004; Gong et al., 1997). UCP3 protein has been detected in mouse and rat skeletal muscle (Cadenas et al., 2002; Cunningham et al., 2003; Gong et al., 2000; Harper et al., 2002; Vidal-Puig et al., 2000; Zhou et al., 2000), BAT mitochondria (Cunningham et al., 2003; Gong et al., 2000; Harper et al., 2002; Jezek et al., 1999) and rat spleen and thymus mitochondria (Carroll and Porter, 2004).

[1.9] Physiological relevance of uncoupling proteins

Apart from UCP1, the function of many of the uncoupling proteins is not clear and is still under investigation. Initially when UCP2 and UCP3 were discovered it was proposed that they may have an uncoupling role like UCP1, and are involved in energy expenditure. This was due to the similarities in their amino acid sequences to that of UCP1. The residues involved in nucleotide binding and pH regulation are well conserved in these proteins (Boss et al., 1997b; Fleury et al., 1997). However one of the histidine residues vital for H^+ transport in UCP1 is not conserved (fatty acid protonophore model) (Bienengraeber et al., 1998). It is now generally agreed that these uncoupling protein homologues do not transport protons in the absence of specific activators. Studies utilizing UCP2 and UCP3 knockout mice showed no difference in basal proton conductance in isolated mitochondria compared to wild-types (Cadenas et al., 2002; Couplan et al., 2002; Echtay et al., 2002; Krauss et al., 2003), but differences were noted when specific activators such as hydroxynonenal were used (Brand et al., 2004a; Brand et al., 2004b; Considine et al., 2003). However the levels of UCP2 and UCP3 are tiny

compared to UCP1 levels in BAT, 0.1% to 1% (Harper et al., 2002; Pecqueur et al., 2001), so any uncoupling effect may be only mild compared to the uncoupling observed in BAT.

This has led to the proposal that UCPs can attenuate mitochondrial production of free radicals and therefore protect against oxidative damage, degenerative diseases and aging. Mitochondrial reactive oxygen species (ROS) production is very sensitive to the proton motive force set up across the inner membrane by electron transport. Any putative mild uncoupling by UCP2 or UCP3 may reduce this proton motive force and thereby reduce ROS production by mitochondria, and protect against ROS-related cellular damage (Brand et al., 2002; Casteilla et al., 2001; Echtay et al., 2002).

A role for UCP2 in signalling is also proposed. This model proposes that activation of UCP2 may attenuate glucose-stimulated insulin secretion by pancreatic β cells (Rutter, 2001). UCP2 knock-out mice have higher islet ATP levels and increased glucose-stimulated insulin secretion suggesting that UCP2 negatively regulates insulin secretion (Zhang et al., 2001).

The proposed roles for UCP2 and UCP3 make them attractive targets for obesity and inefficient insulin signalling in pancreatic β cells. Their proposed role in ROS attenuation and thus protection from oxidative damage, also suggests a role in normal aging and neurodegenerative disorders, and therefore make them attractive targets in this field also.

Although UCP1 is normally studied in the context of adaptive thermogenesis in newborns and rodents, its discovery in the thymus may propose a new role for UCP 1 in the thymus.

[1.10] Half-life of Uncoupling proteins-indicative of function?

Heat production by UCP 1 in brown adipocytes is generally a long and adaptive phenomenon which is reflected in its half life of 30 hours (Puigserver *et al.*, 1992). UCP 2 is expressed in many tissues, such as spleen, lung, intestine, pancreatic β cells and immune cells (Pecqueur *et al.*, 2001). UCP 2 is very unstable with a half life close to 30

minutes (Rousset *et al.*, 2007). UCP 1 is transcriptionally regulated whereas UCP 2 protein level can change without any alteration in m RNA level, highlighting different physiological functions. UCP 2 is implicated in the immune response by regulating ROS production (Arsenijevic *et al.*, 2000). The regulation of ROS level must be subtle, and it is clear that UCP 2, as a regulator of ROS level, is both rapidly synthesized and degraded. The half life of UCP 1 in the thymus has never been explored. UCP2 also plays an important role in regulation of insulin secretion. Pancreatic β-cells secrete insulin in response to a meal by sensing the ATP/ADP ratio resulting from glucose metabolism in the cell. UCP2, by mildly increasing proton leak, decreases the ATP/ADP ratio of the cell thus reducing the effect of glucose on insulin secretion (Brand & Esteves, 2005)

[1.11] Thymus

In human anatomy, the thymus is an organ located in the upper anterior portion of the chest cavity. It is of central importance in the growth and maturation of T cells.

The thymus is a bi-lobed, greyish organ located in the thoracic cavity just below the neck (Ritter & Crispe, 1992). Curiously, when the thymus is removed from adult mammals, few effects are seen. However, when the thymus is removed at birth, dramatic effects are witnessed. The thymus develops from the endoderm. During its development many cells migrate towards it, most of which are lymphocytes. The thymus is divided into two distinct compartments, the outer cortex and the inner medulla. Both regions are densely populated with lymphocytes (or thymocytes while in the thymus). Most of the cortical lymphocytes are immature and unable to carry out immune functions. Mature immunocompetent cells are found in the medulla in greater numbers. The main function of the thymus is to develop immature T-cells into immunocompetent T-cells. This process begins with the production of pre-T cells in the bone marrow and their subsequent transport to the thymus via the blood. The pre-T cells are then taken into the cortex of the thymus. Here, a series of molecular events take place allowing the cells to recognize certain antigens. Some of the cells recognize self-components, and these

are eliminated by a process of negative selection. Those that fail the selection die and those that live proceed to the medulla and eventually enter the blood stream (Figure 1.10).

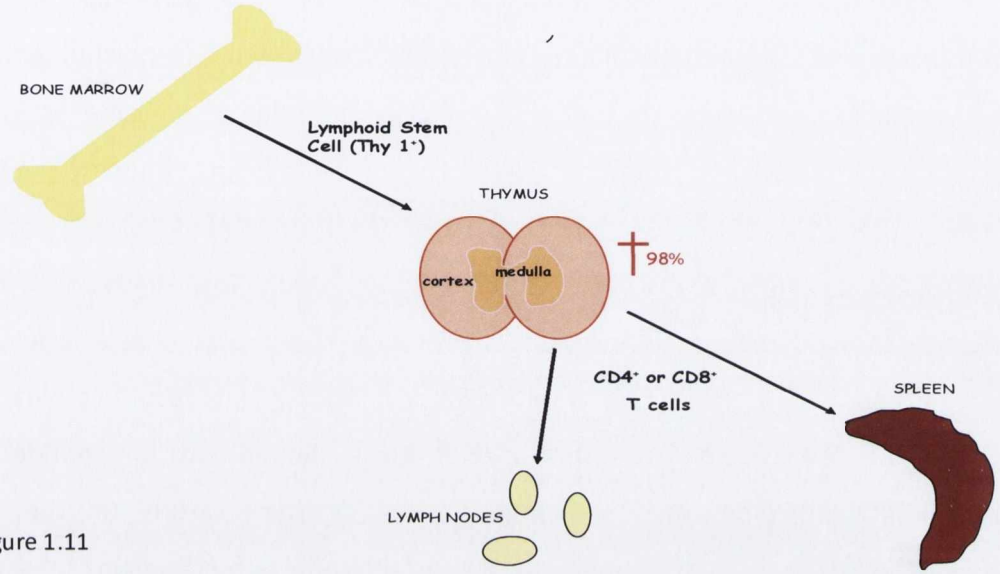

Figure 1.11

[1.11.1] Thymoectomy

Due to the large numbers of apoptotic lymphocytes, the thymus was originally dismissed as a "lymphocyte graveyard", without functional importance. The importance of the thymus in the immune system was discovered by Jacques Miller, by surgically removing the thymus from three day old mice, and observing the subsequent deficiency in a lymphocyte population, subsequently named T cells after the organ of their origin (reviewed by Miller, 2004).

[1.11.2] Function

The thymus plays an important role in the development of the immune system, being the primary site of T cell maturation. The organ is most active between the late stages of gestation and early puberty, when most of the T cells an individual will carry for their

lifetime are formed. With the onset of puberty the organ atrophies, gradually shrinking in size and function. The atrophy is due to the increased circulating level of sex hormones, and chemical or physical castration of adult results in the thymus increasing in size and activity (Miller, 2002). A typically adult thymus weighs about 25g.

In the two thymic lobes, lymphocyte precursors from the bone-marrow become thymocytes, and subsequently mature into T cells. Once mature, T cells emigrate from the thymus and constitute the peripheral T cell repertoire responsible for directing many facets of the adaptive immune system. Loss of the thymus at an early age through genetic mutation or surgical removal results in severe immunodeficiency and a high susceptibility to infection (Schwarz & Bhandoola, 2006). The ability of T cells to recognize foreign antigens is mediated by the T cell receptor. The T cell receptor undergoes genetic rearrangement during thymocyte maturation, resulting in each T cell bearing a unique T cell receptor, specific to a limited set of peptide: major histocompatability complex combinations. The random nature of the genetic rearrangement results in a requirement of central tolerance mechanisms to remove or inactivate those T cells which bear a T cell receptor with the ability to recognize self-peptides.

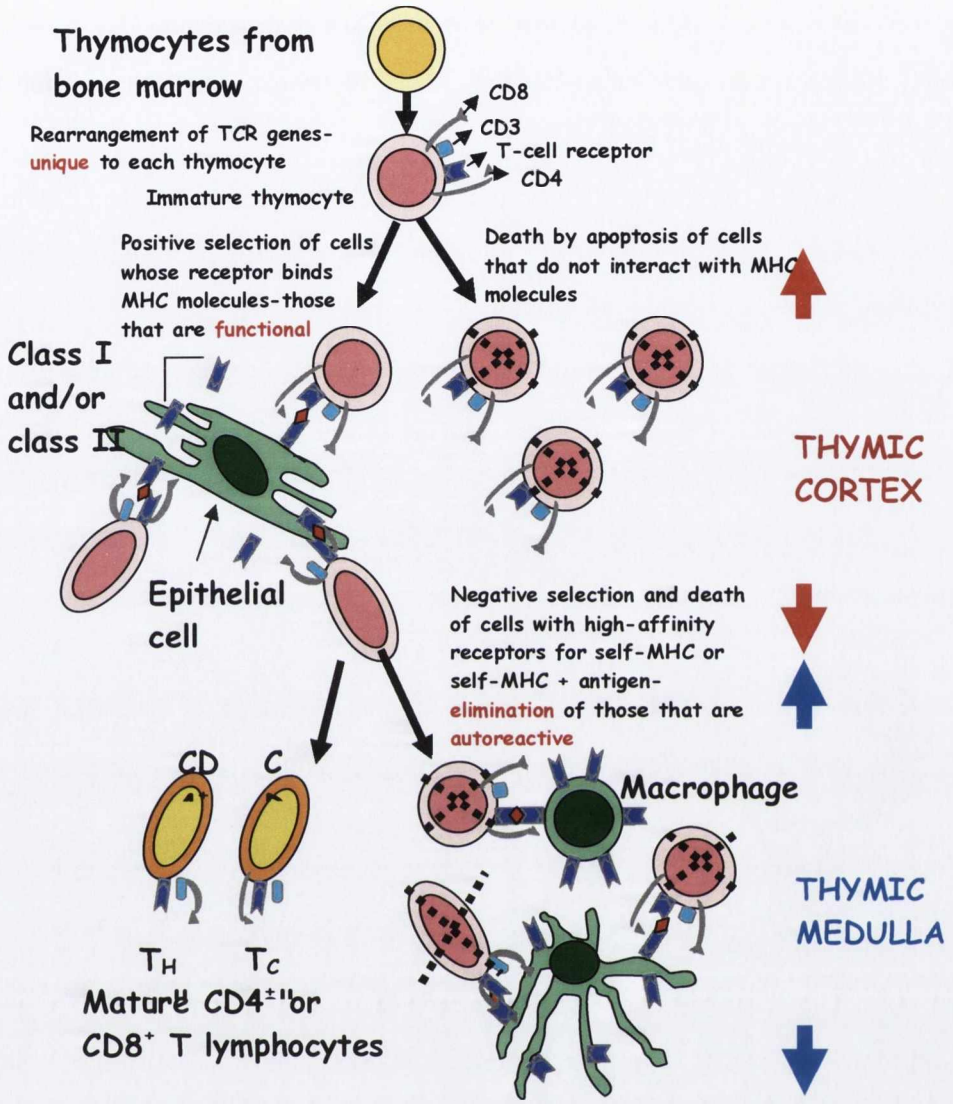

Figure 1.11.3 Maturation of thymocytes in thymus- Positive and Negative selection.

TCR T cell receptor
MHC Major Histocompatability Complex
T_H Helper T cell
T_C Cytotoxic T cell
CD Cluster of Differentiation

[1.11.3] Phases of thymocyte maturation

The generation of T cells expressing distinct T cell receptors occurs within the thymus, and can be conceptually divided into three phases:

a) A rare population of hematopoietic progenitors enters the thymus from the blood, and expands by cell division to generate a large population of immature thymocytes (Sleckman, 2005).

b) Immature thymocytes each make distinct T cell receptors by a process of gene rearrangement. This process is error-prone, and some thymocytes fail to make functional T cell receptors, whereas other thymocytes make T cell receptors that are autoreactive (Baldwin, 2004). Growth factors include thymopoietin and thymosin.

c) Immature thymocytes undergo a process of selection, based on the specificity of their T cell receptors. This involves selection of T cells that are functional (positive selection), and elimination of T cells that are autoreactive (negative selection)

[1.11.4] Minute structure of thymus.

Each lateral lobe is composed of numerous lobules held together by delicate areolar tissue; the entire gland being enclosed in an investing capsule (Ritter & Crispe, 1992) of a similar but denser structure. The primary lobules vary in size from that of a pin's head to that of a small pea, and are made up of a number of small nodules or follicles.

The follicles are irregular in shape and are more or less fused together, especially toward the interior of the gland. Each follicle is from 1 to 2 mm in diameter and consists of a medullary and a cortical portion (Ritter & Crispe, 1992), and these differ in many essential particulars from each other.

[1.11.4.1] Cortex

The cortical portion is mainly composed of lymphoid cells, supported by a network of finely-branched epithelial reticular cells, which is continuous with a similar network in

the medullary portion. This network forms an *adventitia* to the blood vessels.
The cortex is the location of the earliest events in thymocyte development, where T cell receptor gene rearrangement and positive selection takes place.

[1.11.4.2] Medulla

In the medullary portion, the reticulum is coarser than in the cortex, the lymphoid cells are relatively fewer in number, and peculiar nest-like bodies are found there, the concentric corpuscles of Hassall (Terszowski, 2006). These concentric corpuscles are composed of a central mass, consisting of one or more granular cells, and of a capsule formed of epithelioid cells. They are the remains of the epithelial tubes, which grow out from the third branchial pouches of the embryo to form the thymus. Each follicle is surrounded by a vascular plexus, from which vessels pass into the interior, and radiate from the periphery toward the center, forming a second zone just within the margin of the medullary portion. In the center of the medullary portion there are very few vessels, and they are of minute size.
The medulla is the location of the latter events in thymocyte development. Thymocytes that reach the medulla have already successfully undergone T cell receptor gene rearrangement and positive selection, and have been exposed to a limited degree of negative selection. The medulla is specialized to allow thymocytes to undergo additional rounds of negative selection to remove auto-reactive T cells from the mature repertoire.

[1.11.5] Identification of Thymocytes

Thymocytes express many cell surface markers .Thy 1 is expressed at all levels of differentiation within the thymus. Thy 1 (CD90) is a glycoprotein with a molecular weight of 17.5 kDa. Thy 1 is low on prothymocytes in rats and mice. Thy1 is highest on cortical thymocytes and intermediate on medullary thymocytes in rats and mice (figure 1.11.5; Ritter & Crispe, 1992). The only difference is that the Thy 1 marker is lost

Figure [1.11.5]. Expression of Thy 1 (CD90) Cell Marker in rat/mouse thymocytes

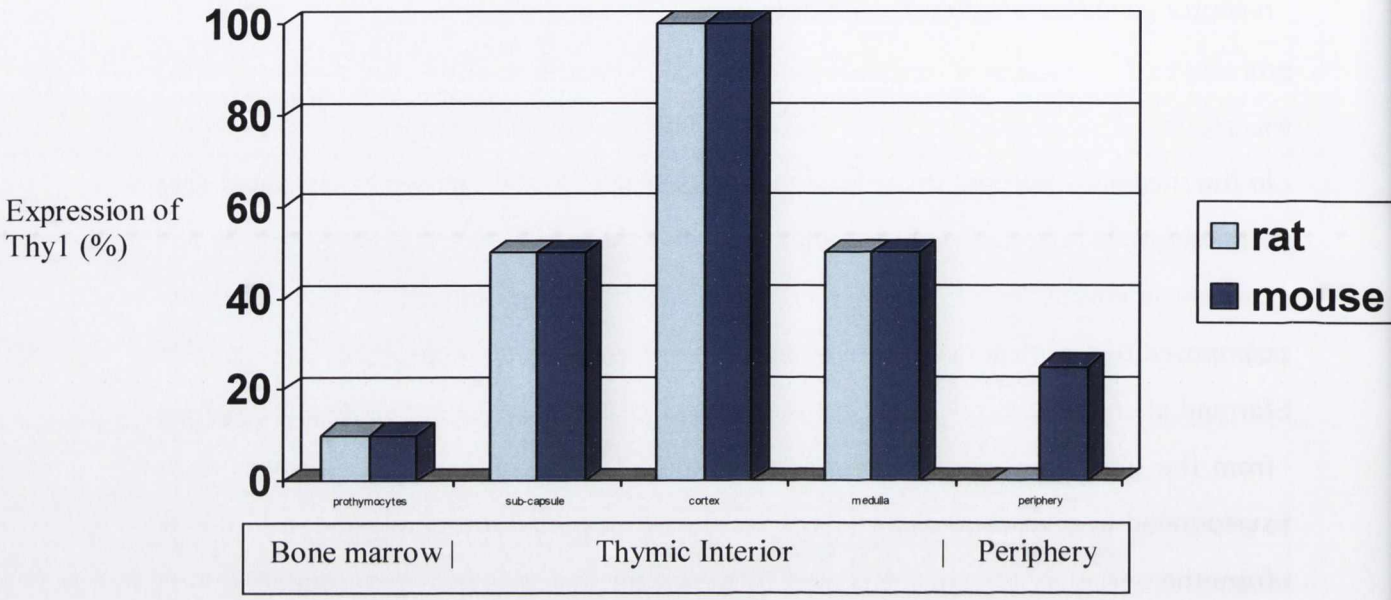

[1.11.6] Cell types in the Thymus

The three-dimensional structure of the rat thymus was studied by combined scanning- and transmission electron microscopy (Ushiki, 1986). The thymus consists mainly of four types of cells: epithelial cells, lymphocytes, macrophages, and dendritic cells (figure 1.11). The epithelial cells form a meshwork in the thymus parenchyma. A continuous single layer of epithelial cells separates the parenchyma from connective tissue formations of the capsule, septa and vessels. Surrounding the blood vessels, this epithelial sheath is continuous in the cortex, while it is partly interrupted in the medulla, suggesting that the blood-thymus barrier might function more completely in the cortex. Cortical lymphocytes are round and vary in size, whereas medullary lymphocytes are mainly small, although they vary considerably in surface morphology (Ushiki, 1986). Two types of large wandering cells, macrophages and dendritic cells could be distinguished, as well as intermediate forms. Dentritic cells sometimes embraced or contacted lymphocytes, suggesting their role in the differentiation of the latter cells. Perivascular

channels were present around venules and some arterioles in the cortico-medullary region and in the medulla. A few lymphatic vessels were present in extended perivascular spaces (Ushiki, 1986).

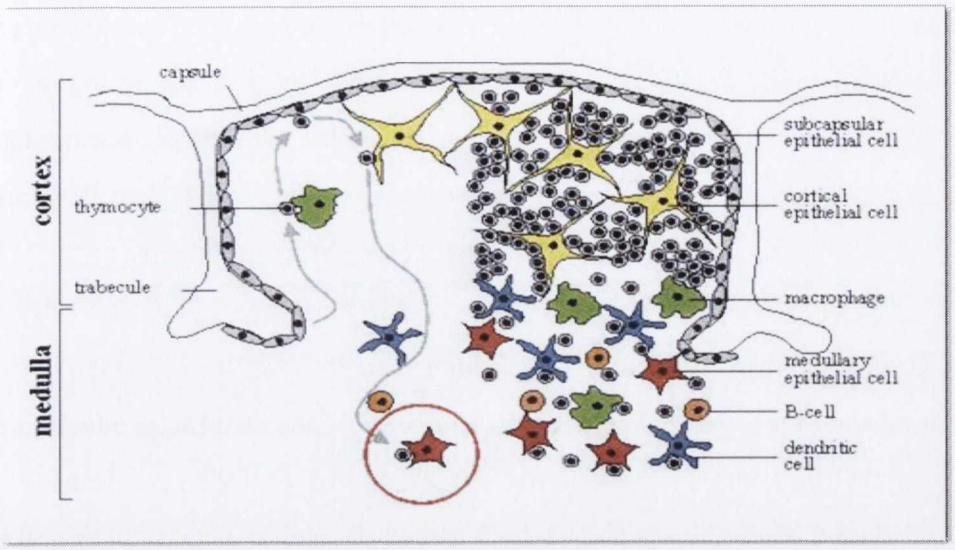

Figure [1.11.6]: Schematic view of the thymus architecture. The major cell types and the sequential cell-cell interactions along the migratory route of developing T cells are depicted.

[1.12] The Immune System

The immune system comprises many different cell types and organs. It can be subdivided into two components, the innate and the adaptive immune systems. The innate immune response is a rapid immediate response while the adaptive response is slower, but provides immunological memory.

[1.12.1] Innate Immune System

The innate immune response is the first line of defense against invading microbes. It recognises antigens associated with microbes, and this recognition triggers an inflammatory response in which certain cells of the immune system attempt to wall of the invader and halt its spread. The activity of these cells e.g. mast cells and of the chemicals they secrete e.g. histamine leads to the redness and swelling at sites of injury and accounts for the fever, body aches and other flu-like symptions that accompany many infections.

The innate immune system contains various cell types responsible for mediating different effector functions. All white blood cells are known as leukocytes, which are able to move freely and interact with and capture cellular debris, foreign particles, or invading micro-organisms. Most innate immune leukocytes are produced by pluripotent hematopoietic stem cells present in the bone marrow (Montecino-Rodriguez & Dorshkind, 2002)). The innate leukocytes include : NK cells, mast cells, eosinophils, basophils ; and the phagocytic cells including macrophages, neutophils and DCs, and function within the immune system by identifying and eliminating pathogens.

The principle functions of the immune system include:

- The recruitment of immune cells to sites of infection, through the production of chemical factors, including specialised chemical mediators, called cytokines.
- Activation of the complement cascade to identify bacteria, activate cells and to promote clearance of dead cells or antibody complexes.
- Identification and removal of foreign substances present in organs, tissues the blood and lymph, by specialized white blood cells.
- Activation of the adaptive immune system occurs through a process known as antigen presentation.

Detection of pathogens is mediated via a variety of receptors, referred to as pattern recognition receptors (PRRs) that recognize molecular patterns on pathogens called pathogen-associated molecular patterns (PAMPs). TLRs are the most common PRRs. Upon TLR activation i.e. when the TLRs sense a pathogen, production of an array of signalling proteins (e.g. cytokines) that induce inflammation and direct the body to mount a fully fledged immune response is triggered. These protein messengers then recruit additional macrophages, DCs and other immune cells to wall off and non-specifically attack the microbes. Macrophages and DCs that have engulfed a pathogen display pieces of it on their surface along with other molecules indicating that a disease-

causing agent is present. This display combined with the cytokines released in response to TLR engagement, ultimately activates T and B cells that recognize those specific antigenic pieces, causing them to proliferate and launch a powerful highly specific assault on the pathogen.

Lipopolysaccharide (LPS) is a cell-wall component of gram-negative bacteria. It acts as an endotoxin and stimulates a powerful immune response through activation of TLR4. TLR4 is crucial for effective responses to LPS (Poltorak et al., 1998). In humans, exposure to LPS causes fever and can lead to septic shock-a deadly vascular shutdown triggered by overwheleming destructive actions of immune cells. LPS induces this inflammatory response in part by prompting macrophages and DCs to release cytokines.

[1.12.2] Adaptive immune system

Adaptive immunity provides the immune system with a memory component and works in tandem with the innate response. The innate system produces cytokines that not only induce inflammation but also recruit and activate the B and T cells that participate in the adaptive response. B cells make antibodies that latch onto specific antigens on the surface of the invading pathogen and T cells have receptors able to recognize pathogen-derived fragments of proteins. This is called the adaptive response because over the course of an infection, it adjusts to optimally handle the particular microorganism responsible for the disease.

The major functions of the adaptive immune system include:

- The recognition of specific "non-self" antigens in the presence of "self", during the process of antigen presentation.
- The generation of responses that are adapted to maximally eliminate specific pathogens or pathogen infected cells.

- The development of immunological memory, in which each pathogen is "remembered" by a signature antibody. These memory cells can be called upon to quickly eliminate a pathogen should subsequent infections occur.

B and T lymphocytes are the main cellular components of the adaptive system. B cells play a major role in the humoral immune response, whereas T cells are closely involved in cell-mediated immune responses. Activated B cells secrete antibody molecules that bind to antigens and destroy the invader directly or mark it for attack (Lebien & Tedder, 2002). T cells recognise antigens displayed on cells. Some T cells help to activate B cells and other T cells; other T cells directly attack infected cells (Rodriguez-Pinto, 2005). When an infection is removed these memory B and T cells persist, priming the body to ward off subsequent attacks.

[1.13.1] B cells

The lymphocytes in the adaptive system are known as T (thymus-derived) and B (bursal or bone marrow-derived) lymphocytes. B lymphocytes (B cells) are a population of cells that express clonally diverse cell surface immunoglobulin (Ig) receptors recognizing specific antigenic epitopes. The development of mammalian B cells involves several stages that begin in primary lymphoid tissue (e.g. human foetal liver and foetal/adult marrow), followed by their maturation in secondary lyphoid tissue (e.g. human lymph nodes and spleen). The functional purpose of B cells is to develop into antibody producing terminally differentiated plasma cells.

[1.13.2] T cells

The antigen-receptor complex expressed by T cells is composed of the T cell receptor (TCR) and CD3. Signalling by the TCR-CD3 complex is iniated by the recognition of peptide antigen in the context of MHC molecules on APCs. Most T-lymphocytes express TCRs on the cell surface comprised of α and β chains, while a small subset express γ and

δ chains (called γδ-T cells). These two T cell populations develop in the thymus. The αβ T cells are comprised of two populations: the cytotoxic $CD8^+$ T cells resposible for killing infected cells and T helper (Th) cells expressing CD4 on their cell surface. $CD4^+$ T cells recognise their antigen in the presence of MHC class II molecules while $CD8^+$ T cells recognise their antigen in association with MHC class I.

[1.13.2 (a)] $CD4^+$ Th cells

$CD4^+$ T cells play a central role in the defense against pathogens through their actions on cells of both the innate and adaptive immune systems. The cells play roles in promoting the production of antibodies by B cells, stimulate macrophages to develop enhanced microbe-killing activity and recruit neutrophils, eosinophils and basophils to sites of infection and inflammation. Many of these effects are mediated by the production of cytokines and chemokines. Regulatory T cells (T_{reg}) are a specialized subpopulation of T cells that act to suppress activation of the immune system and thereby maintain immune system homeostasis and tolerance to self-antigens.

[1.13.2 (b)] $CD8^+$ T cells

Cytotoxic T cells are capable of inducing the death of infected or tumor cells; they kill cells that are infected with viruses (or other pathogens), or are otherwise damaged or dysfunctional. Most cytotoxic T cells express T-cell receptors (TCRs) that can recognize a specific antigenic peptide bound to Class I MHC molecules, present on all nucleated cells, and a glycoprotein called CD8, which is attracted to non-variable portions of the Class I MHC molecule. The affinity between CD8 and the MHC molecule keeps the T_C cell and the target cell bound closely together during antigen-specific activation.

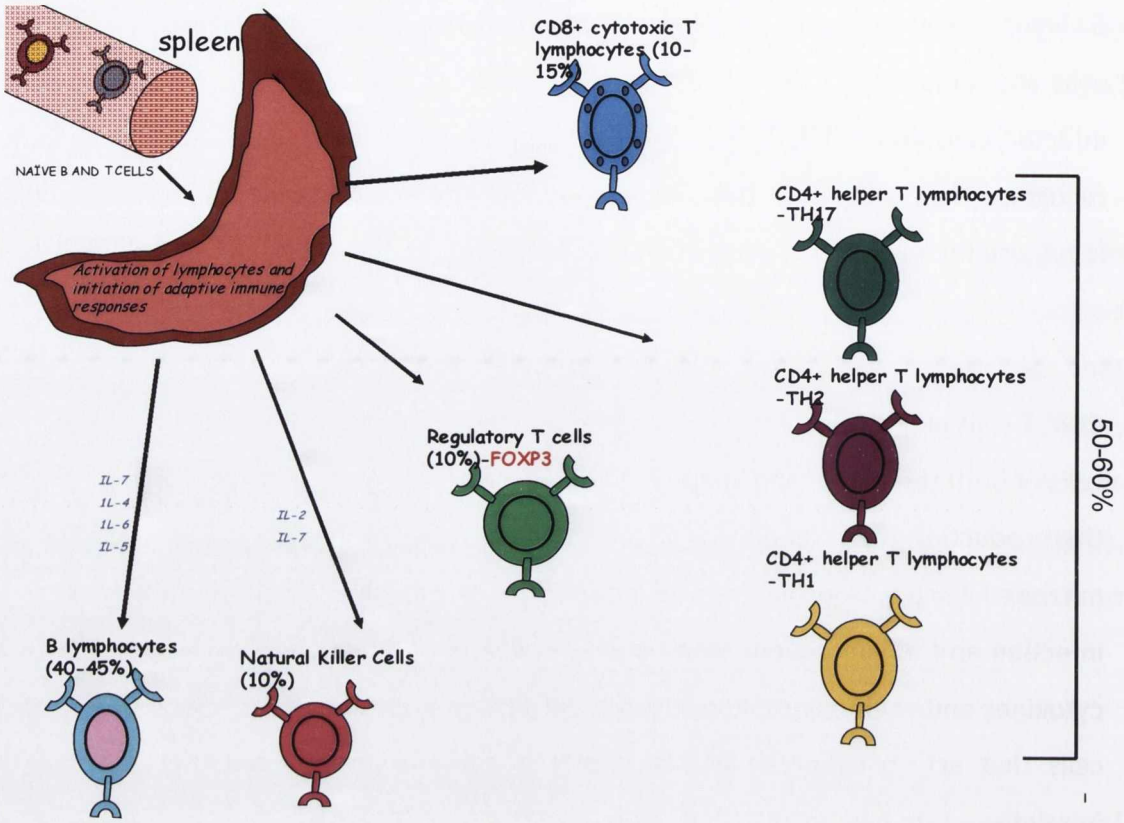

Figure 1.12 T cells in the spleen

The spleen is an immunologic filter of the blood. It is made up of B cells, T cells, macrophages, dendritic cells, natural killer cells and red blood cells. T cells make up about 30% of all spleen cells. The diagram above shows the (%) of each T cell subset (of total T cells)

Chapter 2

Materials and Methods

[2.1] Materials

[2.1] List of Materials used

12 well slides	Medical Supply Company
Aponexin FITC Apoptosis Kit	Millipore
ApoSensor ATP assay kit	BioVision
BSA	Sigma
Caspase-glo 3/7 Assay	Promega
CD4- FITC	BD Biosciences
CD8- R-PE	BD Biosciences
Cycloheximide	Sigma
ECL Western Blotting Reagents	Amersham
Fix and Perm Cell Permeabilization Kit	Invitrogen
Foetal bovine serum	Sigma
Folins-Cioctleau Phenol Reagent	Merck
Hanks Buffered Salt Solution	Sigma
L-glutamine	Sigma
LPS	Alexis Biochemicals
Methylamine	Sigma
PDVF membrane	Millipore
Phytohaemagglutinin	Sigma
Poly-*l*-lysine	Sigma
Propyl-*n*-gallate	Sigma
Protein markers	New England Biolabs
Protogel	National Diagnostics
RPMI-1640	BioSera
Scion Imaging Software	Scion

[2.1.2] Addresses of Suppliers

Biochemical reagents and chemicals used were of analytical grade where possible and were obtained from;

Sigma Chemical Co. Ltd, Fancy Rd., Poole, Dorset, U.K.

BD Biosciences, The Danby Building, Edmund Halley Road, Oxford Science Park, Oxford, OX4 4DQ, U.K.

Jackson Immunoresearch c/o Stratech Scienfic Limited , Unit 7, Acorn Business Center, Oaks Drive, Newmarket, Suffolk, CB8 7SY England.

MERCK BIOSCIENCES LTD., Boulevard Industrial Park, Padge Road, Beeston Nottingham NG9 2JR, UNITED KINGDOM also BDH and Calbiochem and Oncogene

Molecular Probes, 29851 Willow Creek Road, Eugene, OR 97402

Fluka C/O Sigma

Medical Supply Company Ltd., Damastown, Mulhuddart, Dublin 15, Ireland.

[2.2] Methods

[2.2.1] Animals

Source: Wistar Rats were bred and obtained from the Bioresources Unit, Department of Biochemistry, Trinity College Dublin. All animals were kept at room temperature and

allowed free access to rat laboratory chow and water.

UCP 1 knock out mice on a C57BL/6 background, originally provided by Dr. Leslie Kozak (Pennington Biomedical Research Center, Baton Rouge, Louisiana, US) were bred in-house. UCP 1 $^{-/-}$ mice were confirmed to be homozygous by PCR genotyping of tail DNA. All animals were housed in a specific pathogen-free facility and fed ad-libitum. The background of the UCP 1 knock-out mice is essentially congenic with C57 (Hofmann *et al.,* 2001). All animals were killed by cervical dislocation.

[2.2.1.1] LPS/PHA treatment of animals

50 µg of LPS or 100µg PHA dissolved in 200µl PBS or a similar volume of PBS alone was administered to mice by i.p. injection. Three days after injection, animals were killed by cervical dislocation. Thymuses, spleens, brown adipose tissue and livers were harvested and weighed, and mitochondria were isolated from the tissues. Six week old female mice were used unless otherwise stated.

[2.2.2] Mitochondrial isolations:

[2.2.3.1]: Isolation of Brown Adipose Tissue Mitochondria

BAT was prepared by the method of Scarpace *et al.* (1991). BAT was removed from the interscapular region of the rat between the head and shoulder blades. BAT was then placed into a pre-weighed 50 ml beaker containing 30 mls of ice-cold (0-4^{0}C) STE buffer (250 mM Sucrose, 5 mM Trizma-base, 1 mM EGTA, pH 7.4). BAT was weighed and washed several times with STE buffer. BAT was chopped carefully in a beaker and poured into a Potter homogeniser tube to a final volume of about 20 mls. The tissue was then homogenized by hand with four passes using a pestle of 0.26 inch (loose) clearance, followed by homogenization by hand with 6 passes using a pestle of 0.12 inch (tight) clearance. The homogenate was then filtered through 4 layers of muslin and the filtrate

was centrifuged at 8,600 x *g* for 10 minutes at 4^{0}C. The supernatant was discarded and the sides of the centrifuge tubes were wiped with tissue to remove any fat deposits. The pellet was resuspended using a cold-finger (a loose-fitting test-tube filled with ice), that had been suspended in STE buffer, and centrifuged at 750 x *g* for 10 minutes at 4^{0}C. The pellet was discarded and the supernatant was centrifuged at 8,600 x *g* for 10 minutes. The pellet was resuspended in STE buffer with the addition of 2% (w/v) de-fatted BSA using a cold finger that had previously been suspended in STE buffer (containing fatty-acid free BSA) and centrifuged at 8,600 x *g* for 10 minutes. The pellet was then resuspended in STE buffer and centrifuged as above. The resulting mitochondrial pellet was resuspended gently and thoroughly using a cold-finger with 0.05 ml of STE buffer per weight (gram) of original tissue and frozen at -20^{0}C.

[2.2.2.2] Isolation of Liver and Spleen Mitochondria

Mitochondria were prepared essentially by the method of Chappell and Hansford, (1972). Tissues were removed, trimmed of connective tissue and fat and placed into a pre-weighed beaker containing 50 mls of ice-cold (0-4^{0}C) STE buffer (250 mM Sucrose, 5 mM Trizma-base, 2 mM EGTA, pH 7.4). Tissues were weighed, chopped finely using a scissors and washed several times with ice-cold STE buffer. The tissues were poured into a Potter homogenizer tube to a final volume of about 40 mls. The tissues were then homogenized by hand, with 4 passes using a pestle of 0.26 inch (loose) clearance followed by homogenization by hand with 6 passes using a pestle of 0.12 inch (tight) clearance. The homogenates were centrifuged at 800 x *g* for 3 minutes at 4^{0}C, pelleting blood and debris. The pellets were discarded and the supernatants were centrifuged at 12,000 x *g* for 10 minutes at 4^{0}C yielding a "mitochondrial" pellet. The supernatants were discarded and the pellets were resuspended in ~25 mls of STE buffer (± 2% (w/v) de-fatted BSA) and re-centrifuged at 12,000 x *g* for 10 minutes at 4^{0}C The pellets were resuspended in STE buffer and centrifuged as above. The resulting pellets containing the mitochondrial fraction were resuspended in STE buffer to the desired concentration and frozen at -20^{o}C.

[2.2.2.3] Isolation of thymus mitochondria

Thymus mitochondria were prepared essentially by the method of Chappell and Hansford (1972). Any BAT present in the vicinity of the thymus was clearly visible and distinguishable from the thymus and was removed prior to removal of the thymus. The thymus was removed from the abdominal cavity, trimmed of connective tissue and fat and placed into a beaker containing ice-cold (0-4^{0}C) STE buffer (250 mM Sucrose, 5 mM Trizma-base, 2 mM EGTA, pH 7.4). The thymus was weighed, chopped finely using a scissors and washed several times with ice-cold STE buffer. The tissue was poured into a Potter homogenizer tube to a final volume of about 40 mls. The tissue was then homogenized by hand, with 4 passes using a pestle of 0.26 inch (loose) clearance followed by homogenization by hand with 6 passes using a pestle of 0.12 inch (tight) clearance. The homogenate was centrifuged at 800 x *g* for 3 minutes at 4^{0}C, pelleting blood and debris. The pellet was discarded and the supernatant was centrifuged at 12,000 x *g* for 10 minutes at 4^{0}C yielding a "mitochondrial" pellet. The supernatant was discarded and the pellet was resuspended in STE buffer and re-centrifuged at 12,000 x *g* for 10 minutes at 4^{0}C The pellet was resuspended in buffer and centrifuged as above. The resulting pellet containing the mitochondrial fraction was resuspended in STE buffer to the desired concentration and frozen at -20^{o}C.

[2.2.2.4] Isolation of Thymus and Bone Marrow Cell Mitochondria

All spleen cell homogenate, red cells, monocytes, lymphocytes and thymus cells (thymocytes) fractions were spun at 300 x *g* for 5 minutes at 4^{o}C. The supernatants were discarded and all cellular fractions were resuspended in ice-cold (0-4^{0}C) STE buffer (250 mM Sucrose, 5 mM Trizma-base, 2 mM EGTA, pH 7.4). The cell suspensions were poured into a 2 ml Potter homogenizer tube to a final volume of about 1.5 mls. The cellular suspensions were then homogenized by hand, with 6 passes using a pestle of 0.12 inch (tight) clearance. The cell homogenates were centrifuged at 800 x *g* for 3 minutes at 4^{0}C. The pellets were discarded and the supernatants were centrifuged at 12,000 x *g* for 10

minutes at 4^0C yielding a "mitochondrial" pellet. The supernatants were discarded and the pellets were resuspended in STE buffer and re-centrifuged at 12,000 x *g* for 10 minutes at 4^0C. The pellets were resuspended in buffer and centrifuged as above. The resulting pellets containing the mitochondrial fraction were resuspended in STE buffer to the desired concentration and stored at –20°C, prior to analysis.

[2.2.3] Mitochondrial protein determination using the Bicinchoninic Acid Assay

Quantification of protein concentrations in tissue samples was carried out using the Bicinchoninic Acid Assay described by Smith et al., 1985. All of the following solutions (standards or samples) were directly prepared in a 96-well plate. A standard protein solution of BSA was suitably diluted in deionised water from 0 to 0.25 $mg.ml^{-1}$. The amount of mitochondrial protein present in the samples was determined by reference to a standard curve derived from the above known concentrations of BSA. Isolated mitochondria were generally diluted in H_2O before analysis so the final concentration of the samples would fall within the range of the standard curve. Once the samples and the standards were prepared, 200µl of a working solution of BCA (1:49(v/v) BCA:Cu_2SO_4) was added to each well. The plate was then incubated for 30 minutes in an incubator set at 37°C. The absorbance of each sample was measured spectrophotometrically at 550nm.

[2.2.4] SDS PAGE Electrophoresis

Sodium dodecyl sulphate-polyacrylamide gel electrophoresis (SDS-PAGE) was performed by the method of Laemmli (1970), using a Mini-PROTEAN® 3 CELL (Bio-Rad) with a 5% stacking and a 12% resolving gel. Components of a 12% resolving gel are as follows: water (3.35 ml), 1.5 M Tris-HCl, pH 8.8 (2.5 ml), 10% (w/v) SDS (100 µl), Protogel™ (ultra-pure 30% (w/v) acrylamide and 0.8% (v/v) bisacrylamide solution; National Diagnostics; 4.0 ml), TEMED (5 µl) and 10% (w/v) ammonium persulphate (50 µl). The stacking gel (5%) was prepared with water (6.1 ml), 0.5 M Tris-HCl, pH 6.8 (2.5 ml), 10%

(w/v) SDS (100 µl), Protogel™ (ultra-pure 30% (w/v) acrylamide and 0.8% (v/v) bisacrylamide solution; National Diagnostics; 1.33 ml), TEMED (10 µl) and 10% (w/v) ammonium persulphate (50 µl).

Prestained molecular weight marker standards (provided by New England Biolabs) were used. The prestained markers used were *E.coli* MBP-β-galactosidase (175 kDa), *E.coli* MBP-paramyosin (83 kDa), bovine liver glutamic dehydrogenase (62 kDa), rabbit muscle aldolase (47.5 kDa), rabbit muscle triosephosphate isomerase (32.5 kDa), bovine milk β-lactoglobulin A (25 kDa), chicken egg white lysozyme (16.5 kDa) and bovine lung aprotinin (6.5 kDa).

The sample buffer was made up as 4 X strength. Components of the sample buffer are as follows: water (3.8 ml), 0.5 M Tris-HCl, pH 6.8 (1.0 ml), glycerol (0.8 ml), 10% (w/v) SDS (1.6 ml) and 1% (w/v) Bromophenol blue (0.4 ml). 5% β-mercaptoethanol (v/v) was added to the sample buffer immediately prior to use. The sample buffer was added to the mitochondrial protein so that the final concentration of sample buffer was 1 X. Once the sample buffer and mitochondrial protein were added together, the samples were vortexed briefly and boiled for 5 minutes on a heating block set to 100°C. The samples were then pulsed in a bench top centrifuge, loaded into separate wells and electrophoresed at a constant current (200 V) for 45 minutes, until the tracker dye reached the bottom of the resolving gel. A glycine-based running buffer (0.38 M glycine, 0.05 M Tris, 0.1% (w/v) SDS) was used for electrophoresis. Gels were then prepared for Western Blotting.

[2.2.5] Immunodetection

Following SDS-PAGE, resolved proteins were transferred onto polyvinylidene difluoride (PVDF) membranes (Immobilon-P^{SQ}; Millipore). Transfer was achieved using a semi-dry transfer apparatus (Hoeffer) at 110 mA for 2 hours. Firstly, the stacking gel was removed and gels were rinsed briefly in semi-dry transfer buffer (0.192 M glycine, 0.025 M Tris-HCl, pH 8.3, 0.013 M SDS, 15% (v/v) methanol) and carefully arranged in the semi-dry transfer apparatus as directed by the manufacturers. After transfer was complete,

blotted proteins on the PVDF membrane were directly incubated in Ponceau S solution (0.25% (w/v) Ponceau S, in 3% (v/v) trichloroacetic acid) and washed gently with distilled water. The blot was then washed in phosphate-buffered saline (PBS) (0.14 M NaCl, 2.7 mM KCl, 11.5 mM Na_2PO_4, 1.8 mM KH_2PO_4, pH 7.4). Blocking of the membrane was performed by incubating the blot in PWB (PBS containing 0.1% (w/v) Tween 20) containing 5% (w/v) Marvel milk powder at room temperature for 1 hour or overnight at 4°C. This blocking was followed by 3 X 10 minute washes using PWB.

Blots were then incubated in primary antibody (in PWB containing 5% (w/v) Marvel milk powder) overnight at 4°C or at room temperature for 1 hour containing a 1:1,000 dilution of an affinity-purified anti-UCP 1, a 1,1000 dilution of a commercial anti-UCP 1 (Calbiochem), a 1:1,000 dilution of a peptide antibody to pyruvate dehydrogenase (PDH; Cambridge Biosciences). Following this primary antibody incubation, the blots were washed for 3 X 10 minute in PWB. The blots were then incubated with a horse-radish peroxidase (HRP) conjugated goat anti-rabbit secondary antibody (1:10,000 dilution) in PWB containing 5% Marvel milk powder for 1 hour at room temperature. Following this, blots were further washed for 3 X 10 minute in PWB. Blots were developed using an enhanced chemiluminescence (ECL) detection system (Amersham-Pharmacia) for detecting horse-radish peroxidase labeled antibody, by means of the HRP catalyzed oxidation of luminol under alkaline conditions and the results were visualized by exposure to Kodak X-Omat LS film.

[2.2.6] Coomasie Blue G-250 staining of SDS-PAGE gels

Following SDS-PAGE, the Laemilli gels were stained using Coomassie blue G250 according to the method of Laemilli (1970) so as to ensure all the protein was transferred to the membranes successfully. Laemilli gels were stained using 0.5% (w/v) Coomassie Blue G250 in 50% (v/v) methanol, 10% (v/v) acetic acid for 30 minutes on a shaking platform. The Coomasie Blue R stain was then discarded and the gels were destained on a shaking platform for 30 minutes using a 50% (v/v) methanol and 10% (v/v) acetic acid.

[2.2.7] Densitometry

Following Western blot analysis, the relative abundance to UCP 1 was determined using densitometry. The band intensities of the exposed film were analyzed using Scion Imaging Software.

[2.3] Immunofluorescence Studies

[2.3.1] Isolation of thymocytes for confocal microscopy

The thymus was removed from the abdominal cavity, trimmed of any brown fat and connective tissue and placed in a beaker containing ice-cold Hanks Solution (10% F.C.S.). The thymus and medium were poured onto a nylon mesh (tea strainer will suffice) in a petri dish and using a plunger of a 5ml syringe, the thymus was gently ground until a fine suspension of thymocytes were obtained.

[2.3.2] Cell Counting

The cell density of each stock suspension was determined by counting samples which had been diluted 1:1000 in PBS, pH 7.5, using a Neubauer haemocytometer with a silvered stage and a Zeiss light microscope.

[2.3.3] Preparation of poly-*l* -lysine coverslips/slides

Poly-l-lysine (0.1% w/v) was prepared and stored in fridge for up to a month. 10mls of poly-l-lysine was added to 90mls of deionised water. Coverslips/glass slides were immersed in the poly-l-lysine solution for 5 minutes, removed and allowed to dry.

[2.3.4] Preparation of paraformaldehyde

Paraformaldehyde (6% w/v) was freshly prepared on the day of the experiment or frozen in portions at -20^{0}C . The required weight of paraformaldehyde was added to 5 volumes of distilled ionised water. The insoluble paraformaldehyde was then titrated

with NaOH (5 M) and stirred vigoursly until the paraformaldehyde was fully dissolved. 10 volumes of PBS were then added to the fixative. HCl (12 M) was then added to the fixative until the pH of the solution reached 7.5. Sufficient distilled deionised water was added to bring the solution to the required concentration.

[2.3.5] Mitotracker Red Staining

Thymocytes were isolated for confocal microscopy and were incubated in 80nM prewarmed Mitotracker Red (diluted in Hanks and 10% FCS) for 60 minutes at 37%. Cells were then fixed as normal.

[2.3.6] Preparation of anti-quench

The anti-oxidant n-propyl gallate (4%) was dissolved in PBS buffer containing sodium azide (15 mM) and glycerol (50% w/v).0.1ug/ml of Hoechst was also added. This solution was always made fresh on the day and stored at 4° C in the dark until required.

[2.3.7] Indirect Immunofluorescence

Isolated thymocytes from thymuses were suspended in Hanks medium (and 10% FCS). 0.5% paraformaldehyde was added to 1ml of thymocytes and incubated on ice for 5 minutes. 20µl of cells were added to the slides (poly-*l*-lysine coated) and allowed to dry (phosphate crystals form). Slides were then dipped in methanol at -20°C for 5 minutes. Slides were then dipped in acetone at -20°C for 5 minutes. Slides were then allowed to dry at room temperature.

The cells on the coverslips were then incubated with blocking buffer (PBS containing 5% BSA and methylamine, 0.1M) for 2 hours at room temperature in Petri dishes, to inactivate any remaining formaldehyde and block non specific binding. The cells on the coverslips were incubated with primary antibody diluted in PBS containing 5 %(w/v) BSA overnight at room temperature. Following washing with PBS the cells on the coverslips were incubated with the secondary antibody conjugated to a fluor diluted with PBS for 3 h at room temperature. The cells on the coverslips were then washed

with PBS (and sodium azide) and finally mounted onto glass slides using 5ul of anti-quench solution.

[2.3.8] Confocal microscopy

The 12 well plates with antiquench solution were covered with coverslips and were affixed to the glass slide by applying a thin film of nail varnish to the edges of the coverslip. This procedure also prevented the samples from drying out. The slides were examined by phase contrast and confocal microscopy with an Olympus Fluoview FV1000 Imaging system. The excitation light for imaging was provided by the 457-514 nm lines of a multi-line Argon laser, the 543nm line of a Green Helium - Neon laser and the 633 nm line of a red helium-Neon laser. Images were collected and processed with the Olympus Fluoview software (version 1.3c).

[2.4] Flow Cytometry & Luminescence Assays

[2.4.1] Isolation of Thymus cells (Thymocytes)

Thymocytes were isolated from the thymus as described by Buttgereit *et al.* (1994). An illustration depicting the method used to isolate thymus cells is shown in Figure 2.4.1. The thymus was removed from the rat, trimmed clean of connective tissue and brown fat and transferred to RMPI-1640 medium containing 10% foetal calf serum (FCS) and L-glutamine. The thymus and medium were poured onto a nylon mesh (tea-strainer will suffice) in a petri dish and, using a plunger of a 5 ml syringe, the thymus was disaggregated into a suspension of thymus cells. This thymus suspension was transferred to a 15ml centrifuge tube, using a Pasteur pipette, and allowed to stand for 10 minutes at room temperature, thus ensuring that debris and cell clumps settle to the bottom of the centrifuge tube. The thymus cells (thymocytes) in the supernatant were aspirated off and transferred to a fresh 15 ml centrifuge tube. The thymus cells were centrifuged at 300 x *g* for 5 minutes in a bench-top centrifuge. Any fat droplets present on the surface of the supernatant were removed. Similarly, the supernatant was

discarded and the thymocyte pellet was resuspended in RMPI-1640 (10% FCS, L-Glutamine), labeled and aliquoted for Western blot analysis, cell lysates or flow cytometry. Prior to Western blot analysis, thymocytes were centrifuged at 300 x *g* for 5 minutes, and washed twice in phosphate buffered saline (PBS) prior to mitochondrial isolation.

[2.4.2] Isolation of Spleen cells

Spleen cells were isolated according to the method of Mills *et al.* (1996). An illustration depicting the method used to isolate spleen cells is shown in Figure 2.4. Spleen(s) were removed from the abdominal cavity, trimmed free of connective tissue and transferred to a RMPI-1640 medium containing 10% foetal calf serum (FCS) and L-glutamine. The spleen(s) and medium were poured onto a nylon mesh (tea-strainer will suffice) in a petri dish and, using a plunger of a 5 ml syringe, the spleen(s) were grounded until a fine suspension of spleen cells were obtained. This spleen suspension was transferred to a 15 ml centrifuge tube and allowed to stand for 10 minutes at room temperature, thus ensuring that debris and cell clumps settle to the bottom of the centrifuge tube. The spleen cells in the supernatant were aspirated off and transferred to a fresh 15 ml centrifuge tube. The spleen cells were centrifuged at 300 x *g* for 5 minutes in a bench-top centrifuge. The pellet was re-suspended in RPMI-1640 containing 10% FBS and L-glutamine. 2 mls of this resuspended pellet was labeled (spleen cell homogenate) and aliquoted for western blot analysis, cell lysates or flow cytometry.

[2.4.3] Isolation of bone marrow cells

Femurs and tibiae were removed from rats and dissected from the surrounding muscle and fatty tissue. The ends of the bones were cut until the bone marrow was visible. The bone marrow was obtained from the femurs and tibiae by insertion of a sterile 27G needle attached to a syringe containing complete RPMI-1640 (warmed to 37ºC). On insertion of the needle into the bone, the plunger was pushed down and the bone marrow was flushed out onto a petri dish. Cells were then centifuged at 1200rpm for 5

minute at 4ºC. Cells were then analysed by flow cytometry or mitochondria was isolated for blots.

[2.4.4] Thymocyte incubations/ Induction of Apoptosis

Thymocytes were isolated as previously described. Thymocytes were seeded in RPMI-1640 medium supplemented with 10% heat-inactivated FBS, 2µM glutamine , penicillin (100U/ml) and streptomycin (100µg/ml) in the presence or absence (just vehicle) of 0.1 µM dexamethasone for up to six hours in a 37° C humidified incubator under an atmosphere of 5% CO_2 .

[2.4.5] FITC-Annexin V /PI Staining

The apoptosis of isolated thymocytes treated with dexamethasone, was examined. To determine early membrane and DNA changes, whole thymocytes were stained with FITC-conjugated Annexin V and PI according to manufacturer's instructions (Millipore. Cells (.75 x 10^6) were suspended in 100µl of annexin-binding buffer, and 5µl of FITC-annexin V and 1µl of PI (100µg/ml) was added to each 100µl cell suspension. Cells were incubated for 15 minutes at room temperature. Stained cells were suspended in 400µl of binding buffer and immediately processed by flow cytometry.

[2.4.6] Flow Cytometry

Thymocytes/Splenocytes were washed and adjusted to 5x10^6/ml in PBSA (1%BSA-PBS) and 50µl used for each sample. Cells were incubated on ice for 15 minutes in the dark with the surface staining antibodies (FITC-CD4 and R-PE-CD8). Fixation medium (Caltag A; Invitrogen) was added to each tube, followed by incubation on ice for 15 minutes. Cells were washed (1500 rpm for 3 minutes) twice in PBSA, followed by resuspension with permeabilization medium (Caltag B: Invitrogen) and intracellular anti-UCP 1 or Cidea antibody for 15 minutes on ice in the dark. Cells were washed twice in PBSA, and resuspended in catlag B and Alexa 647 labelled secondary antibody, incubated on ice for

15 minutes, cells were washed twice and 30,000 events collected with a Dako CyanADP flow cytometer. Data was analysed using Flowjo Software.

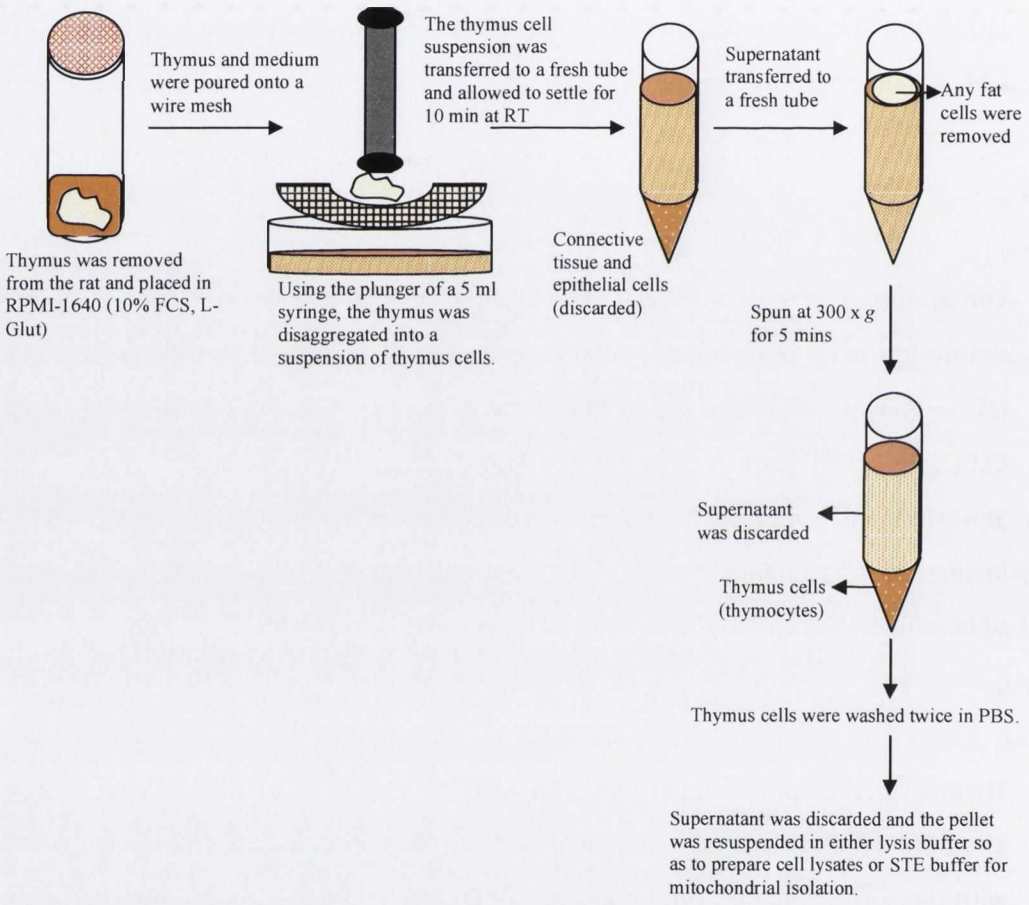

Figure 2.4.1: Schematic illustration of the method used to isolate thymus cells (thymocytes).

[2.4.7] Measurement of ATP and ADP levels

The ApoSENSOR ADP/ATP ratio assay kit (BioVision) utilizes the enzyme luciferase to catalyze the formation of light from ATP and luciferin, and the light can be measured using a luminometer. ADP level is measured by its conversion to ATP that is subsequently detected using the same reaction.Thymocytes from UCP 1 $^{-/-}$ mice and C57BL/6 mice were isolated and resuspended at $1x10^6$/ml in PBS. Triplicate cell samples (10 µl per well) were placed in a white walled 96 well luminometer plate. Nucleotide releasing buffer was then added to each well (100µl), to lyse the cells, and left at room temperature for 5 minutes. To measure the ATP levels in the thymocytes from UCP 1 $^{-/-}$ mice and C57BL/6 mice, 1µl of the ATP monitoring enzyme was added to the resulting lysates.

[2.4.8] Caspase 3/7 Activity

The Caspase-Glo 3/7 Assay (Promega) is a luminescent assay that measures caspase 3 and caspase 7 activities in suspension cells. This assay provides a proluminescent caspase 3/7 substrate, which contains the tetrapeptide sequence DEVD. The substrate is cleaved to release aminoluciferin, a substrate of luciferase used in the production of light. The addition of the single caspase glo 3/7 reagent results in cell lysis, followed by caspase cleavage of the substrate and generation of a luminescent signal. Thymocytes from UCP 1 $^{-/-}$ mice and C57BL/6 mice were isolated and induced into apoptosis (0.1µM dexamethasone) or with the vehicle for 5 hours at 37^{o} in 5% CO_2. After the incubation period, cells were resuspended at $2x10^6$ /ml in RPMI-1640. 100µl of caspase glo 3/7 reagent was added to each well of a white walled 96-well plate containing 100µl of control or drug treated thymocytes in RPMI-1640. Contents of the wells were gently mixed on a plate shaker for 30 seconds, and incubated at room temperature for 1 hour. The luminescence of each well was measured on a plate reading luminometer.

[2.5] DNA fragmentation

DNA electrophoresis was performed using 10^7 thymocytes incubated at 37° C in medium containing ethanol (vehicle) or 0.1μM dexamethasone-supplemented medium. Cells were harvested and resuspended in 1ml cell lysis buffer (20mM EDTA, 100mM Tris pH 8.0 0.8% (w/v) sodium lauryl sarcosinate) and incubated at 37° C for 1 hr. 0.5mg/ml RNAse was then added to each sample and left for a further 2h at 37° C. Finally the samples were treated with 6mg/ml proteinase K and left overnight at 37° C. An aliquot of each sample (45μl) was mixed with 5μl DNA loading dye and resolved on a 1% agarose gel in 0.4M Tris-acetate, 0.01M EDTA, pH 8.3 (TAE), pre-stained with ethidium bromide. DNA was electrophoresised at a constant voltage of 55V for 2 hours 30 mins.

[2.6] UCP 1 half-life

Thymocytes were isolated from mouse thymi by standard methods. Thymocytes were seeded at 2 x 10^6 cells/ml in fully supplemented RPMI-1640 medium, containing 10% heat-inactivated fetal bovine serum at 37° C /5% CO_2. Thymocytes were treated with 10μg/ml cycloheximide at time point zero to arrest protein translation. At various time points, they were pelleted by centrifugation. The resulting cell pellet was washed twice in ice cold PBS and lysed on ice for 30 mins with lysis buffer. Insoluble material was removed by centrifugation.

[2.7] Measurement of oxygen consumption rates of cells

All measurements of respiration rates were made using and Oxygraph-2K respirometer (Oroboros Instruments, Innsbruck, Austria), and oxygen was resolved using DATLAB software. The oxygraph-2k is a two chamber titration-injection respirometer with a limit of oxygen flux detection of 1p/mol/ml^{-1}. Standardized instrumental and chemical calibrations were performed to correct for back diffusion of oxygen into the chamber from the various components; leak from the exterior, oxygen consumption by the chemical medium and sensor oxygen consumption. The cell suspension was stirred using

a PDVF magnetic stirrer and thermostatically maintained at 37° C. Before each experiment, medium was equilibrated for 30-40 mins with air in the oxygraph chambers until a stable signal was achieved to calibrate for oxygen saturation. Quiescent thymocyte steady state oxygen consumption was measured, 1μg/ml oligomycin was added to determine proton leak and FCCP was titrated to reach the maximum uncoupled rate of respiration.

[2.8] LPS/PHA Treatment of Isolated thymocytes

1 X 10^6 /ml thymocytes were placed in RPMI-1640 medium containing 10% FCS and stimulated with LPS (1μg/ml) or phytohemagglutinin (10μg/ml) for 24 hours. After 24 hours, thymocytes were pelleted by centrifugation, and lysed using lysis buffer, for 30 minutes on ice. Lysates were cleared of cellular debris by centrifugation at 14000rpm at 4 °C for 20 mins. Protein concentration was determined by using the BCA protein assay. Fifty micrograms of protein was separated on SDS-PAGE, and Western blotted as described. Antibodies were used at the following dilutions: anti-UCP 1 (1:1000) and horseradish peroxidise-conjugated goat anti-rabbit secondary antibody (1:10000).

[2.9] Antibodies and fluorescent dyes used

[2.9.1] Primary Antibodies

Anti-UCP 1 (Calbiochem/Sigma) (Figure 2.5)

Host: Rabbit

Isotype: IgG

Immunogen: a synthetic peptide [(C)SHLHGIKPRYTGTYN] corresponding to amino acids 145-159 of mouse UCP 1

Dilution used for confocal microscope: 1:50

Immunodetection : 1:1000

Flow cytometry : 1:50

Anti-Thy 1 (Molecular Probes) conjugated to FITC

Host: Rat

Isotype : IgG1

Immunogen: Mouse

Dilution used for confocal microscope: 1:100

Anti-Thy 1 (Abcam)

Host: Rat

Isotype: IGg1

Immunogen: Mouse

Dilution used for confocal microscope: 1:100

Flow cytometry 1:50

Anti PDH (Cambridge Biosciences)

Host: Mouse

Isotype: IGg1

Immunogen: Human

Dilution used for Immunodetection: 1:1000

R-PE- Conjugated CD8 (BD Biosciences)

Host: Rat

Isotype: IGg2

Immunogen: Mouse

Dilution for flow cytometry: 1:50

FITC- Conjugated CD4 (BD Biosciences)

Host: Rat

Isotype: IGg2

Immunogen: Mouse

Dilution for flow cytometry: 1:50

Anti –β-actin (Sigma)

Host: mouse

Isotype: IGg

Immunogen: raised against 16 amino acids near amino terminus of human β-actin

Dilution for Immunodetection: 1:4000

Anti- Full-length UCP 1 (gift from Daniel Ricquier)

Host: Sheep

Isotype: IGg

Immunogen: mouse UCP 1

Dilution for Immunodetection: 1:10000

[2.9.2] Secondary Antibodies

Alexa Fluor 488 donkey anti—rabbit IgG (Invitrogen)

Confocal microscopy 1:1000 dilution

Alexa Fluor 488 goat anti -mouse IgG1 (Invitrogen)

Confocal microscopy 1:1000 dilution

Flow cytometry 1:100 dilution

Alexa Fluor 647 goat anti-rabbit IgG (Invitrogen)

Confocal microscopy 1:1000 dilution

Flow Cytometry 1:100 dilution

Cy5 Goat Anti-Rabbit IgG (Jackson Immunoresearch)

Confocal microscopy 1:250 dilution

Cy3 Donkey Anti-Sheep IgG (H+L) (Jackson Immunoresearch)

Confocal microscopy 1:1000 dilution

[2.9.3] Mitochondria & DNA Stains

Hoechst 33342 (Molecular Probes)

Hoechst 33342 is part of a family of fluorescent stains for labeling DNA in fluorescence microscopy. Because these fluorescence stains for label DNA, they are also commonly used to visualize nuclei. Excited by ultraviolet light at around 350nm, they emit blue

fluorescence light around an emission maximum at 461nm. The Hoechst stains may be used on fixed cells.

Dilution used 1:100,000

M7512 Mitotracker Red (Molecular Probes)

MitoTracker probes are cell-permeant mitochondrion-selective dyes that contain a mildly thiol-reactive chloromethyl moiety. The chloromethyl group appears to be responsible for keeping the dye associated with the mitochondria after fixation. To label mitochondria, cells are simply incubated in submicromolar dilution s of the MitoTracker probe, which passively diffuses across the plasma membrane and accumulates in active mitochondria. Once their mitochondria are labeled, the cells can be treated with aldehyde-based fixatives to allow further processing of the sample;

Dilution Used: 80 Nm Mitotracker Red

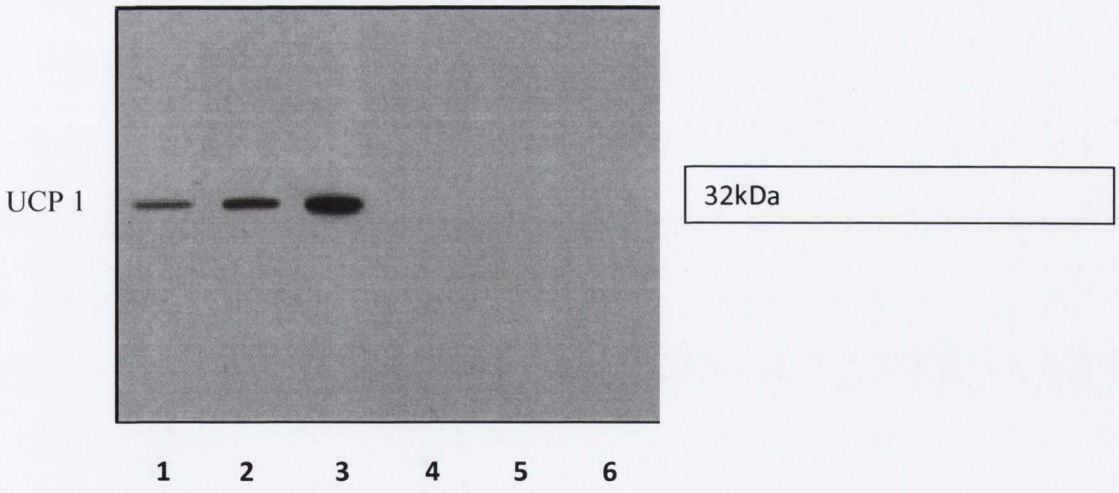

Figure 2.5 Specificity of Commercial UCP 1 peptide antibody (Sigma)

1 10µg wild-type thymus mitochondria
2 20µg wild-type thymus mitochondria
3 30µg wild-type thymus mitochondria
4 10µg knock-out thymus mitochondria
5 20µg knock-out thymus mitochondria
6 30µg knock-out thymus mitochondria

Chapter 3 - Mitochondrial UCP 1 in thymus

[3.1] Introduction

Until recently, mitochondrial uncoupling protein 1 has only ever been associated with brown adipose tissue (Nicholls & Locke, 1984, Ricquier & Bouillaud, 2000, Cannon & Nedergaard, 2004), where it uncouples mitochondria, resulting in the production of heat in a process called non-shivering thermogenesis.

However, extensive direct empirical evidence for the detection of UCP 1 in thymocytes was recently demonstrated in our laboratory (Carroll *et al.*, 2004, Carroll *et al.*, 2005, Porter, 2006). The thymus is the site of T-helper and cytotoxic T cell maturation (Ritter & Crispe, 1992). The thymus is involved in determining self from non-self and its size and activity is greatest in younger mammals. Evidence from Carroll et al. ,(2005) for the evidence of UCP 1 in thymus mitochondria includes (i) reverse transcriptase-polymerase chain reaction detection of RNA transcripts for UCP 1 in whole thymus and in isolated thymocytes of rats and mice (isolated thymocytes were not contaminated with brown adipocytes , but contained > 99% Thy-1(CD90) positive lymphocytes as identified by FACS analysis) , (ii) peptide antibodies specific for UCP 1, detected protein of appropriate molecular mass in mitochondria isolated from whole thymus and thymocytes of rats and mice, but not in thymus mitochondria from UCP 1 knock-out mice and (iii) UCP 1 was purified from thymus mitochondria and identified by mass spectrometry.

Interestingly, Frontini *et al.* (2007) have recently produced histological images of UCP 1 detection associated with BAT in the vicinity of thymus tissue from mouse/rat. These authors suggest that any detection of UCP 1 in thymus in solely due to associated BAT. It is also noteworthy that, reports of UCP 1 expression in uterine longitudinal smooth muscle cells by Nibbelink et al., (2001) were later refuted by Rousset at al. (2003), as being due to UCP 2. Recently, Mori et al., (2008), reported UCP 1 expression in human skin, with immunohistochemistry, placing UCP 1 in the granular layer of the epidermis, sweat glands, hair follicles and sebaceous glands of various sites in the human body. Of course these latter observations require further scrutiny.

The initial objective of this investigation was to build upon the aforementioned empirical evidence for the existence of UCP 1 in thymocytes in our laboratory and to provide a definitive visual image of UCP 1 in thymocytes, paving the way for investigations into the role of UCP 1 in the thymus. To that end we investigated whether we could visualize UCP 1 expression in thymocytes from another species, namely rat.

As there are data refuting the existence of UCP 1 in thymus, we addressed discrepancies in these studies. Using an antibody to full-length UCP 1, Frontini et al. (2007) have produced histological images of protein detection which they describe as BAT in the vicinity of thymus tissue from mouse and rat. These authors suggest that any detection of UCP 1 in thymus is solely due to associated BAT. Thus we assessed the sensitivity of the antibody to full length UCP 1, as used by Frontini et al., relative to the antibody raised against a UCP 1 peptide used in our previous studies (Carroll *et al.*, 2006, Adams *et al.*, 2007).

Since the thymus is most active up to puberty, we investigated if this had any effect on UCP 1 protein expression in thymus mitochondria, and if UCP 1 was present in all thymocyte subsets present. The half-life of UCP 1 in the thymus was also investigated as this might help pave the way for investigations into the function of UCP 1 in the thymus.

In addition we also looked at the level of expression of the *C*ell death *I*nducing *D*NA fragmentation factor (DFF), alpha subunit-like *E*ffector *A* (CIDEA) in wild-type and UCP 1 knock-out mice. Zhou et al. (2003) have proposed a role for CIDEA in directly regulating UCP 1 in BAT. CIDEA has been shown to activate apoptosis. This activation of apoptosis is inhibited by the DNA fragmentation factor DFF45. Mice that lack functional CIDEA have higher metabolic rates, higher lipolysis in brown adipose tissue and higher core body temperatures when subjected to cold. Consequently, we set out to determine whether native CIDEA expression was affected by UCP 1 expression in mouse thymocytes.

[3.2] Results

The first challenge was to identify thymocytes from the various different cells present in the thymic environment including epithelial cells, macrophages, dendritic cells and red blood cells from surrounding vessels (Ushiki, 1986).Using a Neubauer haemocytometer to count the cells in the thymus, it was observed that a rat thymus contains approximately 250 million cells. Flow cytometry analysis has confirmed that >99% of cells in a resulting thymocyte suspension from rats, and also mice, were positive for the thymocyte specific marker, Thy 1. Thymocytes are extremely small cells, with a diameter of ~5μm, especially when compared to, for instance, brown adipocytes (~40 μm in diameter) (Cinti *et al.*, 1997).

The surface marker Thy 1 (conjugated to FITC) was used to exclusively identify thymocytes. Figure 3.1 shows Thy 1 as a green ring completely surrounding the thymocytes. The next step was to identify the mitochondria within the thymocytes. To label the mitochondria, thymocytes were incubated in submicromolar concentrations of the dye, Mitotracker® Red, which passively diffuses across the plasma membrane and accumulates in active mitochondria, due to the high mitochondrial membrane potential. Thymocytes' mitochondria appear to be extremely close to the nucleus and can either completely surround or be dispersed around the nucleus. Hoechst stain was used to detect the nucleus of the thymocytes. The images show that the nucleus is clearly a prominent feature, taking up a large proportion of the thymocyte volume, with the mitochondria apparently located in a relatively smaller volume surrounding the nucleus, within the plasma membrane as determined by the Thy 1 antigen.

The visual evidence for the presence of UCP 1 in thymocytes is clearly demonstrated in Figure 3.2. All cells investigated from wild-type and UCP 1 knock-out mice were thymocytes as determined by a monoclonal antibody specific for the thymocyte surface marker Thy 1(CD 90) pre-coupled to a fluorescently labelled

secondary antibody (Alexa 488, green). Mitochondrial within thymocytes were stained using Mitotracker® Red. Using a primary peptide antibody specific to UCP 1, and a secondary fluorescently-labelled antibody (Alexa 647, magenta) , it is demonstrated that UCP 1 is associated with mitochondria in thymocytes from wild type mice but not thymocytes from UCP 1 knock-out mice. A merged image clearly demonstrates the relative location of the plasma membrane, mitochondria and UCP 1 (in wild-types).

The detection of UCP 1 in situ in mitochondria is not unique to mice. Figure 3.3 demonstrates visual evidence for the presence of UCP 1 in Thy 1 positive (green staining) thymocytes isolated from rat thymus. Mitochondria were stained using Mitotracker Red. The association of UCP1 with mitochondria is shown in the merge image (figure 3.3) when UCP 1 is detected using the specific peptide antibody (magenta).

In an attempt to resolve the discrepancy between data reported by our group and data reported in studies by others, Frontini *et al.,* (2007), the specificity of the retrospective antibodies used in these studies was compared.

It was predicted that the discrepancy could be due to the use of a UCP 1-specific peptide antibody rather than an antibody raised against the whole UCP 1 protein. Confocal analysis showed that using an antibody raised to full length UCP 1; a protein is detected (magenta staining) in Thy 1 positive thymocytes from wild type mice and also from UCP 1 knock out mice (Figure 3.5). Figure 3.4 confirms the specificity of the peptide UCP 1 antibody, as no UCP 1 is detected in the thymocytes from UCP 1 knock out mice.

Thymocytes (Thy 1^{+}) originate from the bone marrow, and thymocytes that survive positive and negative selection in the thymus migrate to the spleen. Figure 3.6 shows an immunoblot on mouse mitochondrial samples from brown adipose tissue, thymocytes, bone marrow and spleen. Using the UCP 1 peptide antibody, a band at ~ 32 kDa denotes

the presence of UCP 1. This blot shows the presence of UCP 1 in BAT and thymus but not in bone marrow or spleen mitochondria. The bar chart in figure 3.6 shows the relative abundance of UCP 1 expression as a ratio of PDH, as determined by densitometry for BAT and thymus mitochondria. This confirms the previously reported RT-PCR evidence that UCP 1 protein is only evident in mitochondria from thymus and not in mitochondria from bone marrow or spleen cells.

The thymus is largest and most active during the neonatal and pre-adolescent periods, after which the thymus begins to atrophy and thymic stroma are replaced by adipose (fat) tissue. This atrophy is due to the increased circulating level of sex hormones (Sutherland, 2005). Therefore it would be interesting to see if age had an effect on UCP 1 expression in thymus mitochondria. Figure 3.7 shows the time-dependant profile of UCP 1 expression in mouse thymus mitochondria. Three week old mice were selected for the initial profiling based on the observation that UCP 1 expression in mitochondria from thymi of wild type mice was persistently evident in mice of less than five weeks old.

Figure 3.8 gives a typical profile of the thymocyte cells present in the thymus of mice, indicating, as expected, that the majority of the cells are CD4/CD8 double positive. Figure 3.8 (b) demonstrates that mitochondrial UCP 1 is associated with all thymocyte cell types: CD4/CD8 double positive (DP) thymocytes, CD4/CD8 double negative (DN) thymocytes, CD4 single positive (CD4SP) thymocytes and CD8 single positive (CD8SP) thymocytes. The association of UCP 1 with CD4/CD8 double positive (DP) thymocytes is visually demonstrated in the confocal images in Figure 3.9.

To investigate the role of protein degradation on the variation of UCP 1 levels, thymocytes were treated with cycloheximide to arrest protein synthesis, and UCP 1 levels were measured at different times by immunoblotting. Thymocyte mitochondrial

UCP 1 was found to have a relatively short half-life of approximately 3 hours, as seen in figure 3.10., compared to the 30 hour half-life of UCP 1 in BAT (Puigserver *et al.*, 1992).

We were also able to demonstrate that CIDEA, a protein suggested to be directly associated with UCP 1 in brown adipose tissue, was also present in mouse thymocytes (Figure 3.11).However, CIDEA was not associated with UCP 1 in thymocytes, with equivalent abundance of CIDEA in thymocytes from UCP 1 wild-type and UCP 1 knock-out mice (Figure 3.11).

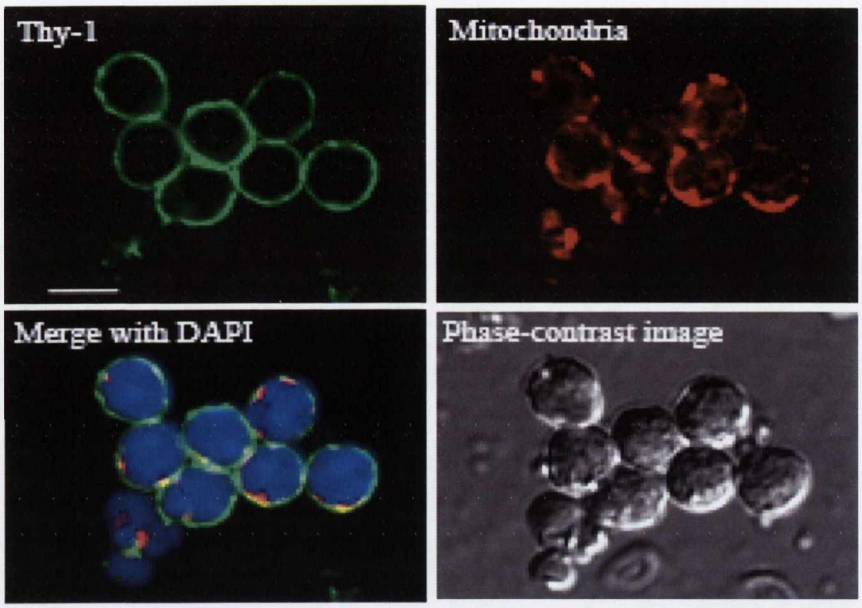

Figure 3.1 Detection of Thy-1, a cell surface marker, mitochondria and nucleus of thymocytes isolated from mice.

Isolated thymocytes were incubated with Mitotracker Red for 60 min at 37 °C and fixed and permeabilized consecutively in methanol and acetone at −20 °C for 5 min each on poly-L-lysine slides and subsequently probed with the polyclonal anti-Thy-1 IgG. Thy-1 was detected using anti-mouse Alexa 488 (green). The nucleus was stained with Hoechst stain (blue). The merge image shows the large nucleus of thymocytes and the small cytoplasmic space between the nucleus and the plasma membrane, in which the mitochondria are located. The phase contrast image shows the thymocytes. (×4200 zoom; Bar 5 µm).

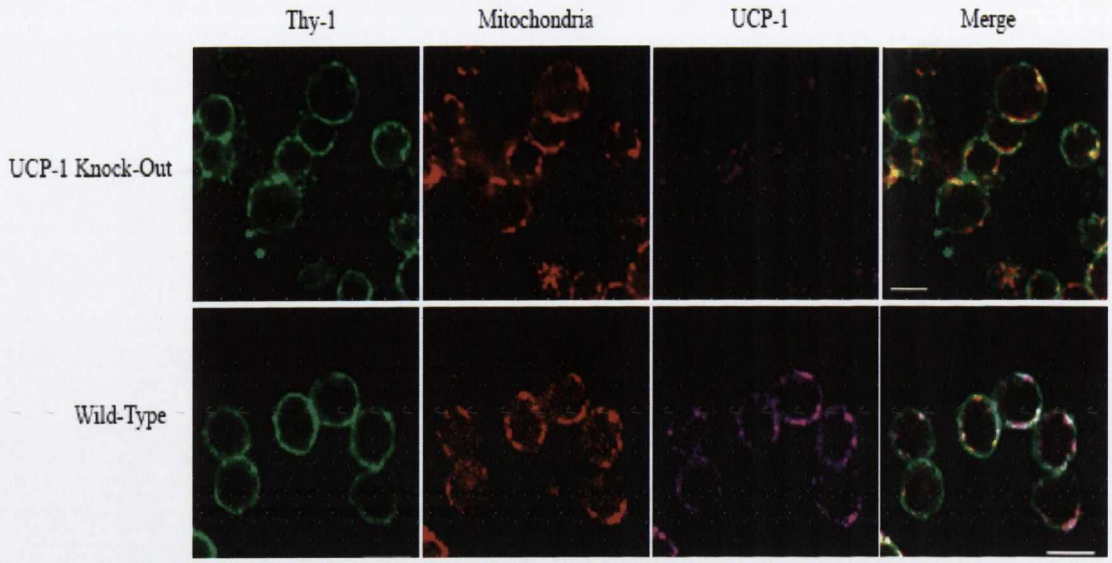

Figure 3.2 In situ identification of UCP 1 in the mitochondria of thymocytes from wild-type mice, but not thymocytes from UCP-1 knock-out mice.

Isolated thymocytes were incubated with Mitotracker Red for 60 min at 37 °C and fixed and permeabilized consecutively in methanol and acetone at −20 °C for 5 min each on poly-L-lysine slides and subsequently probed with the polyclonal anti-UCP 1 IgG and anti-Thy-1 (CD-90) IgG antibodies. UCP1 was detected using primary antibodies to UCP 1 and an anti-rabbit Alexa 647 (magenta) labelled secondary antibody. Thy-1 was detected using an IgG primary antibody to Thy-1 and an anti-mouse Alexa 488 (green) labelled secondary antibody. Accumulated Mitotracker Red stains the mitochondria red. (×4200 zoom; Bar 5 µm).

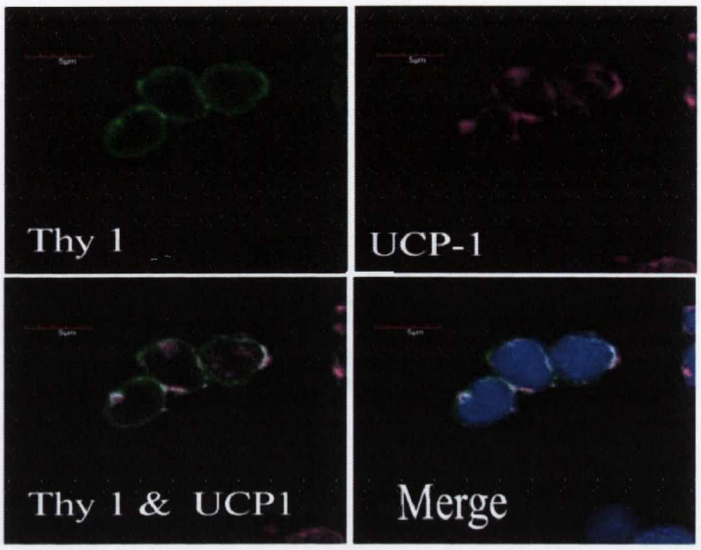

Figure 3.3 In situ identification of UCP 1 in thymocytes from rat.

In situ identification of UCP 1 in thymocytes isolated from a wistar rat using the UCP 1 antibody (Calbiochem). The UCP 1 antibody was detected using an anti-rabbit Cy5 (Jackson Immunoresearch-magenta) labeled secondary antibody. Thymocytes were detected using Thy 1 (Ab Serotec) primary antibody and detected using an anti-mouse Alexa 488 labeled secondary antibody (Invitrogen-green). Hoechst (Invitrogen) was used to stain the nucleus blue (x 4200 zoom; Bar 5µm).

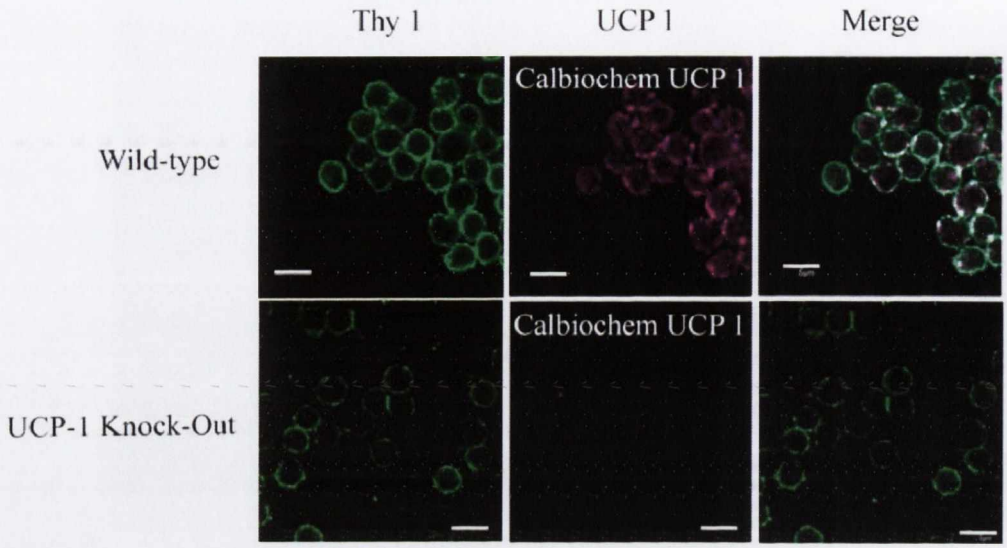

Figure 3.4. Identification of UCP 1 in thymocytes. In situ identification of UCP 1 in thymocytes from UCP 1 wild-type mice using a primary antibody specific to UCP 1 peptide (Calbiochem).

UCP 1 is not detected in thymocytes isolated from UCP 1 knock-out mice. The anti-UCP 1 peptide antibody was detected using an anti-rabbit Alexa 647 (magenta) labelled secondary antibody.Thymocytes were detected using an anti-Thy-1 primary antibody and detected using an anti-mouse Alexa 488 (green) labelled secondary antibody. (×2400 zoom; Bar 5 μm).

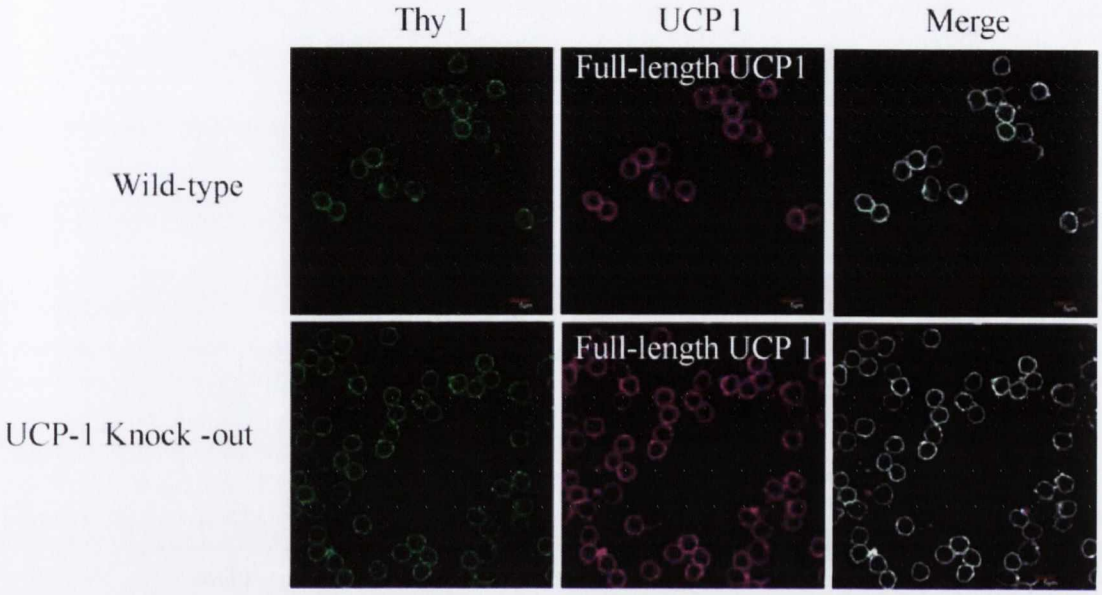

Figure 3.5. Non-specific in situ detection of protein in thymocytes using antibody to full-length UCP 1.

Thymocytes were isolated from the thymus of wild-type and UCP 1 knock-out mice using an antibody raised to full-length UCP 1. Thymocytes were identified using a Thy1 primary antibody and detected using an anti-mouse Alexa 488 (green) labelled secondary antibody. The antibody to full-length UCP 1was detected using an anti-sheep Cy3 (magenta) labelled secondary antibody. (×2400 zoom; Bar 5 μm);

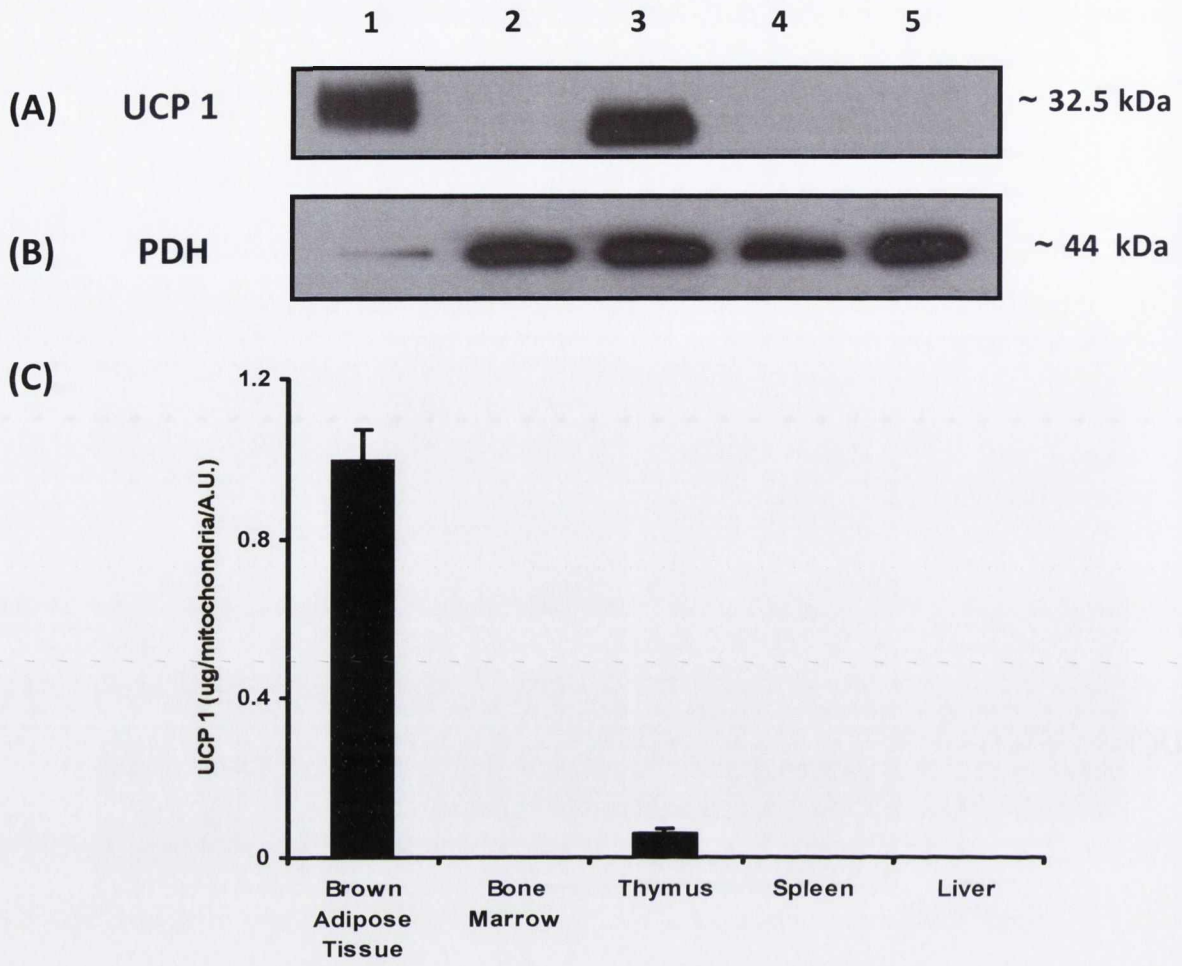

Figure 3.6 UCP 1 expression in mitochondria isolated from BAT, bone marrow, thymus , spleen and liver using a commercial UCP 1 peptide antibody (Sigma).

Mitochondria were isolated from wild-type mice as described in Section [2.2.2].Following isolation, mitochondria were subjected to SDS-PAGE (12% resolving gel) and transferred to PDVF membrane and immunoreactive proteins were detected using anti-UCP 1 peptide antibody (Sigma (A)) and anti-PDH (Cambridge Biosciences (B)). All antibodies were used at a 1:1000 dilution. A ~32.5 kDa and ~44 kDa protein band denotes the expression of UCP 1 and PDH respectively. The bar chart (C) shows the relative abundance of UCP 1 µg/mitochondria, as determined by densitometry, for BAT and thymus mitochondria

1.1µg BAT mitochondria

2.10 µg Bone Marrow mitochondria

3.10 µg Thymus mitochondria

4.10 µg Spleen mitochondria

5.10 µg Liver mitochondria

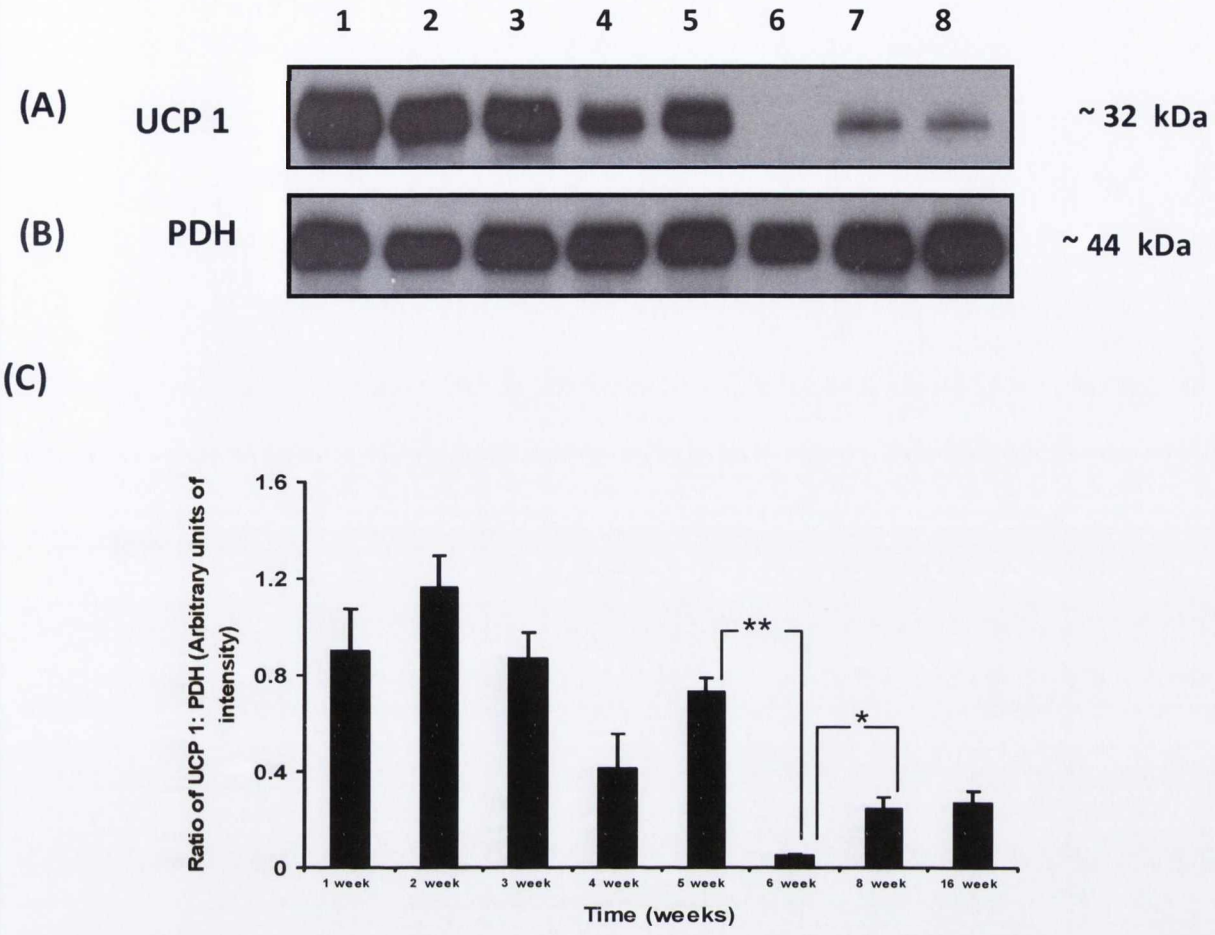

Figure 3.7 Time-dependant profile of UCP 1 expression in isolated thymus mitochondria.

Thymus mitochondria were isolated from 1, 2, 3, 4, 5, 6, 8 and 16 week old wild-type mice. 10μg of each sample was used for SDS-PAGE analysis, as described in Section [2.2.2]. Following isolation, mitochondria were subjected to SDS-PAGE (12% resolving gel) and transferred to PDVF membrane and immunoreactive proteins were detected using anti-UCP 1 peptide antibody (Sigma) and anti-PDH (Cambridge Biosciences (B)). A ~32.5 kDa and ~44 kDa protein band denotes the expression of UCP 1 and PDH respectively. The bar chart (C) shows the relative abundance of UCP 1 expression as a ratio of PDH, as determined by densitometry, for 3 separate preparations. Data is presented as mean ± S.E.M. An extremely significant decrease in UCP 1 expression is observed between 5 and 6 week old mice (p= 0.0003**, n=3) and a significant increase in UCP 1 expression is observed between 6 and 8 week old mice (p= 0.02*, n=3).

1. 1 week thymus mitochondria
2. 2 week thymus mitochondria
3. 3 week thymus mitochondria
4. 4 week thymus mitochondria
5. 5 week thymus mitochondria
6. 6 week thymus mitochondria
7. 8 week thymus mitochondria
8. 16 week thymus mitochondria

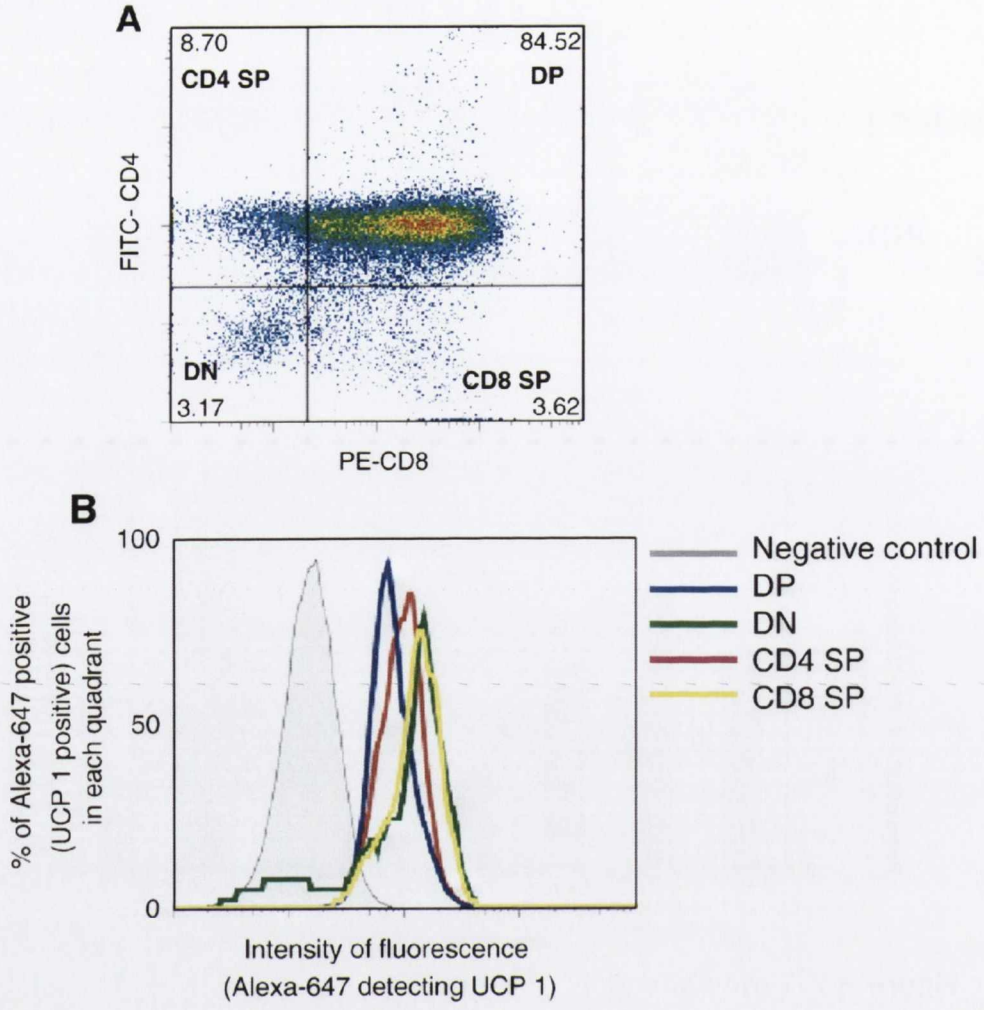

Figure 3.8. Characterization of thymocytes isolated from wild-type mice.

A. Representative two colour flow cytometry analysis of thymocyte subsets from wild type mice. Numbers in the dot plot represent percentage of cells in each quadrant using 10,000 cells. Thymocytes were probed with FITC-conjugated anti-CD4,R-PE-conjugated anti-CD8 (both from BD Biosciences) B. All thymocytes were simultaneously labelled for mitochondrial UCP1, and a profile of the proportion of each thymocyte subset containing UCP 1 was expressed as a percentage. Each thymocyte subset was defined by the number of cells in each quadrant. Intensity of fluorescence is proportional to the amount of UCP 1 present. The graph shows the FACS Profiles for UCP 1 in CD4/CD8 double positive (DP) thymocytes (blue), CD4/CD8 double negative (DN) thymocytes (green), CD4 single positive (CD4 SP)thymocytes (red) and CD8 single positive (CD8 SP) thymocytes (yellow). UCP 1 was detected with anti-UCP 1 antibody (Calbiochem) and secondary anti-rabbit Alexa-647 antibody (Invitrogen-magenta). The intensity of fluorescence due to non-specific binding by the secondary antibody (negative control) is depicted by the grey lined profile.

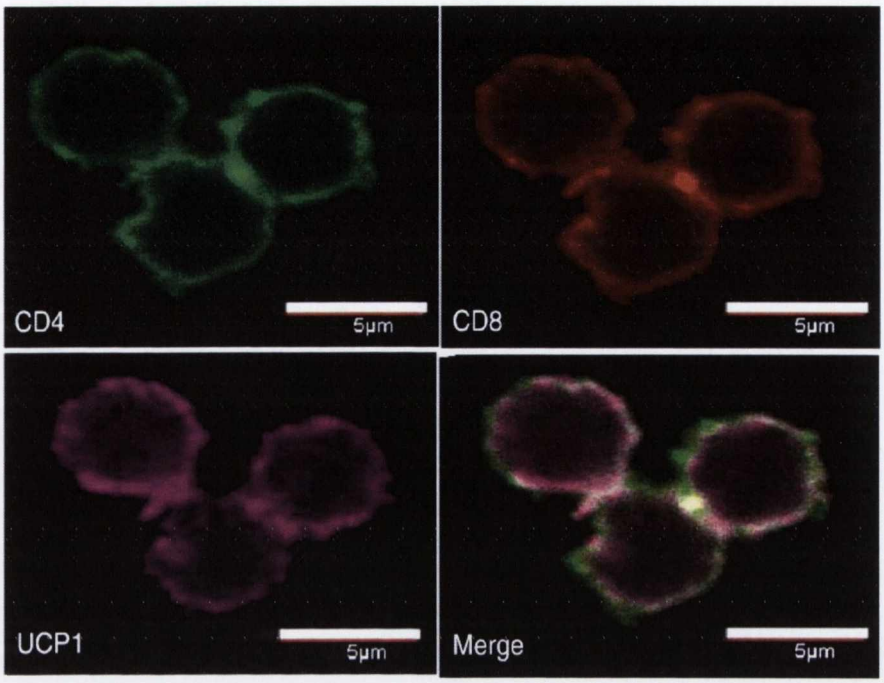

Figure 3.9 Identification of UCP 1 in CD4+/CD8+ thymocytes from wildtype mice.

Isolated thymocytes were fixed and permeabilized as described in the Materials and methods section. Thymocytes were probed with FITC-conjugated anti-CD4 (green), R-PE-conjugated anti-CD8 (red) [both from BD Biosciences] and UCP 1 antibody (Calbiochem) using an anti-rabbit Alexa 647 labelled secondary antibody (Invitrogen-magenta)(4200 zoom; Bar 5 µm).

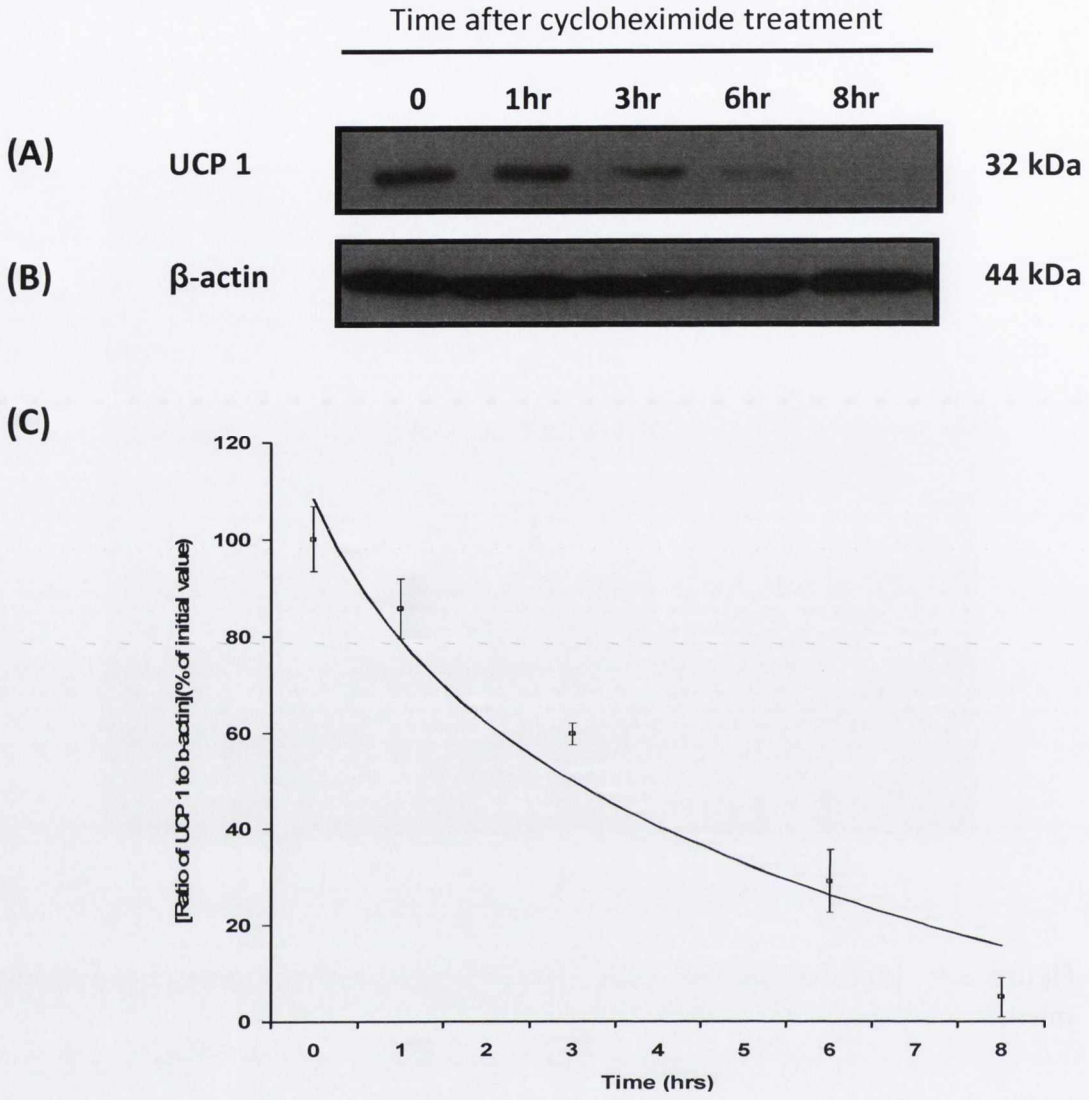

Figure 3.10 Half-life of UCP 1 in mice thymi.

(A) Thymocytes were isolated into fully supplemented RPMI at 2 x 10^6 cells/ml, then treated with 10 μg/ ml cycloheximide to arrest protein synthesis, harvested at the times shown and immunoblotted for UCP 1. Membranes were re-blotted for β-actin as a control (the lower immunoblot shows an example (B)). 50μg of cell lysate was used per lane. (C) Cell UCP 1 content (expressed as a ratio of β-actin by densitometry)-normalised to time point zero- as a function of time after cycloheximide treatment. Values are means ± S.E.M. from n=3 mitochondrial preparations.

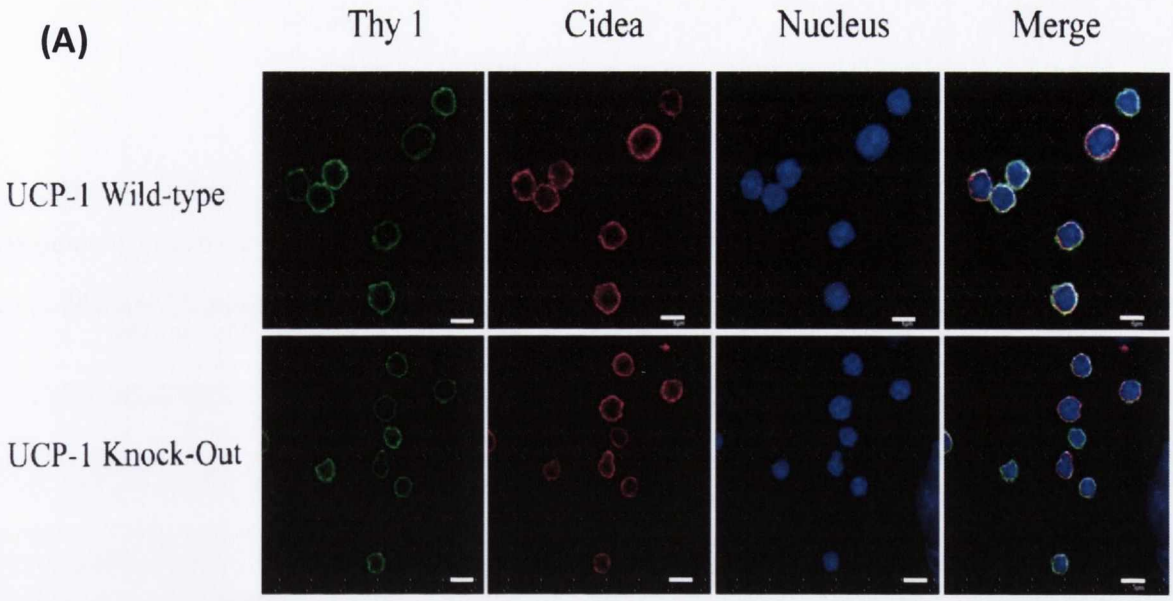

Figure 3.11. Identification of CIDEA in thymocytes from wild-type and UCP 1 knock-out mice thymocytes.

(A) Thymocytes were fixed and permeabilized as described in Materials and methods, probed with anti-Thy1 IgG and anti-CIDEA IgG antibody. Thy 1 was detected using a secondary labelled Alexa 488 (green) secondary antibody and CIDEA was detected using a secondary labelled Alexa 647 (red) secondary antibody. The nucleus was detected using Hoechst stain. (×3600 zoom; Bar 5 μm).

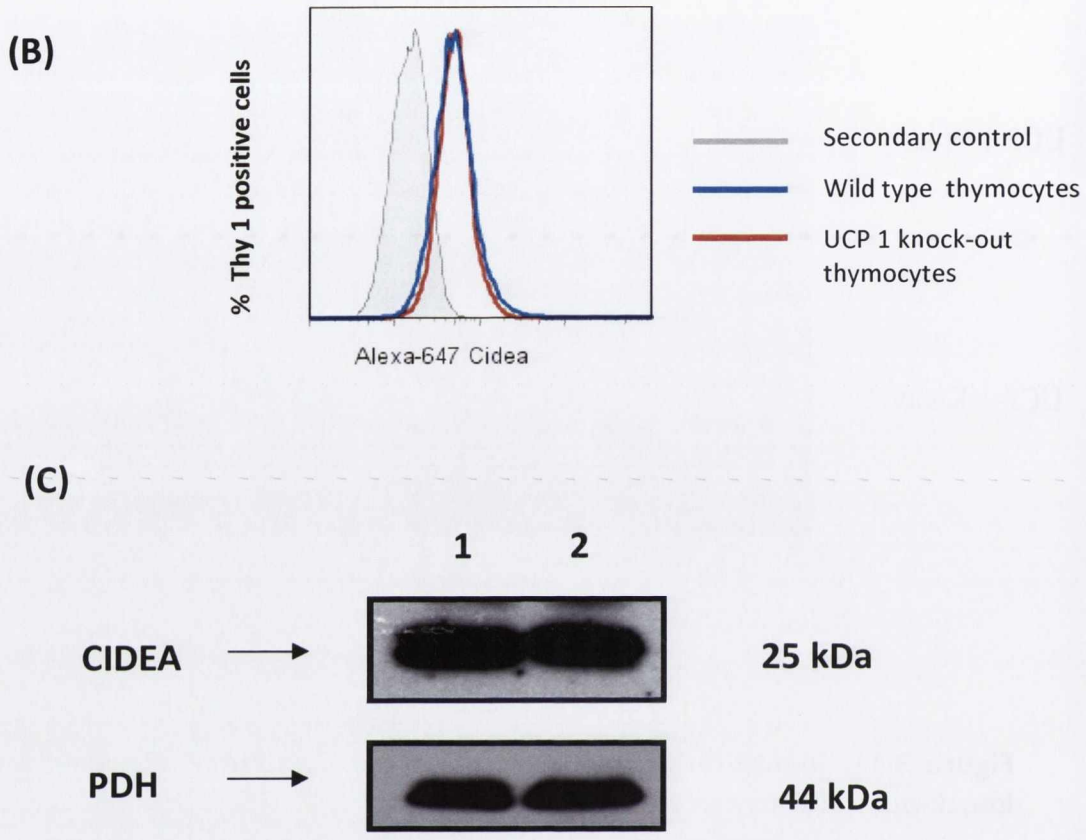

Figure 3.11 (continued) . Identification of CIDEA in thymocytes from wild-type and UCP 1 knock-out mice thymocytes.

(B) FACS Profile of wild-type and UCP 1 knockout thymocytes stained with CIDEA antibody (Millipore) and detected using Alexa 647 labeled secondary antibody (Invitrogen).(C) Immunoblotting was performed on mitochondrial samples prepared from (1) wild-type thymocytes and (2) UCP 1 knock-out thymocytes . The antibodies used were the CIDEA antibody (Millipore) and PDH (Millipore) antibody was used as a loading control for mitochondria. A ~25kDa and ~44kDa band denotes the presence of CIDEA and PDH respectively.

1 50µg Wild-type Thymocyte mitochondria

2 50µg UCP 1 knock-out Thymocyte mitochondria

[3.3] Discussion

Up until recently, UCP 1 was only ever associated with BAT mitochondria (Cannon *et al.,* 1982). UCP 1 has been reported to be found in white fat, however, in such cases it was always related to the presence of brown adipocytes dispersed in white fat depots (Cinti *et al.,* 2002). UCP 1 expression in other tissues has occasionally been reported; For instance UCP 1 has been shown to be expressed in skeletal muscle of mice chronically treated with a ß-adrenoreceptor agonist and in the longitudinal muscle layer of peristalic organs such as the intestine (Yoshhida *et al.,* 1998) and uterus (Nibblelink *et al.,* 2001).

However, the former data have never been confirmed, whereas the presence of UCP 1 in the longitudinal muscle layer of uterus has been conclusively disproved (Rousset *at al.,* 2003). The work of Carroll *et al.,* (2006), has shown that a functional UCP 1 is present in the thymus mitochondria of rats and mice. This work was recently challenged by Frontini *et al.,* (2007), who argued that any UCP 1 present in the thymus is due to brown adipose tissue contamination.

Once thymi were cleared of all (if any) surrounding tissue, thymocytes were isolated and we set out to determine whether UCP 1 could be demonstrated to exist in whole cells. Figure 3.1 shows laser confocal microscopy images of thymocytes with fluorescently labelled Thy 1/CD90 antibody (green), fluorescently labelled mitochondria (Mitotracker Red; red), a merged image with the nucleus stained using a DNA dye (Hoeshst; blue) and a phase contrast image. It is interesting to note from the scale, that thymocytes are rather small cells (~ 5 µm in diameter) when compared to, for instance, brown adipocytes (~40 µm in diameter) (Cinti *et al.,* 1997). This figure shows that the nucleus is clearly a prominent feature of thymocytes (identified by Thy 1), taking up a large proportion of the volume, with the mitochondria apparently located in a relatively smaller volume surrounding the nucleus.

The visual evidence for the presence of UCP 1 in thymocytes is clearly demonstrated in Figure 3.2. This figure demonstrates that all cells investigated from

wild-type and UCP 1 knock-out mice were thymocytes as determined by the monoclonal antibody specific for the thymocyte surface marker Thy 1(pre-conjugated to Alexa 488). Mitochondrial location was determined using Mitotracker red, which accumulates in viable mitochondria. Using a commercial antibody specific to UCP 1 (Calbiochem), and fluorescently labelled secondary antibody (Alexa 647; magenta) it is clearly demonstrated that UCP 1 is associated with mitochondria in thymocytes from wild-type mice but not thymocytes from UCP 1 knock-out mice. The merged image clearly demonstrates the relative location of the plasma membrane, mitochondria and UCP 1 in wild-type mice (Adams *et al.*, 2007).

The detection of UCP 1 insitu in mitochondria of thymocytes is not unique to mouse. Figure 3.3 demonstrates visual evidence for the presence of UCP 1 (magenta) in Thy 1 (green) thymocytes isolated from rats.

In an attempt to resolve the discrepancy between data reported by us, (Adams *et al.,* 2007), and data reported in studies by others (Frontini *et al.,* 2007), the specificity of the respective UCP 1 antibodies used in these studies was compared.

We predicted that the discrepancy could be due to the relative specificity of the peptide antibody used by us and the full length antibody used by Frontini *et al.,* (2007) Confocal analysis shows that using the full-length UCP 1 antibody, a protein is detected (figure 3.5) in Thy 1 positive thymocytes from wild-type mice and also UCP 1 knock out mice. The full-length UCP 1 antibody detects a ~32 k Da band in mitochondria from BAT, spleen, liver and also BAT mitochondria from mice deficient in UCP 1 (Adams *et al.*, 2008). Clearly, the antibody to full-length UCP 1 is detecting other proteins at ~32kDa and possibly at other masses.

Figure 3.4 shows that using the commercial UCP 1 antibody from Calbiochem, that UCP 1 is associated with mitochondria in thymocytes from wild-type mice but not thymocytes from UCP 1 knock-out mice. This highlights the specificity of the Calbiochem antibody raised against a peptide of UCP 1 (residues 145-159) used by Carroll *et al.,*

(2006) and Adams *at al.,* (2008), which detected a 32.5k Da protein, consistent with the size of UCP 1 , in BAT and thymus mitochondria and not other tissues.

As mentioned in the introduction all thymocytes (Thy 1^{+}; pre-thymocytes) originate from a progenitor cell in the bone marrow. Approximately 30-45% of rat bone marrow cells express Thy 1 (so are the pre-thymocytes) (Williams, 2005). These cells are transported to the thymus via the blood. While in the thymus, thymocytes that survive positive and negative selection migrate to the peripheral immune system such as the spleen (the mature T cells; either CD4SP or CD8SP) (Abbas A.K. *et al.,* Cellular and Molecular Immunology 2^{ND} Edition)

Having established that UCP 1 is present in thymocytes we decided to ask the question of whether UCP 1 was present in thymocyte progenitor cells and/or circulating T cells. An immunoblot on rat mitochondrial samples from BAT, thymus, bone marrow and spleen was performed. Using the UCP 1 peptide antibody, a band at ~ 32 k Da denotes the presence of UCP 1 protein. Figure 3.6, demonstrates that UCP 1 is not present in bone marrow or spleen; it is only expressed in thymus mitochondria. The bar chart in figure 3.6 shows the relative abundance of UCP 1 in BAT and thymus as a ratio of PDH, and that the level of UCP 1 in thymus is at a much less prominent compared to BAT.

Figure 3.7 shows the time-dependant profile of UCP 1 expression in isolated thymus mitochondria. It is shown for the first time, that UCP 1 protein expression decreases significantly after 5 weeks of age, coinciding with the suckling/weaning transition, when mice would be weaned from their mothers. The connection between mother and her offspring could be an important factor in the expression of UCP 1 in thymus mitochondria, as newborns receive all their antibodies and nutrients from their mothers whilst suckling and maturation of their own immune system

We next had to establish the role of UCP 1 in thymus and our first line of investigation centred on T-cell maturation and differentiation, to that end we compared thymocyte distribution in wildtype and UCP 1 knock-out mice. The thymus contains many thymocytes at different stages of maturation. The most immature are the double negatives (DN; $CD4^-CD8^-$), then the double positives (DP; $CD4^+CD8^+$) and then those that survive positive and negative selection (~2%) go on to become mature T cells- either CD4SP or CD8SP.

Figure 3.8(A) shows a representative dot-plot of CD4 and CD8 expression on thymocytes from a wild-type mouse, giving a typical profile to those being in the literature (Starr *et al.,* 2003) with $CD4^+CD8^+$ cells being the most prominent cell type in the thymus. It is clearly demonstrated that mitochondrial UCP 1 is apparent in all thymocytes [Figure 3.8(B)] with a clear microscopic demonstration of UCP 1 in $CD4^+CD8^+$ cells [Figure 3.9].

To investigate the role of protein degradation on the variation of UCP 1 levels in thymocytes, isolated thymocytes were treated with cycloheximide to arrest protein synthesis, and UCP 1 levels were measured at different times by immunoblotting. UCP 1 was found to have a relatively short half-life of approximately 3 hours, presumably allowing dynamic fluctuation and perhaps accounting for the low abundance of UCP 1 in the thymus. This short half-life contrasts with the much longer half-life of approximately 30 hours of UCP 1 in BAT (Puigserver *et al.*, 1992). This suggests a unique role for UCP 1 in thymus and might account for its low abundance, and allows rapid fluctuation depending on conditions.

Our data also clearly demonstrate that CIDEA is expressed in thymocytes. However, using UCP 1 deficient mice we have shown that the absence of UCP 1 does not affect native expression of CIDEA. It would still be interesting to discover whether the absence of CIDEA affects mitochondrial function in thymocytes as has been demonstrated for BAT (Zhou *et al.*, 2003).

Confirmation of UCP 1 in thymocytes from wildtype mice and rats highlights the need to address the biological functions of UCP 1 in such cells. There is already circumstantial evidence that UCP 1 does not play a thermogenic role in the thymus (Brennan *et al.*, 2006). Future experiments will address alterations in metabolic and physiological functions of UCP 1 knock out mice.

[3.4] Conclusion

Our data provide unequivocal evidence for the presence of UCP 1 in thymocyte mitochondria in situ and are the first images to demonstrate UCP 1 expression in cells other than brown adipocytes. The demonstration by Frontini *et al.* , that UCP 1 is associated with BAT tissue in the vicinity of the thymus is not disputed, but their assertion that any UCP 1 associated with the thymus is due to BAT alone, is clearly not the case. We conclude and clearly demonstrate that mouse thymocytes contain UCP 1 in their mitochondria. Our data also highlight the specificity of the commercial antibody raised against UCP 1 peptide, used in our published studies (Carroll *et al.*, 2004; Carroll *et al.*, 2005; Porter, 2006; Adams *et al.*, 2007; Brennan *et al.*, 2006; Cunningham *et al.*, 2003) which reacted against a ~ 32.5 kDa protein, consistent with the size of UCP 1, in BAT and thymus mitochondria and not other tissue. In striking contrast, there was marked lack of specificity in reactivity of the antibody raised against the full-length UCP 1 protein, with a ~ 32.5 kDa protein detected in rat BAT and thymus mitochondria and also mitochondria from spleen, kidney, skeletal muscle and liver and crucially BAT from UCP 1 knock out mice. We also demonstrate UCP 1 is prominent in the thymus is young mice, and also that UCP 1 is present in all thymocyte subsets. We also demonstrate UCP 1 has a half-life of approximately 3 hours in the thymus.

Chapter 4
Phenotypic and apoptotic differences in UCP 1 knock-out mice

[4.1] Introduction

The thymus is a primary lymphoid tissue where progenitor thymocytes from bone marrow develop into mature thymocytes and via antigen selection processes develop into naïve T-cells which migrate to peripheral lymphoid tissue, such as spleen and lymph nodes (Starr *et al.*, 2003, Zuniga-Pflucker, 2004, Hayday & Pennington, 2007). Thus the thymus contains thymocytes contains thymocytes that are at different stages of maturation. The most immature of these cells are easily identified due to the lack of the CD4/CD8 surface antigens (also called double negatives (DN)) and account for up to ~5% of the cells present in the thymus. Progress to maturation can be followed firstly by the expression of both CD4 and CD8 antigens on the thymocyte surface (double positives (DP)), which account for up to 85% of cells in the thymus. The DP cells undergo positive selection for antigen and negative selection for self-antigen resulting in attrition of up to 95% of these cells through apoptosis. The remaining 5% of selected DP cells generate either naïve CD4 single positive or naïve CD8 single positive cells which enter the medulla of the thymus before they migrate to the peripheral immune tissues.

In a peripheral immune tissue such as the spleen, CD4 single positive T-cells account for approximately 20% of all cells, CD8 single positive T-cells account for approximately 10% of all cells, whereas the amount of DP is negligible (Mebius & Kraal, 2005). The remainder of the cells in the spleen are composed mainly of reticulocytes, monocytes and B-lymphocytes (Adams & Cory, 2001).

For many apoptotic events the Bcl-2 family of mitochondrial proteins play a central role (Mills *et al.*, 1996)). For instance, Bim, a BH3-only Bcl-2 family member, is required for apoptosis of thymocytes in response to negative selection (Bouillet *et al.*, 2002)). Furthermore, there is a hierarchy of ATP usage in thymocytes (Buttgereit & Brand, 1995) and although ATP is necessary for apoptosis (Stefanelli *et al.*, 1997), low intracellular ATP levels can trigger nitric oxide induced apoptosis (Honda *et al.*, 2003).

Until relatively recently, mitochondrial uncoupling protein 1 had only ever been associated with mitochondria of brown adipose tissue. Under conditions of cold-stress, brown adipose tissue UCP 1 activity results in uncoupling of mitochondrial ATP synthesis, from oxygen consumption, by dissipating the proton electrochemical gradient, generated by the electron transport chain across the inner membrane. The resulting increased metabolic flux, increased heat production by brown adipose tissue and ultimately distribution of that heat through-out the whole body, is a process termed non-shivering thermogenesis (Nicholls & Locke, 1984, Cannon & Nedergaard, 2004, Nicholls, 2006). UCP 1 has also, however shown to be present in thymocyte mitochondria, and although the original empirical evidence has been contested (Frontini *et al.*, 2007), the cell imaging evidence demonstrating UCP 1 present in thymocytes from wild-type mice but absent in thymocytes from UCP 1 knock-out mice, is very convincing (Carroll *et al.*, 2004, Carroll *et al.*, 2005, Adams *et al.*, 2007, Adams *et al.*, 2008). Interestingly, despite the fact that T-cells in the spleen are derived from the thymus, no transcripts for UCP 1 have been detected in spleen (Carroll & Porter, 2004). Until this study we had no indication of a role for UCP 1 in thymus function, but the laboratory had established that UCP 1 did not have a thermogenic role in the thymus, as cold acclimation did not result in increased UCP 1 expression there (Brennan *et al.*, 2006).

In this study we investigated whether the absence of UCP 1 in thymocytes resulted in a difference in thymus and spleen cell composition profile and function when compared to wild-type mice of the same back-ground, sex, age and strain.

[4.2] Results

Three week old mice were selected for this study based on the previous chapter that UCP 1 expression in mitochondria from thymi of wild-type mice was prominent in the first 5 weeks of life. In light of the observation that mitochondrial UCP 1 is present in thymocytes (but not spleen) of mice, and because the T-cell profile of the spleen is contributed to by the thymus, a variety of tissue and cell parameters from both thymus and spleen of wild-type and UCP 1 knock-out mice were compared, to ascertain whether there are differences in cell profile and function. Table 4.1 holds data for thymus and spleen tissue masses from wildtype and UCP 1 knock out mice. No significant difference was observed in a comparison of tissue mass from wild-type and UCP 1 knock out mice; however there is a trend for the spleen masses of knock out mice to be lower than that of wildtype mice.

Despite the fact that no significant difference in thymus or spleen tissue mass between wildtype and UCP 1 knock out mice was seen, a cell count was nevertheless performed on these tissues. No difference in cell numbers was observed in a comparison of the thymus from wild-type and UCP 1 knock out mice (Figure4.1(A)), but a significant 3-fold decrease in cell number in a comparison of the spleens from wild-type and UCP 1 knock out mice was observed, Figure 4.1(B).

Furthermore, the cells within the thymus were profiled (Figure 4.2(A-F)) and those from wild-type and UCP 1 knock out mice were compared. Figure 4.2(A) and 4.2(B) are typical examples of the primary FACS analysis data for mouse thymus. From the collated data, a significant 2-fold decrease in the CD8 single positive cells (Figure 4.2(C)) and a significant ~ 10% increase in CD4/CD8 double positive cells (Figure 4.2(D)) from UCP 1 knock out mice was observed when compared to those from wild-type mice. No significant difference was observed in the proportion of CD4/CD8 double negatives or CD4 single positive thymocytes isolated from wildtype mice compared to UCP 1 knock out mice (Figure 4.2(E) and Figure 4.2 (F))

As there is a significant contribution to T cells in the spleen from the thymus , the relative abundance of CD8 single positive and CD4/CD8 double positives within the spleen were identified (Figure 4.3) and compared to those from wild-type and UCP 1 knock out mice. An example of the FACS analysis primary data for mouse spleen is given in Figure 4.3(A) and Figure 4.3 (B).

A significant ~2 fold decrease in the CD8 single positive cells (Figure 4.3 (C)) and a significant ~2 fold increase in CD4/CD8 double positive T-cells (Figure 4.3 (D)) in the spleen of UCP 1 knock out mice was observed compared to the cells from spleen of wild-type mice. No significant difference was observed in the proportion of other cells (which includes CD4/CD8 double negative T-cells) (Figure 4.3 (E)) or CD4 single positive T cells (Figure 4.3 (F)) isolated from wildtype compared to UCP 1 knock out mice.

The decrease in the proportion of CD8 single positive thymocytes in the thymus (Figure 4.2 (C)) and CD8 single positive T cells in the spleen (Figure 4.3 (C)), together with the increase in CD4/CD8 double positive thymocytes in the thymus (Figure 4.2 (D)) and the doubling of CD4/CD8 double positive circulating T cells (Figure 4.3 (D)) led to questioning whether there was a differential effect in apoptotic potential in a comparison of thymocytes from wild-type and UCP 1 knock out mice.

Figure 4.4 contains the primary data and collated data for annexin V plasma membrane phosphatidylserine binding and propidium iodide DNA staining, as measures of the extent of apoptosis , after 5 hr (Figure 4.4 (A,B and C)) and 18 hr (Figure 4.4 (D,E and F)) for dexamethasone and vechicle-treated thymocytes from wild-type and UCP 1 knock out mice.

The data shows no significant difference in apoptotic potential in a comparison of dexamethasone treated thymocytes from wild-type and UCP 1 knock out mice after 5 hr (Figure 4.4 (C)) and no significant difference in apoptotic potential in a comparison of dexamethasone treated thymocytes from wildtype and UCP 1 knock out mice after 18 hr (Figure 4.4 (F)).

However there is a significant decrease in apoptotic potential in vechicle treated thymocytes from UCP 1 knock out mice after 5 hr compared to cells from wildtype mice (Figure 4.4 (C)) and a significant decrease in apoptotic potential in vechicle treated thymocytes from UCP 1 knock out mice after 18 hr when compared to those from wildtype mice (Figure 4.4 (F)).

Additional indices of apoptosis, namely Caspase 3 and 7 activities in dexamethasone-treated, vechicle-treated and untreated control thymocytes from wildtype and UCP 1 knock out mice, indicated less caspase activity in thymocytes from UCP 1 knock out mice for dexamethasone-treated, vechicle-treated and untreated control thymocytes (Figure 4.5).

These data, depicting caspase activity in figure 4.5, are consistent with the independent indices of apoptosis, namely annexin V binding and propidium iodide staining laid out in figure 4.4. The data in Figure 4.4 and 4.5 are further endorsed by the observation of increased DNA laddering in dexamethasone-treated and control thymocytes from wild-type mice compared to UCP 1 knock-out mice (Figure 4.6)

The decreased apoptotic potential of thymocytes from UCP 1 knock out mice when compared to thymocytes from wildtype mice (Figure 4.4, 4.5 and 4.6) is consistent with the further observation of an increased abundance of ATP in thymocytes from UCP 1 knock out mice when compared to thymocytes from wildtype mice (Figure 4.7). Intracellular ADP levels were not significantly different in thymocytes from UCP 1 knock out mice compared to wildtype mice (Figure 4.8).

Despite the increase in ATP levels in thymocytes isolated from knock out mice, there appears to be no impact of the absence of UCP 1 on the total oxygen consumption rate by thymocytes (Figure 4.9).

Animal source/tissue	Thymus (grams)	Spleen (grams)
Wild-type mice	0.073±0.006(9)	0.073±0.009(9)
UCP 1 KO mice	0.087±0.009(9)	0.067±0.006(9)

Table 4.1 Thymus and spleen mass in wild-type and UCP 1 knock-out mice.

Data represents the mean ± SEM of 9 separate measurements. p values≤0.05 on an unpaired Student's 't'-test were deemed significant. No significant difference was observed in a comparison of tissue mass between wild-type and UCP 1 knock-out mice.

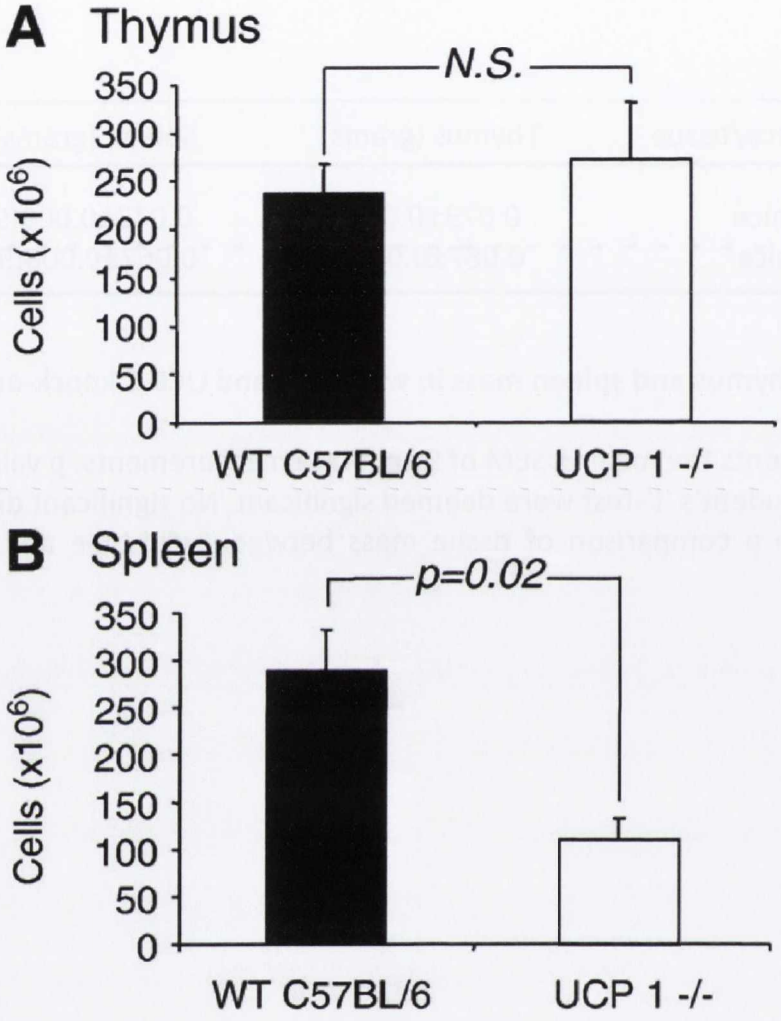

Figure 4.1. Number of cells per thymus and spleen from 3 week old wild-type and UCP 1 knock-out mice.

The bar chart depicts the collated data for cell number for (A) thymus and (B) spleen of wild-type (■) and UCP 1knock-out (□)mice. Data are from three separate experiments each performed in at least triplicate (mean ± SEM (3)). p values ≤0.05 on an unpaired Student's 't'-test were deemed significant.

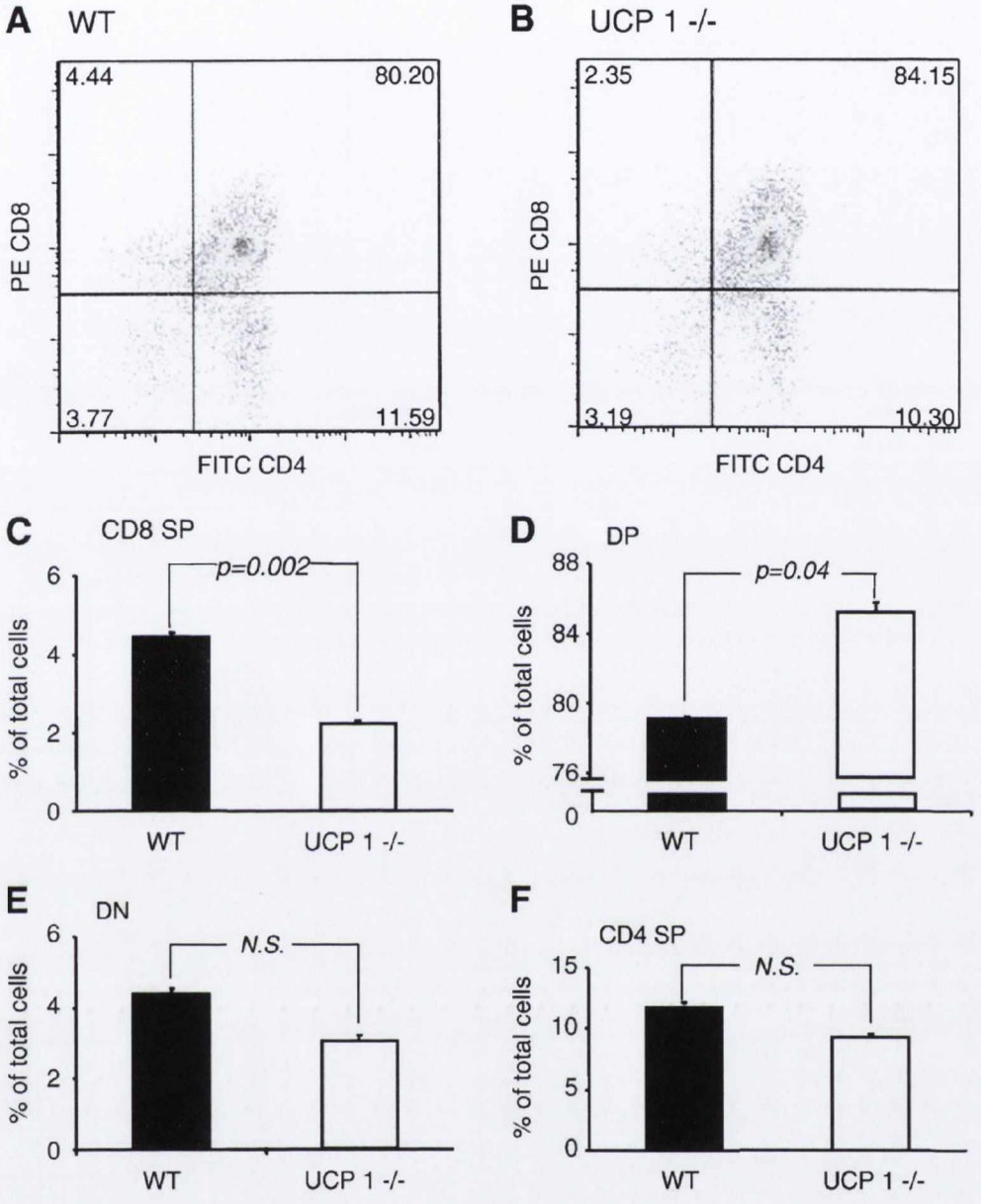

Figure 4.2 Cell subsets in thymus of 3 week old wild-type and UCP 1 knock out mice.

Thymocytes from 3 week old wild-type (■) and UCP 1 knock-out (□) mice were isolated and the cells were stained with FITC-conjugated anti-CD4, R-PE-conjugated anti-CD8 (both from BD Biosciences) and analyzed on the FACS Cyan. Representative dot-plots for thymocytes from (A) wild-type and (B) UCP 1 knock-out mice are shown. Numbers represent percentage of total cells in each quadrant using 10,000 cells. The percentage of cells that are (C) CD8 single positive (CD8 SP), (D) CD8/CD4 double positive (DP), (E) CD8 and CD4 double negative (DN) and (F) CD4 single positive (CD4 SP) are indicated. Data are mean ± SEM of six experiments performed in at least triplicate. p values ≤ 0.05 on an unpaired Student's 't'-test were deemed significant.

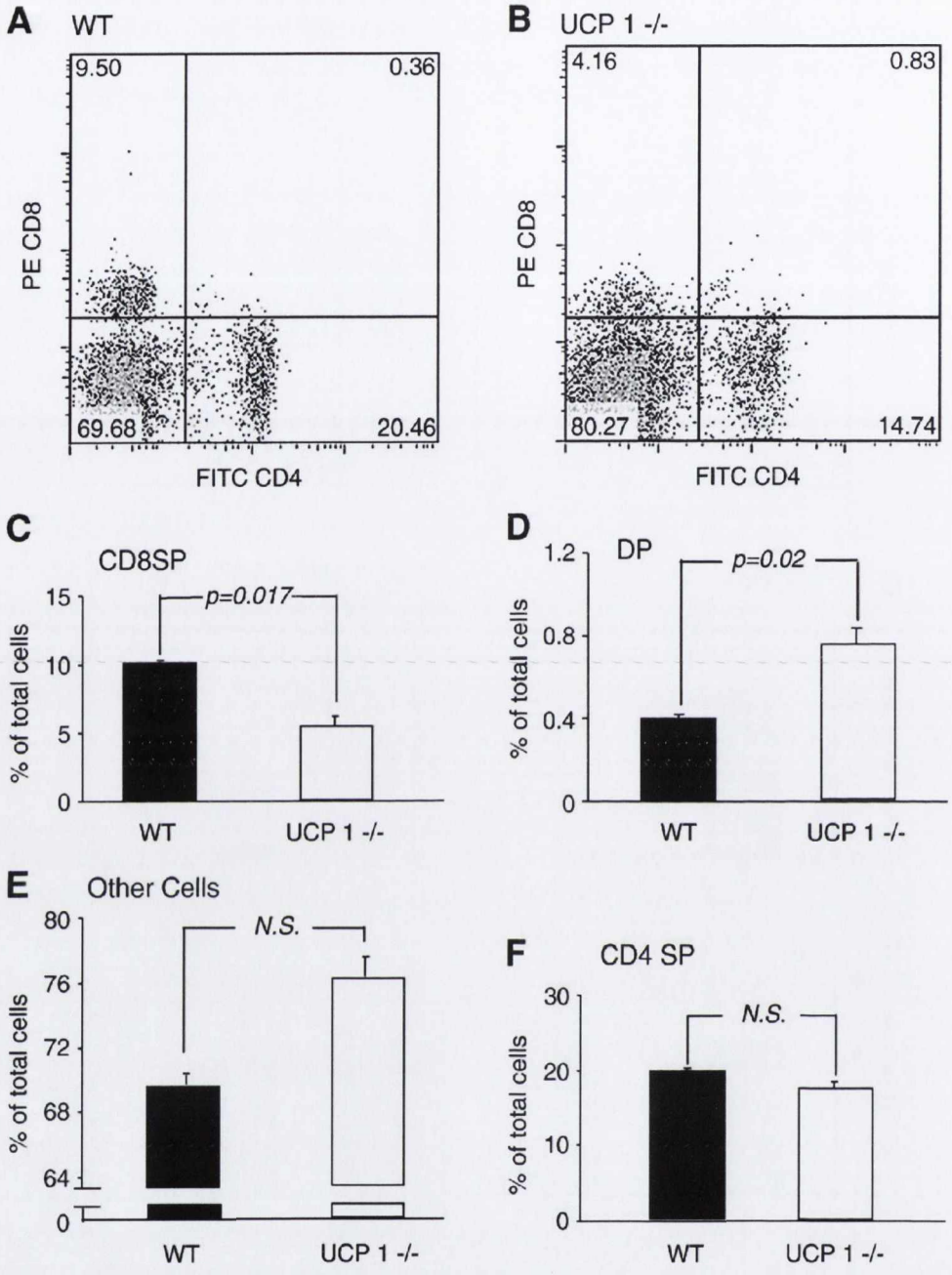

Figure 4.3 Cell subsets in spleen of 3 week old wild-type and UCP 1 knock out mice.

Spleen cells from 3 week old wild-type (■) and UCP 1 knock-out (□) mice were isolated and the cells were stained with FITC-conjugated anti-CD4, R-PE-conjugated anti-CD8 (both from BD Biosciences) and analyzed on the FACS Cyan. Representative primary data for spleen cell from (A) wild-type and (B) UCP 1 knock-out mice are shown. Numbers represent percentage of total cells in each quadrant using 10,000 cells. The percentage of T-cells that are (C) CD8 single positive (CD8 SP), (D) CD8/CD4 double positive (DP), (E) Other cells including CD8 and CD4 double negative (other cells) and (F) CD4 single positive (CD4 SP) are indicated. Data are mean ± SEM of six experiments performed in triplicate. p values ≤ 0.05 on an unpaired Student's 't'-test were deemed significant.

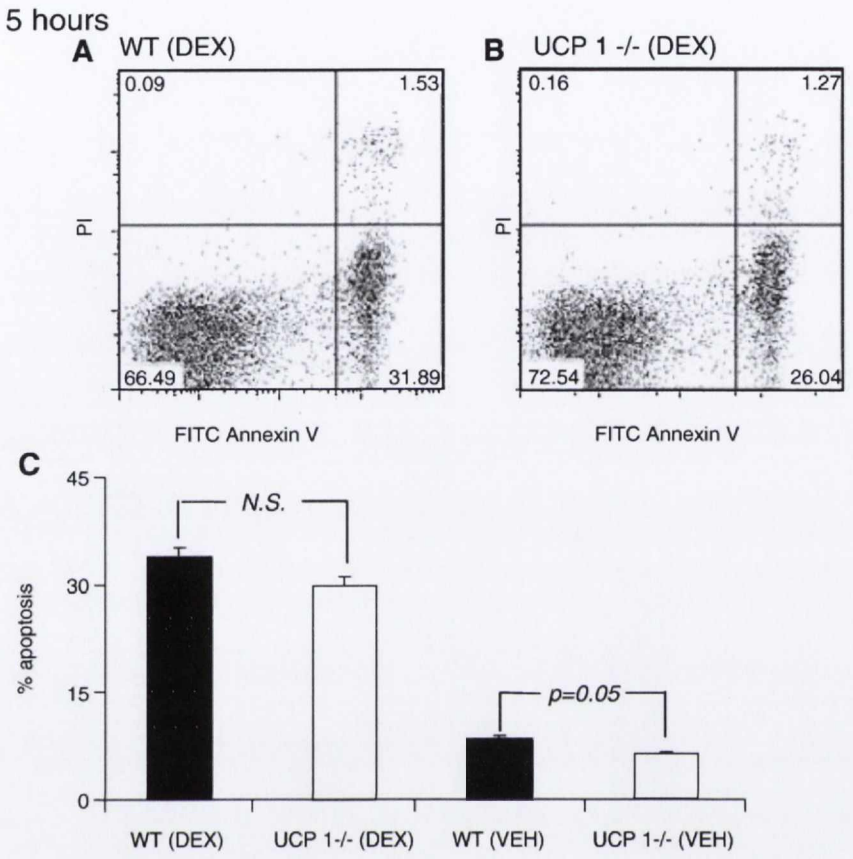

Fig.4.4. Percentage of apoptosis in vehicle-treated and dexamethasone-treated thymocytes from wildtype and UCP 1 knock out mice, as determined by annexin V and propidium iodide (PI) staining.

Thymocytes from wild-type (■) and UCP 1 knock-out (□)mice were isolated and treated with either the vehicle (VEH) or dexamethasone (DEX) (0.1 μM) for 5 (A–C) and 18 (D–F) hours. Cells were collected and stained with Annexin V (conjugated to Alexa 488— Millipore) and Propidium iodide (PI). 10,000 events per measurement were then collected on a FACS Cyan. Representative dot plots of dexamethasone-treated thymocytes after (5 h)(A and B) and 18 h (D and E) are indicated. Collated data for dexamethasone and vehicle-treated thymocytes after (5 h) (C) and 18 h (F) are indicated. Data are mean ± SEM of four experiments performed in at least triplicate. p values ≤ 0.05 on an unpaired Student's 't'-test were deemed significant.

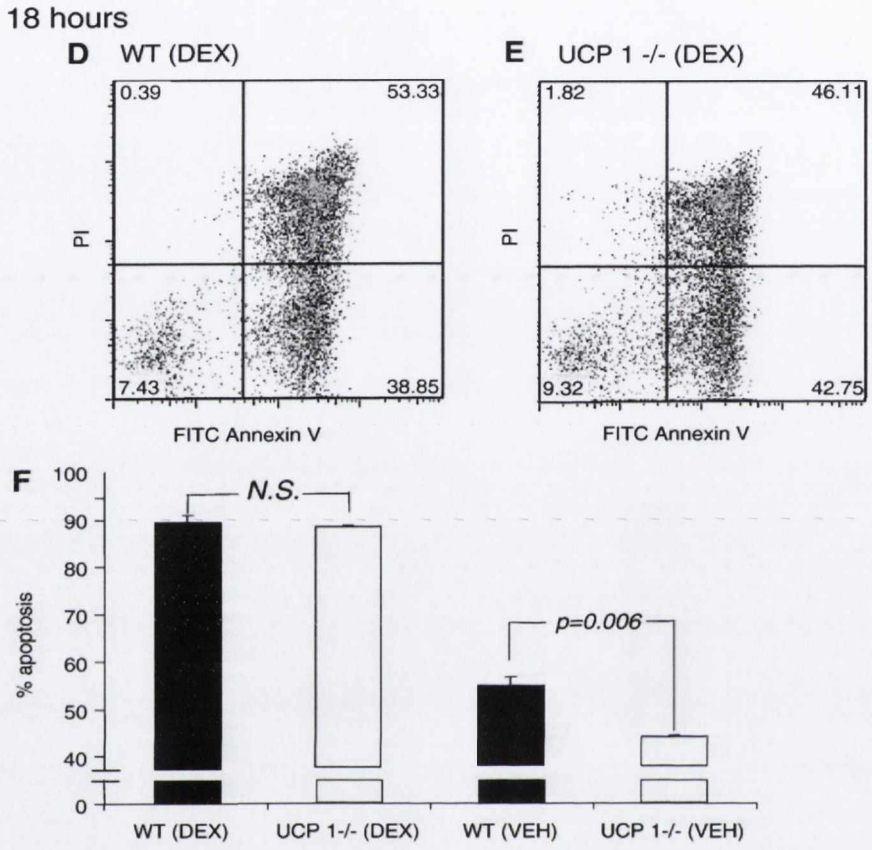

Fig.4.4. (continued) . Percentage of apoptosis in vehicle-treated and dexamethasone-treated thymocytes from wild-type and UCP 1 knock out mice, as determined by annexin V and propidium iodide (PI) staining.

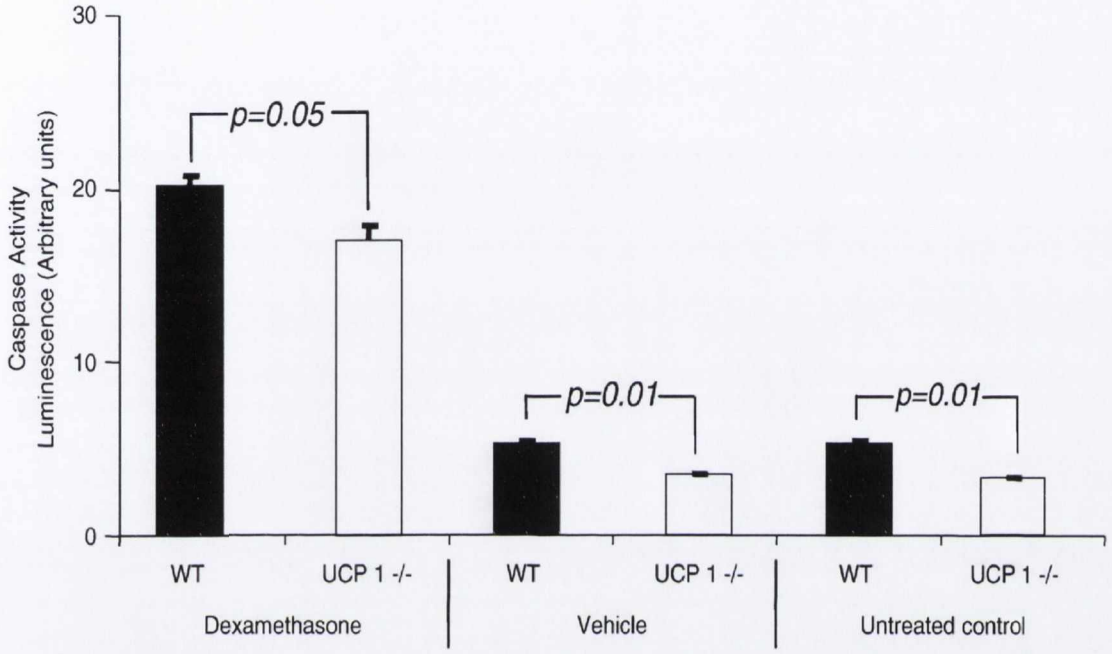

Figure.4.5. Caspase activation in dexamethasone-treated, vehicle-treated and untreated (control) thymocytes from3 week old wild-type and UCP 1 knock out mice, as determined by the Caspase-Glo 3/7 assay.

Thymocytes from wild-type (■) and UCP 1 knock-out (□)mice were isolated and treated with either dexamethasone (0.1 μM), vehicle or were untreated. After 5 h, 10 000 cells were placed in each well and lysed. A substrate peptide for caspase 3 and 7 was added. Data are mean ± SEM of three experiments performed in at least triplicate. p values ≤ 0.05 on an unpaired Student's 't'-test were deemed significant.

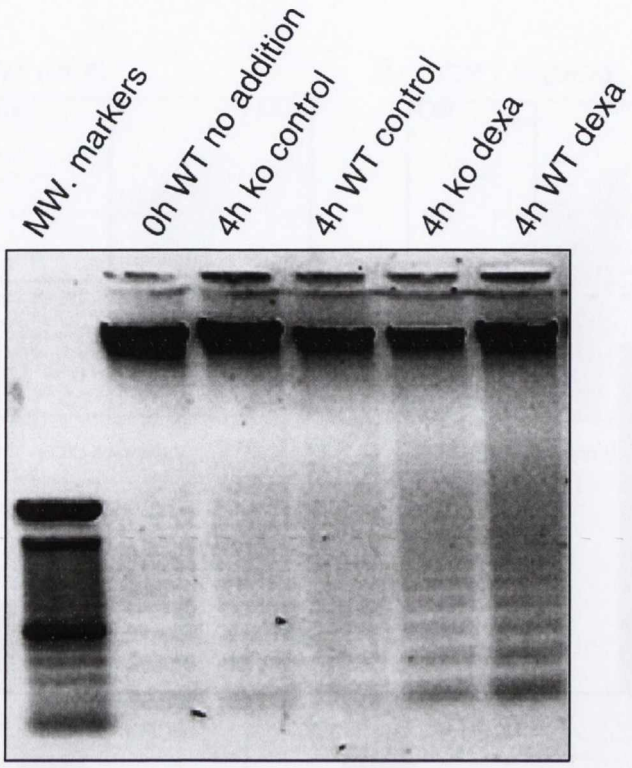

Figure 4.6. DNA fragmentation in untreated (control), vehicle-treated and dexamethasone treated thymocytes from wild-type and UCP 1 knock out mice.

The lanes on the agarose gel show DNA markers and DNA isolated from untreated (0 h), vehicle-treated (4 h) and dexamethasone-treated (4 h) thymocytes from wildtype and UCP 1 knock out mice.

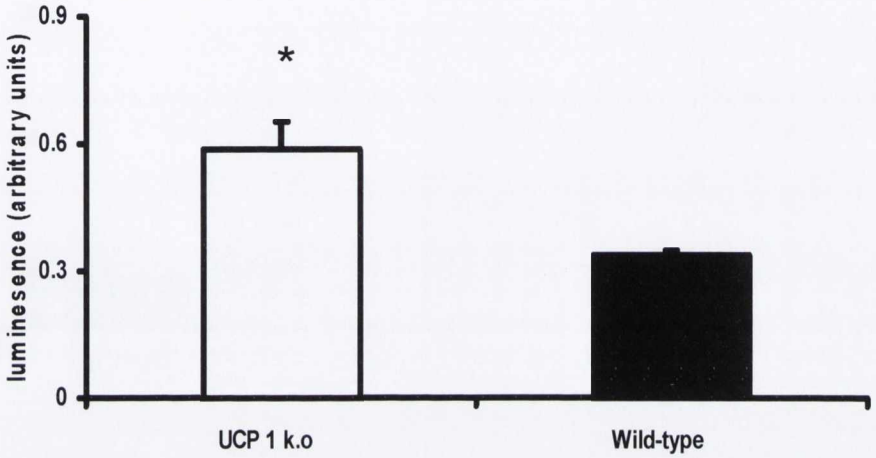

Figure 4.7 Intracellular ATP levels of 3 week old thymocytes from UCP 1 knock out mice compared to wildtype mice.

ATP levels were determined using Aposensor ADP/ATP Ratio Assay Kit from Biovision. 10000 cells were used for each sample. Data are expressed as mean +/- SEM of each group (n=3). * Statistical significance for the difference in ATP levels, as determined by the student's t test ($p = 0.019$)

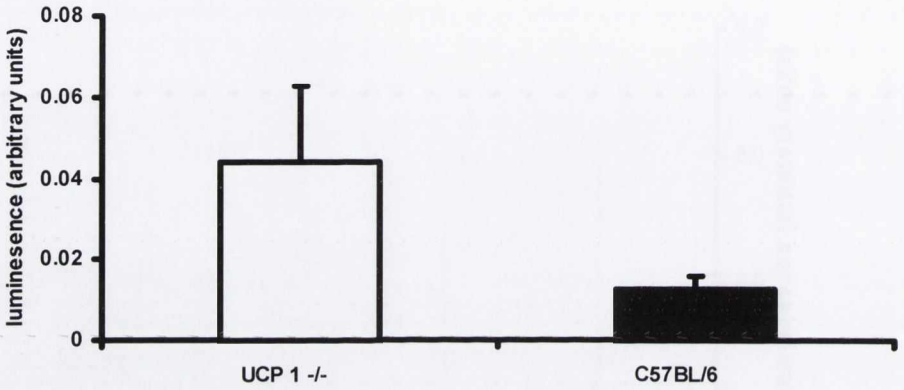

Figure 4.8 Intracellular ADP levels in thymocytes from UCP 1 knock out 3 week old mice compared to thymocytes from 3 week old wild-type mice.

Thymocytes were isolated and 10 min after initial ATP levels were read , residual ATP was measured. Then ADP was converted to ATP and luminescence was measured again. The residual value was subtracted from the final reading. 10000 cells were used for each reading. Data are expressed as mean +/- SEM of each group (n=3). No statistical difference between UCP 1 knock out and wild-type mice (p= 0.17).

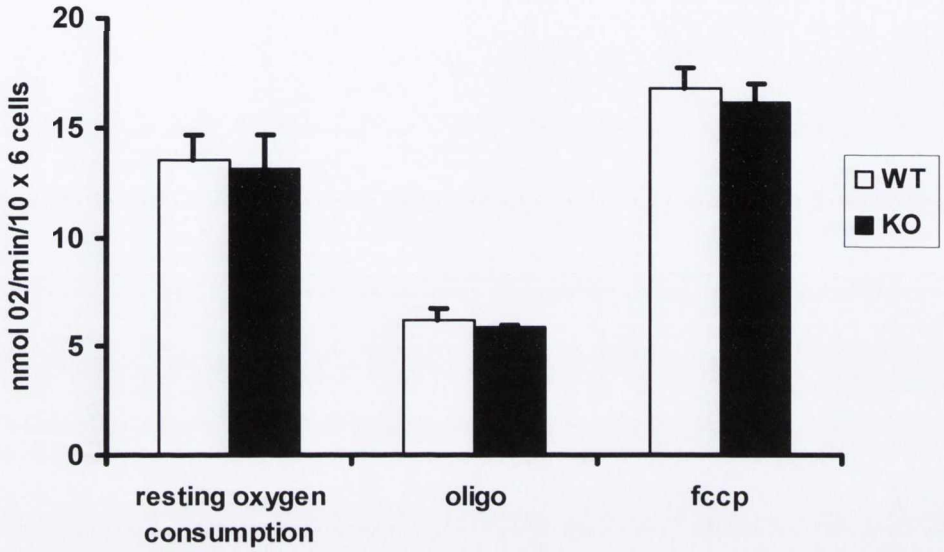

Figure 4.9 Resting, state 4 and maximum oxygen consumption rates by thymocytes isolated from 3 week old female wild-type mice compared to thymocytes isolated from three week old female UCP 1 knock out mice.

Thymocytes were isolated as described in section 2.3. Subsequent oxygen consumption rates by thymocytes ($5x10^6$/ml) were determined at 37°C in RPMI-1640 in a precalibrated Oroboros Oxygraph. Steady –state oxygen consumption rates were then obtained. 1 µg/ml oligomycin was added followed by titration with 0.25 µM FCCP to achieve the state 4 uncoupled rate. Data are expressed as mean ± SEM of at least three independent experiments, each experiment performed in triplicate. No significant differences were observed.

[4.3] Discussion

We have previously demonstrated empirically and using confocal microscopy that thymocytes from mice have uncoupling protein 1 (UCP 1) associated with their mitochondria (Carroll *et al.*, 2004, Carroll *et al.*, 2005, Adams *et al.*, 2007, Adams *et al.*, 2008). In light of this observation we set in this study to demonstrate whether there was any difference in thymus function by comparing profiles and function of thymocytes isolated from wild-type and UCP 1 knock out mice. Initial anatomical investigations gave no indication of any cellular phenotypic difference as there was no detectable difference in the mass of thymus and spleen from wild-type and UCP 1 knock out mice (Table 4.1). However, when cell numbers from thymus and spleen are compared, there is a significant ~3-fold reduction in cell numbers in spleen, with no significant difference in cell number in thymus in a comparison of wild-type and UCP 1 knock-out mice (Figure 4.1). Interpreting the data so far would suggest that the absence of UCP 1 in thymus may affect cell number in spleen.

Analysis of the cell populations in a comparison of thymocytes (Figure 4.2) and spleens (Figure 4.3) clearly demonstrates a significant incremental increase in DP cells in the thymus (Figure 4.2(D)) and a significant doubling of DP cells in the peripheral tissue of UCP 1 knock-out mice compared to wild-type mice (Figure 4.3(D)). We conclude from these data that there is either an alteration in the positive or negative selection process in the thymus so that DP cells are in excess in the thymus and spill over into the spleen.

In addition we observed a significant halving of CD8 single positive cells in the thymus (Figure 4.2(C)) concomitant with a halving of CD8 cells in the spleen (Figure 4.3(C)), but no significant changes in CD4 cells in the thymus when comparing cell profile from UCP 1 knock out mice with those from wild type mice. We conclude from these data that the process of determining SP cell type after negative selection is affected by the absence of UCP 1.

The high attrition rate of cells in the thymus, through positive and negative selection by apoptosis, led us to investigate whether our observations of decreased spleen cell numbers (Figure 4.1) and the decreased CD8 and DP cells in the thymus

and spleen of UCP 1 knock-out mice. (Figure 4.2 & 4.3) , might be due to differences in apoptotic potential of thymocytes from wild-type and UCP 1 knock-out mice. Our data clearly demonstrate that apoptotic potential is reduced in thymocytes from UCP 1 knock-out mice when compared to wild type mice (Figure 4.4, 4.5 & 4.6). Our interpretation from these data, in the context of Figures 4.4-4.6, is that the reduced apoptotic potential of thymocytes from UCP 1 knock-out mice probably explains (a) the halving of cell numbers in the spleen (b) the disrupted selection processes of DP cells and (c) the maturation of SP cell type following negative selection.

In light of the fact that we have observed a significant decrease in spontaneous, non-dexamethasone treated, apoptosis in thymocytes from wild-type mice compared to thymocytes from UCP 1 knock-out mice, and in light of the fact that steady state UCP 1 activity may reduce intracellular ATP status in thymocytes, we measured the ATP levels in quiescent thymocytes from wild type and UCP 1 knock out mice. Our observation that quiescent thymocytes from UCP 1 knock out mice have higher ATP levels (Figure 4.7) is consistent with an increased steady-state mitochondrial efficiency in thymocytes from UCP 1 knock out mice compared to the wild-type controls. Furthermore, in light of the fact that nitric oxide mediated induced apoptosis in thymocytes is dependant on efficient mitochondria (Migita *et al.*, 2003) and reduced intracellular ATP levels trigger nitric oxide induced apoptosis (Honda *et al.*, 2003), our observations of higher intracellular ATP levels in cells of a lower apoptotic potential is interesting and may hint at its mechanism. If we thus presume that the higher ATP concentrations in thymocytes of UCP 1 knock-out mice are instrumental in reducing apoptosis, we would hypothesis that the absence of UCP 1 increases the efficiency of the insitu mitochondria resulting in the higher steady state ATP concentration in knock-out mice. Consequent to that, one might expect the proton leak in these quiescent thymocytes of UCP 1 knock-out mice to be reduced compared to thymocytes from wild-type mice which in turn might manifest itself as a decrease in oxygen consumption at the whole cell (thymocyte) oxygen consumption level. This was not apparent though, as there was no significant difference in the whole cell oxygen consumption rates in a comparison of thymocytes from UCP 1 knock out mice and from wild type mice (Figure 4.9). However an equivalent observation was made by Krauss et al., (2002), who observed

no significant difference in the rate of thymocyte oxygen consumption rates in a comparison of UCP 2 knock-out and wild type mice, yet they did manage to detect a difference in insitu proton leak. Future work by us will explore whether insitu proton leak is affected in thymocytes by the absence of UCP 1.

One could argue that the effects we observe on thymus and spleen cell profiles, numbers and apoptotic potential may not in fact be due to absence of UCP 1 directly, but due to secondary effects on BAT function in vivo. There is no doubt that brown fat has been reported to play a role in the development of immune potential (Jankovic, 2006) and that the ablation of UCP 1 can effect mitochondrial proton leak in skeletal muscle, a tissue that does not contain UCP 1(Monemdjou *et al.*, 2000). Such a metabolic influence, if it exists, may well explain differences in profiles and numbers of the immediately accessed thymus and spleen cells. However it is probably less likely that brown adipose tissue is affecting our observed apoptotic potential differerences in thymocytes, as in this instance we are working with isolated cells, no longer under the influence of whatever regulation might be imparted by brown adipose tissue.

Finally, the potential consequence of increased circulating DP cells and reduced CD8 T-cells in the UCP 1 knock-out mice (compared to wild-type controls) are , on the face of it, quite similar, in that CD8 T-cells are anti-cancer and anti-viral whilst increased circulating DP T-cells have been associated with increased cancers and viral infection (Mebius & Kraal, 2005, Nascimbeni *et al.*, 2004). Thus extrapolating from our cell data to the whole animal, one might expect UCP 1 knock-out mice to be more susceptible to cancers and viral infection compared to wild-type controls, however , I am not aware of any whole animal studies, as yet, indicating such vulnerability, but in light of our observations, future investigations may highlight them.

[4.4] Conclusion

In our endeavours to understand the role of mitochondrial uncoupling protein 1 in thymocyte function, we compared cell profiles in thymus and spleen of wild-type mice with those of UCP 1 knock-out mice. We demonstrate that spleen cell

numbers were reduced ~ 3 fold in UCP 1 knock –out mice compared to wild-type mice. Using flow cytometry, we show that there is a halving of CD8 thymocytes in thymus with a significant incremental increase in DP in the thymus of UCP 1 knock-out mice compared to wild-type mice. These data were mirrored by ~ halving of CD8 thymocytes, and a doubling of DP cells in the spleen of UCP 1 knock-out mice compared to wild-type mice. We also show that thymocytes from UCP 1 knock-out mice have a decreased apoptotic potential and higher ATP levels compared to wild-type controls. We conclude that constitutively expressed UCP 1 may play a role in determining T-cell selection in mice.

Chapter 5

Effect of mitogens on UCP 1 expression in thymus

[5.1] Introduction

The thymus is a lymphoid organ that selects T cells for release to the peripheral immune system. Proportional to thymic size, thymic activity (T-cell output) is most active before puberty. Although the need for the thymus to generate a continuous supply of T cells decreases with advancing age, the thymus continues to serve as the site of T-cell differentiation and maturation throughout life (Shimosato & Mukai, 1997). It is now known that various inductive, hormonal, and proliferative signals from epithelial cells contribute to the maturation of thymocytes (Shimosato & Mukai, 1997).

All T cells originate from haematopoietic stem cells in the bone marrow. Haematopoietic progenitors derived from haematopoietic stem cells populate the thymus and expand by cell division to generate a large population of immature thymocytes (Schwarz & Bhandoola, 2006). The earliest thymocytes express neither CD4 nor CD8, and are therefore classed as double-negative ($CD4^-CD8^-$) cells. As they progress through their development they become double-positive thymocytes ($CD4^+CD8^+$), and finally mature to single-positive ($CD4^+CD8^-$ or $CD4^-CD8^+$) thymocytes that are then released from the thymus to peripheral tissues. About 98% of thymocytes die during the development processes in the thymus by failing either positive selection or negative selection; whereas the other 2% survive and leave the thymus to become mature immunocompetent T cells (Baldwin, 2004). Apoptosis plays a critical role in selecting the thymocyte pool, deleting cells expressing an unproductive T cell receptor (TCR), or exhibiting hypo- or hyper-responsiveness upon encountering MHC/self-peptide complexes (Zacharchuk *et al.*, 1991; Page *et al.*, 1996). Apoptotic "checkpoint" reside at the developmental boundary separating double negative (DN) from double positive (DP) thymocytes, and the DP to single positive (SP) transition point (Minter & Osbourne, 2003).

Positive selection "selects for" T-cells capable of interacting with MHC. Double-positive thymocytes ($CD4^+/CD8^+$) move deep into the thymic cortex where they are presented with self-antigens complexed with MHC molecules on the surface of cortical epithelial cells (Hettmann *et al.*, 1999; Lagresle *et al.*, 2002). Only those

thymocytes that bind the MHC/antigen complex with adequate affinity will survive. The implication of this binding is that all T cells must be able to recognize self antigens to a certain degree. Developing thymocytes that do not have adequate affinity cannot serve useful functions in the body. Also, the thymocyte must be able to recognize antigens that are self from non-self. Because of this, the thymocytes with no affinity for self antigens die by apoptosis and are engulfed by macrophages (von Boehmer, *et al.*, 1989).

A thymocyte's fate is also determined during positive selection. Double-positive cells ($CD4^+/CD8^+$) that are positively selected on major histocompatability complex (MHC) class II molecules will eventually become $CD4^+$ cells, while cells positively selected on major histocompatability complex (MHC) class I molecules mature into $CD8^+$ cells (von Boehmer, *et al.*, 1989). A T cell becomes a $CD4^+$ cell by downregulating expression of its CD8 cell surface receptors (Sawada & Littman, 1991; Sawada *et al.*, 1994). If the cell does not lose its signal through the immunoreceptor tyrosine–based activation motif (ITAM) pathway, it will continue downregulating CD8 and become a $CD4^+$, single positive cell. But if there is signal drop, the cell stops downregulating CD8 and switches over to downregulating CD4 molecules instead, eventually becoming a $CD8^+$, single positive cell (Leung *et al.*, 2001; Ellmeier *et al.*, 1997).This process does not remove thymocytes that may cause autoimmunity. The potentially autoimmune cells are removed by the process of negative selection.

Negative selection removes thymocytes that are capable of strongly binding with "self" peptides presented by MHC. Thymocytes that survive positive selection migrate towards the boundary of the thymic cortex and thymic medulla (Wolfer *et al.*, 2001; Izon *et al.*, 2001). While in the medulla, they are again presented with self-antigen in complex with MHC molecules on antigen-presenting cells (APCs) such as dendritic cells and macrophages. Thymocytes that interact too strongly with the antigen receive an apoptotic signal that leads to cell death (von Boehmer *at al.*, 1989). The vast majority of all thymocytes end up dying during this process. The remaining cells exit the thymus as mature naive T cells. This process is an important

component of immunological tolerance and serves to prevent the formation of self-reactive T cells that are capable of inducing autoimmune diseases in the host.

However even in normal individuals, negative selection is fool proof; autoreactive T lymphocytes can be quite easily detected in the periphery (Sun *et al.*, 1991; Liblau *et al.*, 1991). These potentially pathogenic cells must be kept in check by the diverse mechanisms of peripheral tolerance induction, such as dominant suppression by Treg cells. From Chapter 4 it was seen that thymocytes isolated from UCP 1 knock-out mice were less susceptible to apoptosis, this could ultimately lead to auto-reactive thymocytes entering the circulation, and possibly causing damage. This led us to provide wild-type and UCP 1 knock-out mice with a challenge from either lipopolysaccharide (LPS) or phytohaemagglutinin (PHA), both of which have effects on the thymocytes and lead to proliferation of T cells. LPS treatment leads to acute thymic atropy in mice, through apoptosis of DP thymocytes in the cortex of the thymus. LPS also leads to more efficient selection of CD4 and CD8 thymocytes and they are activated through antigen presenting cells such as macrophages or dendritic cells. PHA is a lectin, from red kidney bean, that directly acts on the thymocytes in the medulla, leading to their proliferation.

Given that the thymus is the primary site of T cell maturation in the body, that maturation of T cells is a tightly regulated process, errors in the process of selecting functional T cells can be detrimental for an individual leading to a variety of autoimmune diseases. We decided to investigate if UCP 1 expression was affected by T cell proliferation. We also investigated if lack of UCP 1 in the thymus led to differences in thymus weights, total thymocyte number, frequencies of thymocyte subsets, oxygen consumption rates and proton leak when compared to wild-type mice.

[5.2] Results

Since the thymus is most active during the development of the immune system (from the late stages of gestation to early puberty), this is also when UCP 1 expression is maximal. The thymus is also very sensitive to a variety of stresses e.g. bacterial infection, which led to acute thymic atrophy. To investigate if UCP 1 plays a role in the immune response to thymic challenges, wild type mice were injected with mitogenic stimulants, namely LPS (stimulates B cells, and indirectly T cells (through macrophage activation)) and PHA (stimulates thymus derived T cells).

Wild-type 6-10 week old female mice were injected with 50ug LPS in 200ul of PBS, 100ug of PHA in 200ul PBS or 200ul PBS (control) i.p. After injection mice were left for 3 days, as this was when the immune response was maximal (Gruver & Sempowski, 2008). Mice were then sacrificed and mitochondria were isolated from thymus, brown adipose tissue, spleen and liver.

Figure 5.1(A) illustrates the effect of LPS and PHA treatment on UCP 1 protein expression in isolated thymus mitochondria. We observed a significant ($p = 0.03$) ~2 fold increase in UCP 1 in thymus mitochondria from LPS treated mice compared to PBS treated mice while PHA treatment increases significantly ($p= 0.002$) UCP 1 expression in the thymus ~3 fold compared to thymus mitochondria from PBS treated wild-type mice.

UCP 1 knock-out mice were also treated with PBS, LPS and PHA as negative controls. Mitochondria were also isolated from thymus tissue of these knock-out mice as shown in lanes 4-6 of Figure 5.1(A) and as expected no UCP 1 protein was detected. Figure 5.1(B) shows a mitochondrial loading control for the same blot. The bar chart in Figure 5.1(C) shows the relative expression of UCP 1 protein expression as a ratio to PDH expression (loading control).

Mitochondria were also isolated from brown adipose tissue of PBS, LPS and PHA treated wild-type mice, as UCP 1 was initially thought to be exclusively expressed in brown adipocytes (Cannon et al., 1982). UCP 1 is the key molecule in the thermogenic function of BAT, due to its capacity to dissipate the proton gradient (Nicholls and Locke, 1984) leading to more fuel being oxidised and the liberated energy is dissipated as heat instead of being captured as ATP. We observed that LPS

and PHA treatment has no affect on UCP 1 expression in isolated BAT mitochondria compared to BAT from PBS treated wild-type mice (Figure 5.2(A)). BAT mitochondria from UCP 1 knock-out mice were also used as a negative control, lanes 4-6 in Figure 5.2 (A).

Figure 5.1 and Figure 5.2 suggest that UCP 1 might have a unique role in thymus mitochondria. Since the T cells present in the spleen are derived from the thymus, mitochondria were also isolated from the spleens of the PBS, LPS and PHA treated wild-type mice (and the UCP 1 knock-out treated mice). Figure 5.3 illustrates that LPS or PHA treatment of wild type mice does not induce the expression of UCP 1 in spleen mitochondria.

Isolated liver mitochondria are frequently used as a negative control for UCP 1 protein expression. Liver mitochondria were isolated from PBS, LPS and PHA treated wild-type mice (and UCP 1 knock-out mice), and as expected no UCP 1 protein was detected (Figure 5.4).

Since UCP 1 protein appears to play a unique role in the thymus, experiments were focused on UCP 1 expression in the thymus. As Figure 5.1 shows a increase in UCP 1 expression in thymus mitochondria after LPA and PHA treatment of wild-type mice, a variety of thymus tissue and cell parameters of wild-type and UCP 1 knock-out mice after treatment with PBS, LPS or PHA were measured , to ascertain whether there were differences in thymocyte sub-sets and function. Figure 5.5 shows the effect of LPS and PHA on thymus mass and thymus cell number.

LPS causes a dramatic decrease in thymic mass (Figure 5.5 (A)) ($p = 0.005$) and in total cell number (Figure 5.5(B)) ($p < 0.0001$) between PBS and LPS treated wild-type mice. PHA had no effect on thymic mass (Figure 5.5(A)) and total cell number (Figure 5.5(B)) between PHA treated wild-type mice compared to PBS treated wild-type mice.

Figure 5.6 shows the effect of LPS and PHA treatment on thymus mass and total cell number in 6-10 week old female UCP 1 knock-out mice. LPS treatment caused significant decrease in thymus mass (Figure 5.6(A))($p = 0.0007$) and thymocyte cell

number (Figure 5.6 (B)) ($p = 0.0001$) in a comparison of the PBS treated UCP 1 knock-out mice and LPS treated UCP 1 knock-out mice.

No significant difference was observed in a comparison of thymus mass (Figure5.6(A)) or thymocyte number (Figure 5.6(B)) in a comparison of PHA treated UCP 1 knock-out mice compared to PBS treated UCP 1 knock-out mice.

Figure 5.7 compares thymus mass and thymus cell number in PBS, LPS and PHA treated wild-type mice and UCP 1 knock out mice. As in Adams et *al.*, 2010, thymus mass in PBS treated UCP 1 knock-out mice when compared to PBS treated wild type mice (Figure 5.7(A)) are consistently heavier. There is no significant difference in thymi mass between LPS treated wild-type and LPS treated UCP I knock-out mice, however thymi from PHA treated UCP 1 knock-out mice are consistently heavier than the PHA treated wild-type mice, if not quite significant.

In Adams et *al.*, 2010, we observed no significant difference in total cell number from 3 week old wild type and UCP 1 knock-out mice. Figure 5.7(B), confirms this in 6-10 week old female mice.

There was no significant difference in the total thymus cell number between LPS treated wild-type and LPS treated UCP 1 knock-out mice (Figure 5.7(B)) or in total cell number between PHA treated wild-type and PHA treated UCP 1 knock- out mice.

Furthermore, we profiled the thymocyte subsets within the thymus of PBS, LPS and PHA treated wild-type mice (Figure 5.8 (A-G)). Figure 5.8 (A-C) are typical examples of primary FACS data for frequency of thymocyte subsets in thymi of PBS, LPS and PHA treated wild-type mice. From the collated data, we are able to demonstrate a significant increase in CD8 cells (Figure 5.8(D)) (LPS, $p = 0.008$)(PHA, $p = 0.01$) and CD4 cells (Figure 5.8(G)) (LPS, $p = 0.02$)(PHA, $p = 0.025$) after LPS and PHA treatment in thymi of wild type mice, and also a significant increase in DN cells (Figure 5.8 (F)) in LPS compared to PBS treated wild-type mice ($p = 0.001$) and in PHA treated mice compared to PBS treated wild-type mice ($p = 0.005$). We also observed a significant decrease in DP cells in the thymi of LPS treated mice compared to the PBS treated wild type mice (Figure 5.8(E)) ($p = 0.01$).

The thymocyte subsets of PBS, LPS and PHA treated UCP 1 knock-out mice were similarly profiled to investigate what effect the lack of UCP 1 has on the selection of T cells after a mitogenic challenge (Figure 5.9). Figure 5.9 (A-C) shows representative primary FACS data for thymocyte subsets from PBS, LPS and PHA treated UCP 1 knock-out mice. Similarly to the wild-type treated mice (Figure 5.8) there is a significant increase in CD8 cells (Figure 5.9 (D)) (LPS, $p = 0.008$) (PHA, $p = 0.0002$) and CD4 cells (Figure 5.9 (G)) (LPS, $p = 0.007$) (PHA, $p < 0.001$) after LPS and PHA treatment of UCP 1 knock-out mice compared to the CD8 and CD4 cell frequency in the thymus of PBS treated UCP 1 knock-out mice. Again there is a very significant (LPS, $p = 0.002$)(PHA, $p < 0.0001$) decrease in DP cells in the thymus of LPS and PHA treated UCP 1 knock-out mice compared to PBS treated UCP 1 knock-out mice (Figure 5.9 (E)). There was no significant difference in the % frequency of DN thymocytes in a comparison of LPS and PHA treated UCP 1 knock-out mice compared to the PBS treated UCP 1 knock out mice (Figure 5.9 (F)).

Figure 5.10 compares the frequency of each thymocyte subset of PBS, LPS and PHA treated mice between wild type and UCP 1 knock-out mice. Figure 5.10(A) compares the % frequency of CD4 thymocytes for each treatment in a comparison of wild-type and UCP 1 knock-out mice. We observed a significant increase in CD4 thymocytes in UCP 1 knock-out mice after both LPS ($p = 0.02$) and PHA ($p = 0.01$) treatment compared to the treated wild-type mice.

Figure 5.10 (B) compares the frequency of CD8 thymocytes after each treatment between wild type and UCP 1 knock-out mice. We observed significantly more CD8 thymocytes in PHA treated UCP 1 knock-out mice compared to the PHA treated wild type mice ($p = 0.02$). We also observed a significant decrease in the frequency of DP thymocytes in both LPS and PHA treated UCP 1 knock-out mice compared to the corresponding LPS and PHA treated wild-type mice (LPS, $p= 0.04$)(PHA, $p= 0.008$)(Figure 5.10 (C)).

No significant difference in frequencies of DN thymocytes in PBS, LPS and PHA treated wild type was observed compared to the corresponding treatment in the UCP 1 knock-out mice (Figure 5.10(D)).

Table 5.1 displays the frequency of T cell subsets (mean ± SEM) in tabular form and the absolute number of each thymocyte subset (mean ± SEM). From the absolute numbers it can be seen that there is a significant ~ 3 fold ($p = 0.0007$) increase in the amount of CD4 thymocytes in a comparison of wild type and UCP 1 knock out mice after the same PHA treatment, ~20 million in wild type mice compared to ~67 million in UCP 1 knock out mice . Similarly there is a significant ($p = 0.0009$) ~ 3 fold increase in the amount of CD8 thymocytes between wild type and UCP 1 knock out after PHA treatment, from ~7 million CD8 T cells to ~ 23 million T cells.

Since LPS and PHA both have a mitogenic response on thymocytes and stimulate cell proliferation, we decided to investigate if this had any effect on the basal oxygen consumption of thymocytes isolated from the treated mice. We also measured the oligomycin rate as UCP 1 protein is increased after LPS and PHA treatment in wild type mice. Maximum oxygen consumption was also measured. Figure 5.11 displays the rates of oxygen consumption for isolated thymocytes from PBS, LPS and PHA treated wild-type mice.

We observed a significant increase in basal oxygen consumption in thymocytes isolated from LPS treated wild-type mice compared to the thymocytes isolated from the PBS treated wild-type mice ($p = 0.0008$). There was no difference in resting oxygen consumption rates of thymocytes isolated from PHA treated wild-type mice compared to PBS treated wild-type mice. There was no significant difference in oligomycin rates obtained between the isolated thymocytes from the LPS and PHA treated wild-type mice compared to the thymocytes isolated from PBS treated wild-type mice. Figure 5.12 illustrates the rates of oxygen consumption for thymocytes isolated from PBS, LPS and PHA treated UCP 1 knock-out mice.

There appears to be no impact of the absence of UCP 1 on the oxygen consumption rates or proton leak for isolated thymocytes from PBS, LPS and PHA treated wild-type mice compared to the rates from treated UCP 1 knock out mice (Figure 5.13).

To investigate if UCP 1 protein expression could be increased in vitro in isolated thymocytes after mitogenic stimulation with LPS or PHA, isolated

thymocytes from wild-type mice were treated with LPS or PHA for 24 hours. After this time, cell lysates were immunoblotted for UCP 1 protein.

In vitro treatment of isolated thymocytes with either PHA (Figure 5.14(A)) or LPS (Figure 5.14 (B)) led to an apparent reduction in UCP 1 protein expression compared to PBS treated control thymocytes after 24 hours. Loading controls for cell lysate using β-actin are also shown.

Since UCP 1 protein expression appears to be increased after an immune challenge in wild-type mice, activated peritoneal neutrophils were lysed and subjected to SDS-PAGE, transferred to PDVF and immunoreative proteins were detected using the anti-UCP 1 peptide antibody (Sigma) (Figure 5.15).

Lane 1 of Figure 5.15 contains 100μg of wild type thymocyte lysate and lane 2 contains 150μg of the activated neutrophils. Figure 5.15 shows the expression of UCP 1 in activated neutrophils.

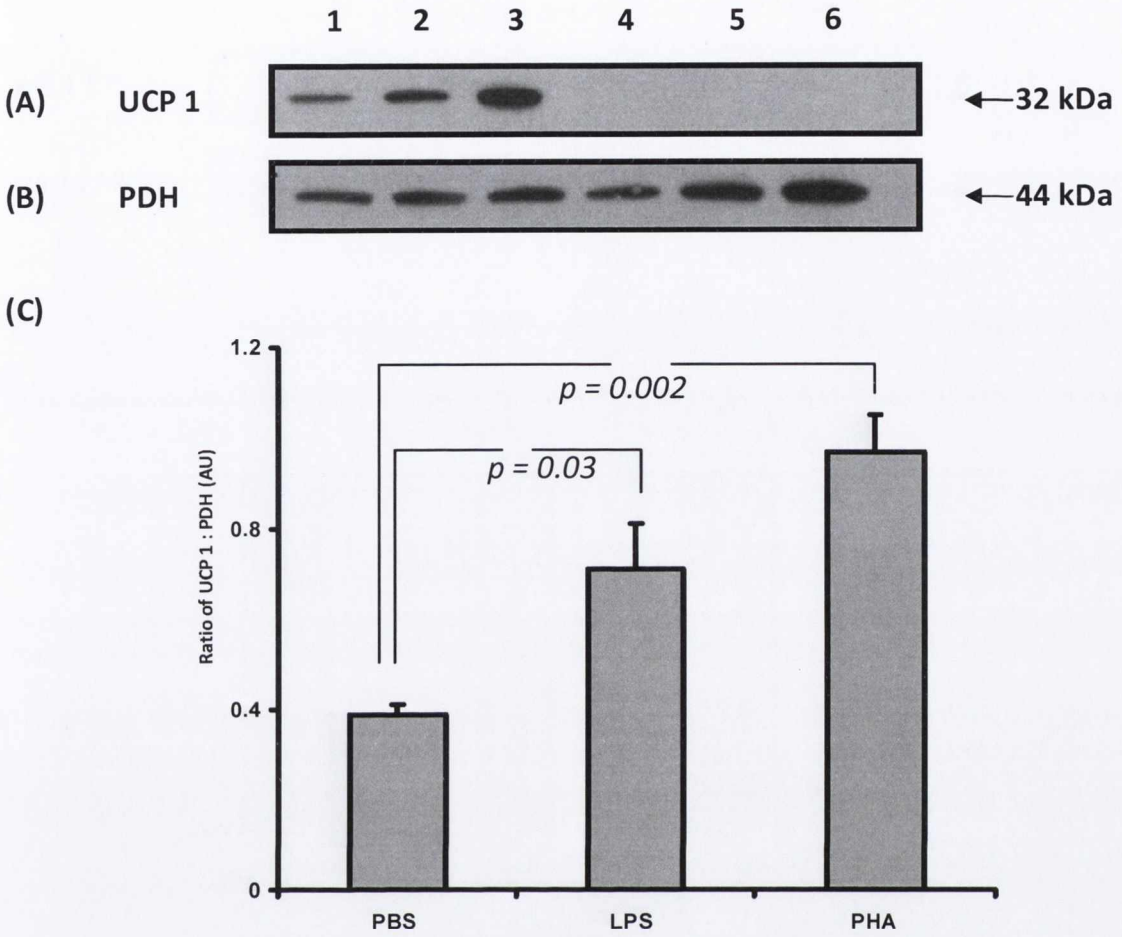

Figure 5.1. The effect of LPS and PHA on UCP 1 expression in mitochondria isolated from thymus of LPS and PHA treated wild-type mice.

UCP 1 protein expression in isolated thymus mitochondria from 6-10 week old ♀ wild-type mice (or control UCP 1 knock out mice) injected with either LPS or PHA or a similar volume of PBS control. Immunoblotting was performed with 10µg of mitochondrial protein per well using an anti-UCP 1 (Sigma) peptide antibody **(A)** and an anti-PDH (Millipore) peptide antibody **(B)** . All antibodies were used at a 1:1000 dilution. The bar chart **(C)** shows the relative abundance of UCP 1 protein expression as a ratio to PDH, as determined by densitometry, for 3 separate preparations. Data is expressed as mean ±S.E.M. Values of p were obtained by unpaired Student's t test (2-tailed), values less than < 0.05 were deemed significant.

1. 10µg thymus mitochondria / Wild-type PBS mouse
2. 10µg thymus mitochondria / Wild-type LPS mouse
3. 10µg thymus mitochondria / Wild-type PHA mouse
4. 10µg thymus mitochondria / UCP 1 knock out PBS mouse
5. 10µg thymus mitochondria / UCP 1 knock out LPS mouse
6. 10µg thymus mitochondria / UCP 1 knock out PHA mouse

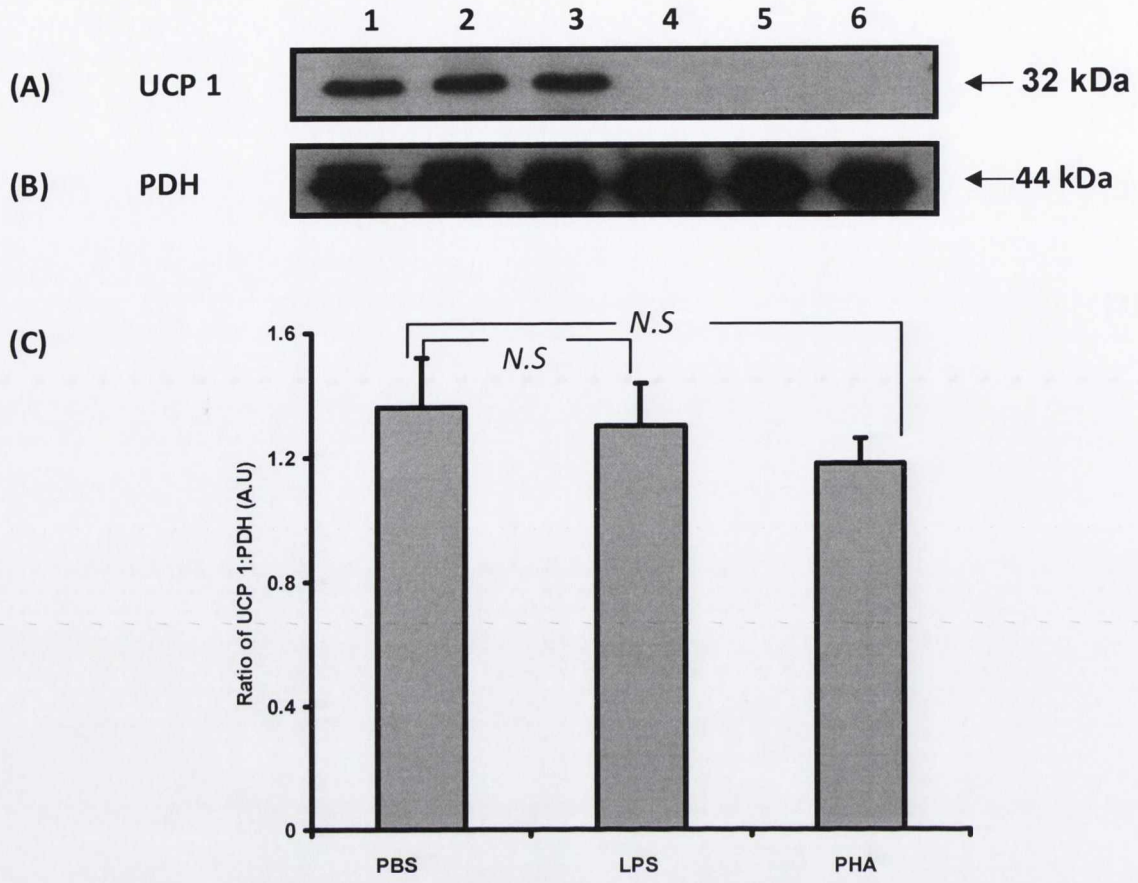

Figure 5.2. The effect of LPS and PHA on UCP 1 expression in mitochondria isolated from BAT of LPS and PHA treated wild-type mice.

UCP 1 protein expression in isolated BAT mitochondria from 6-10 week old ♀ wild-type mice (or control UCP 1 knock out mice) injected with either LPS or PHA or a similar volume of PBS control. Immunoblotting was performed with 10µg of mitochondrial protein per well using an anti-UCP 1 (Sigma) peptide antibody **(A)** and an anti-PDH (Millipore) peptide antibody **(B)** . All antibodies were used at a 1:1000 dilution. The bar chart **(C)** shows the relative abundance of UCP 1 protein expression as a ratio to PDH, as determined by densitometry, for 3 separate preparations. Data is expressed as mean ±S.E.M. Values of p were obtained by unpaired Student's t test (2-tailed), values less than < 0.05 were deemed significant.

1. 10µg BAT mitochondria / Wildtype PBS mouse
2. 10µg BAT mitochondria / Wildtype LPS mouse
3. 10µg BAT mitochondria / Wildtype PHA mouse
4. 10µg BAT mitochondria / UCP 1 knock out PBS mouse
5. 10µg BAT mitochondria / UCP 1 knock out LPS mouse
6. 10µg BAT mitochondria / UCP 1 knock out PHA mouse

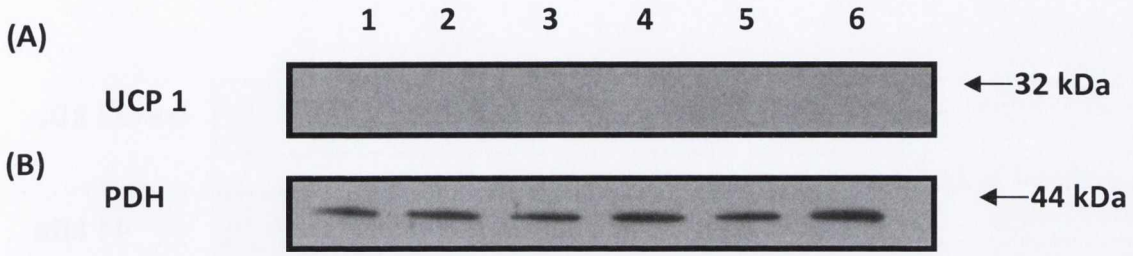

Figure 5.3. The effect of LPS and PHA does on UCP 1 expression in mitochondria isolated from spleen of LPS and PHA treated wild-type mice.

UCP 1 protein expression in isolated spleen mitochondria from 6-10 week old ♀ wild-type mice (or control UCP 1 knock out mice) injected with either LPS or PHA or a similar volume of PBS control. Immunoblotting was performed with 10µg of mitochondrial protein per well using an anti-UCP 1 (Sigma) peptide antibody **(A)** and an anti-PDH (Millipore) peptide antibody **(B)** . All antibodies were used at a 1:1000 dilution.

1. 10µg spleen mitochondria / Wild-type PBS mouse
2. 10µg spleen mitochondria / Wild-type LPS mouse
3. 10µg spleen mitochondria / Wild-type PHA mouse
4. 10µg spleen mitochondria / UCP 1 knock out PBS mouse
5. 10µg spleen mitochondria / UCP 1 knock out LPS mouse
6. 10µg spleen mitochondria / UCP 1 knock out PHA mouse

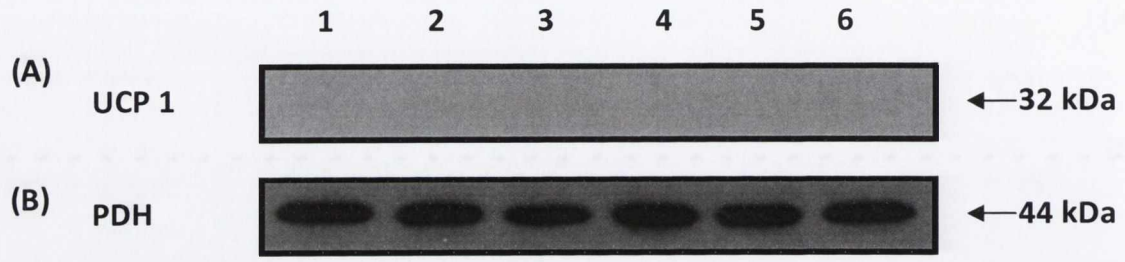

Figure 5.4. The effect of LPS and PHA on UCP 1 expression in mitochondria isolated from liver of LPS and PHA treated wild-type mice.

UCP 1 protein expression in isolated liver mitochondria from 6-10 week old ♀ wild-type mice (or control UCP 1 knock out mice) injected with either LPS or PHA or a similar volume of PBS control. Immunoblotting was performed with 10μg of mitochondrial protein per well using an anti-UCP 1 (Sigma) peptide antibody **(A)** and an anti-PDH (Millipore) peptide antibody **(B)** . All antibodies were used at a 1:1000 dilution.

1. 10μg liver mitochondria / Wildtype PBS mouse
2. 10μg liver mitochondria / Wildtype LPS mouse
3. 10μg liver mitochondria / Wildtype PHA mouse
4. 10μg liver mitochondria / UCP 1 knock out PBS mouse
5. 10μg liver mitochondria / UCP 1 knock out LPS mouse
6. 10μg liver mitochondria / UCP 1 knock out PHA mouse

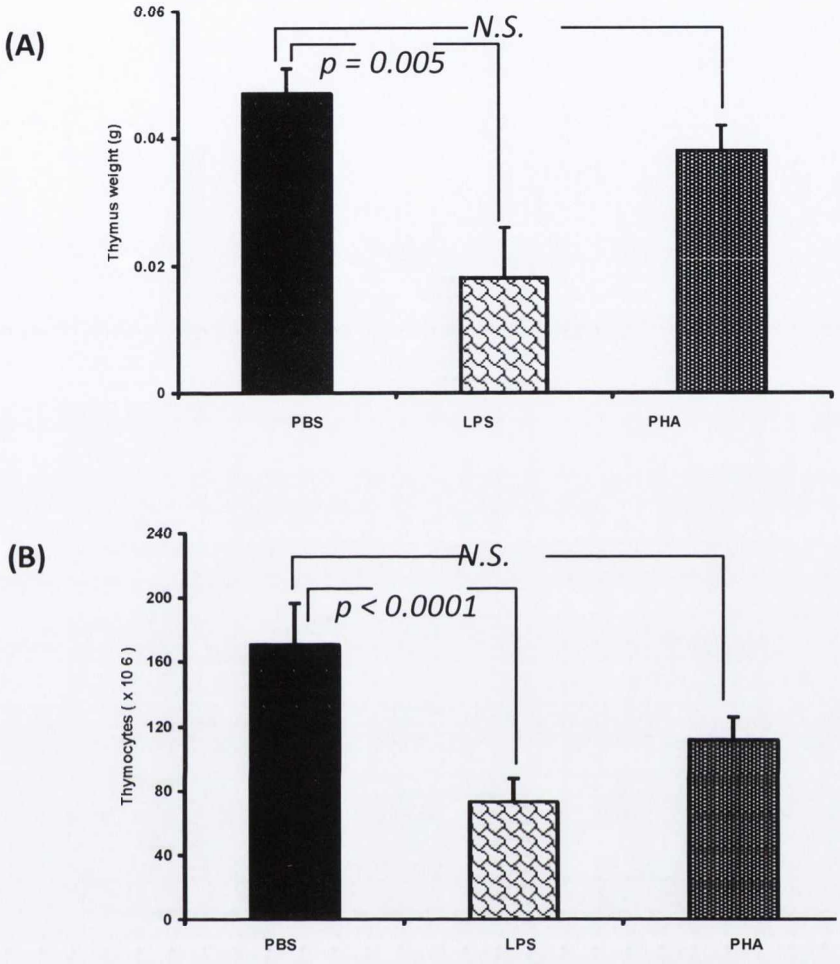

Figure 5.5 Effect of LPS or PHA treatment on thymus weight and thymus cell number in wild-type mice.

Wild-type 6-10 week old ♀ mice were given i.p. injections of LPS (50 ug/mouse), PHA (100ug/mouse) or PBS. Three days after injections the mice were sacrificed, thymus was removed and weighed. Mean thymus weight (A) and absolute number of thymocytes (B) +/- SEM of each group (n= at least 5) are shown. Values of p were obtained by unpaired Student's t test (2-tailed), values less than < 0.05 were deemed significant.

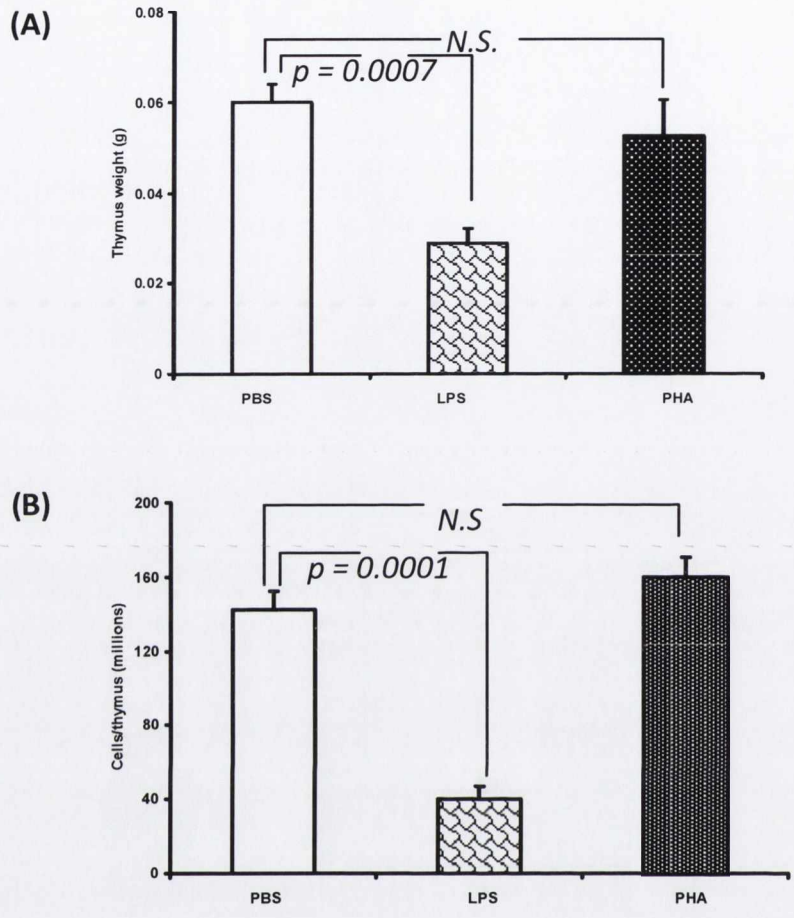

Figure 5.6 Effect of LPS or PHA treatment on thymus weight and thymus cell number in UCP 1 knock-out mice.

UCP 1 Knock-out 6-10 week old ♀ mice were given i.p. injections of LPS (50 ug/mouse), PHA (100ug/mouse) or PBS. Three days after injections the mice were sacrificed, thymus was removed and weighed. Mean thymus weight (A) and absolute number of thymocytes (B) +/- SEM of each group (n=3) are shown. . Statistical significance for the difference in weight of the thymus or cell number post LPS or PHA treatment, were obtained by the unpaired Student's t test (2-tailed), values less than < 0.05 were deemed significant.

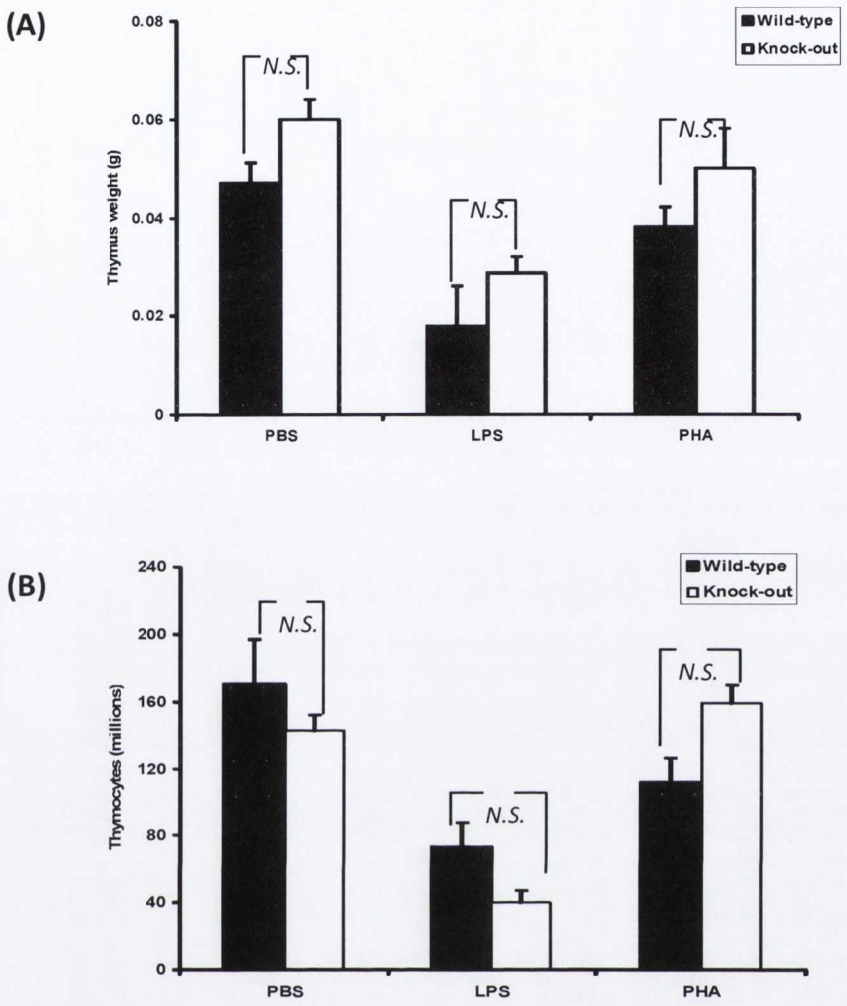

Figure 5.7. A comparsion of thymus mass and cell number in PBS , LPS and PHA treated 6-10 week old ♀ wild-type and UCP 1 knock out mice.

Three days after injections the mice were sacrificed, thymus was removed, weighed and thymocytes counted. Data are expressed as mean +/- SEM of each group (n=3). Values of p were obtained by unpaired Student's t test (2-tailed), values less than < 0.05 were deemed significant.

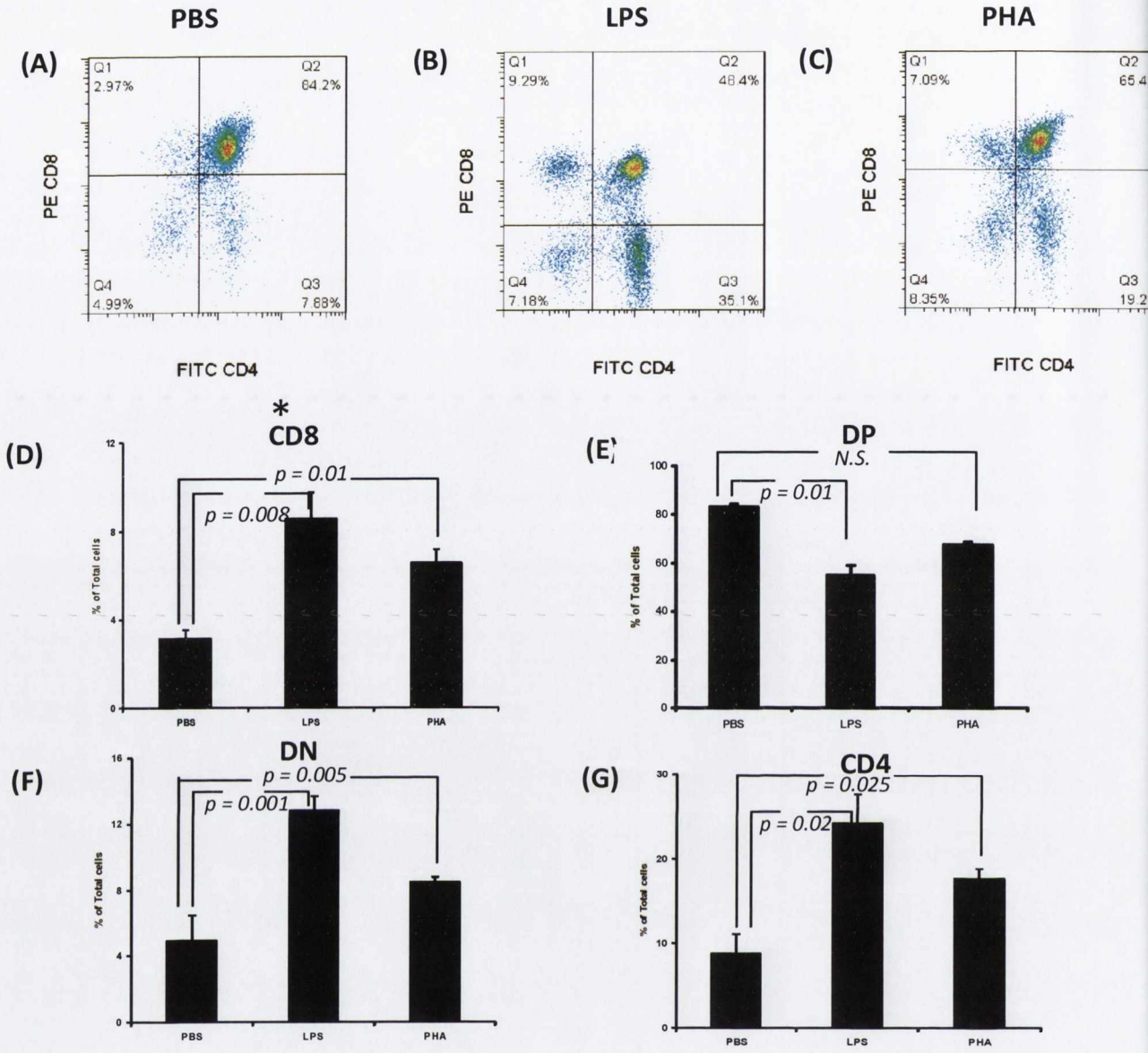

Figure 5.8 Frequency (%) of thymocyte subsets in 6-10 week old ♀ wild-type mice after treatment with PBS, PHA or LPS.

Female 6-10 week old wild-type mice were simultaneously administered (i.p.) either PBS, PHA (100 µg/mouse) or *E. coli* LPS (50 µg/mouse). Three days after injections the mice were sacrificed and thymus was removed. Thymocytes were isolated and the cells were stained with FITC-conjugated anti-CD4, R-PE-conjugated anti-CD8 (both from BD Biosciences) and analyzed on the FACS Cyan. Representative dot-plots for thymocytes from (A) PBS, (B) LPS and (C)PHA mice are shown. Numbers represent percentage of total cells in each quadrant using 10,000 cells. The percentage of cells that are (D) CD8 single positive (CD8), (E) CD8/CD4 double positive (DP), (F) CD8 and CD4 double negative (DN) and (G) CD4 single positive (CD4) are indicated. Data are mean ± SEM of three experiments performed in at least triplicate. p values ≤ 0.05 on an unpaired Student's 't'-test were deemed significant.

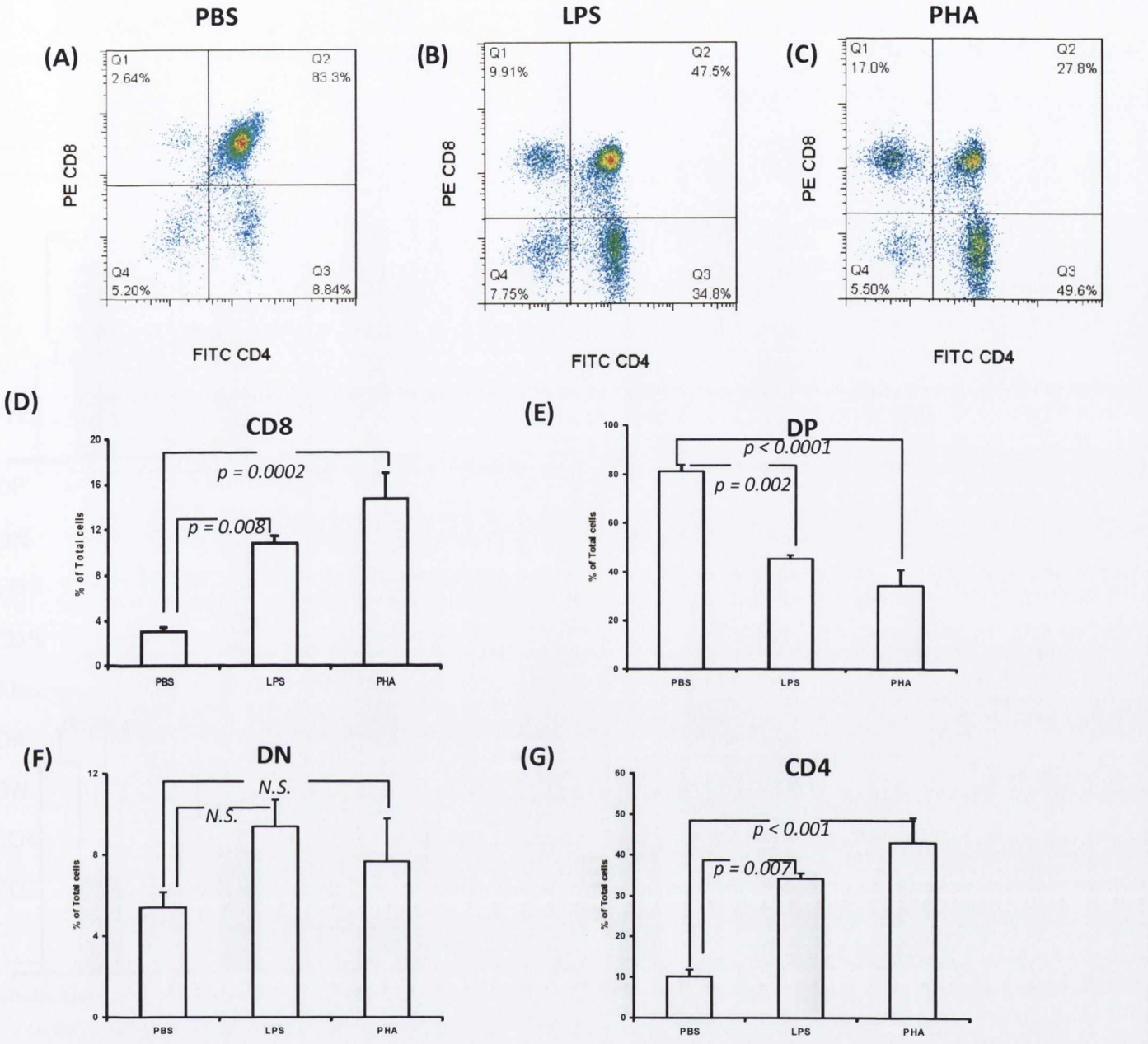

Figure 5.9 Frequency (%) of thymocyte subsets in 6-10 week old ♀ UCP 1 knock-out mice after treatment with PBS, PHA or LPS.

Female 6-10 week old UCP 1 knock-out mice were simultaneously administered (i.p.) either PBS, PHA (100 µg/mouse) or *E. coli* LPS (50 µg/mouse). Three days after injections the mice were sacrificed and thymus was removed. Thymocytes were isolated and the cells were stained with FITC-conjugated anti-CD4, R-PE-conjugated anti-CD8 (both from BD Biosciences) and analyzed on the FACS Cyan. Representative dot-plots for thymocytes from (A) PBS, (B) LPS and (C)PHA mice are shown. Numbers represent percentage of total cells in each quadrant using 10,000 cells. The percentage of cells that are (D) CD8 single positive (CD8), (E) CD8/CD4 double positive (DP), (F) CD8 and CD4 double negative (DN) and (G) CD4 single positive (CD4) are indicated. Data are mean ± SEM of three experiments performed in at least triplicate. p values ≤ 0.05 on an unpaired Student's 't'-test were deemed significant.

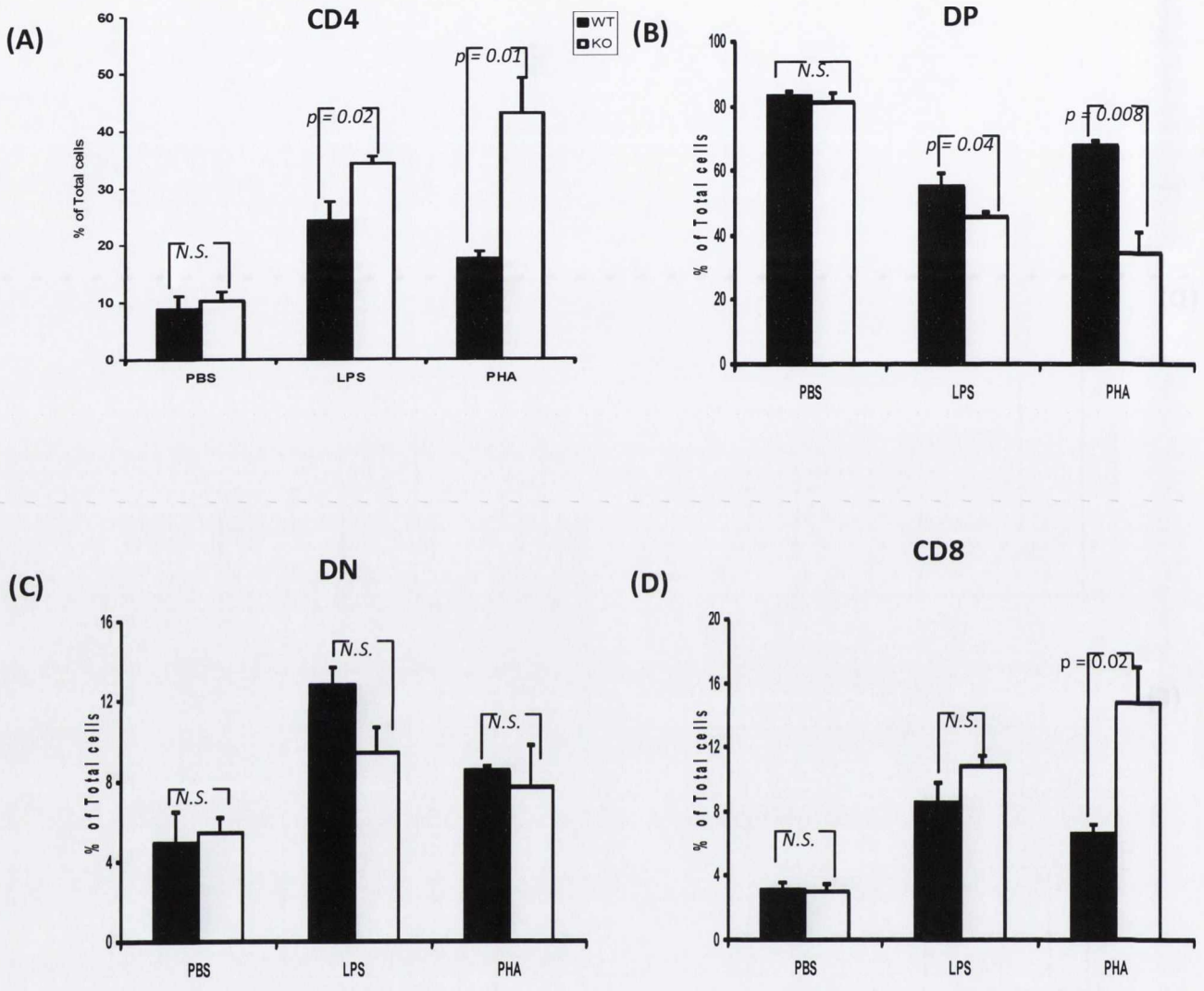

Figure 5.10 Frequency (%) of thymocyte subsets in 6-10 week old ♀ wild-type mice compared to UCP 1 knock-out mice after treatment with PBS, PHA or LPS.

Female 6-10 week old UCP 1 knock-out mice were simultaneously administered (i.p.) either PBS, PHA (100 µg/mouse) or *E. coli* LPS (50 µg/mouse). Three days after injections the mice were sacrificed and thymus was removed. Thymocytes were isolated and the cells were stained with FITC-conjugated anti-CD4, R-PE-conjugated anti-CD8 (both from BD Biosciences) and analyzed on the FACS Cyan. The percentage of cells that are (A) CD4 single positive (CD4) (B) CD8/CD4 double positive (DP) (C) CD8 and CD4 double negative and (D) CD8 single positive (CD8) are indicated. Data are mean ± SEM of three experiments performed in at least triplicate. p values ≤ 0.05 on an unpaired Student's 't'-test were deemed significant.

	Wild -type			UCP 1 Knock-out		
	PBS	LPS	PHA	PBS	LPS	PHA
	(n=3)	(n=3)	(n=3)	(n=3)	(n=3)	(n=5)
Frequency of T cell Subset (%)						
DP	83±1.3	55±4	67.4±1.4	81.2 ± 3	45±1.6*	34.5 ± 6**
DN	4.9±1.5	12.8±0.9	8.5±0.3	5.4 ± 0.7	9.4 ± 1.3	7.6 ± 2
CD4	8.8±2.3	24.1±3.4	17.6±1.1	10.3 ± 1.6	34 ± 1.2*	43 ± 6.2*
CD8	3.1±0.4	8.6±1.2	6.6±0.6	3 ± 0.4	10.8 ± 0.6	14.7 ± 2.3*
Absolute number of T cell subset (x 10^6)						
DP	142 ± 22	40±8	75± 9.3	115 ± 8	18 ±3	55 ± 3.5
DN	8.3 ± 1.2	9.3 ± 2	9.5 ± 1.2	7.7 ± 0.5	3.8 ± 0.6	12 ± .7
CD4	15 ± 2.3	17.6 ± 3.6	19.6 ± 2.5	14.6 ± 1	14 ± 2.4	67 ± 4.4***
CD8	5.3 ± 0.8	6.24 ± 1.3	7.3 ± 0.9	4.3 ± 0.3	4.4 ±0.7	23 ± 1.5***

•Compared to corresponding LPS or PHA wild-type value

* $p < 0.05$

** $p < 0.01$

*** $p < 0.005$

Table 5.1 Frequency and absolute number of thymocytes in thymi from wild-type and UCP 1 knock-out 6-10 week old ♀ mice after treatment with PBS, PHA or LPS.

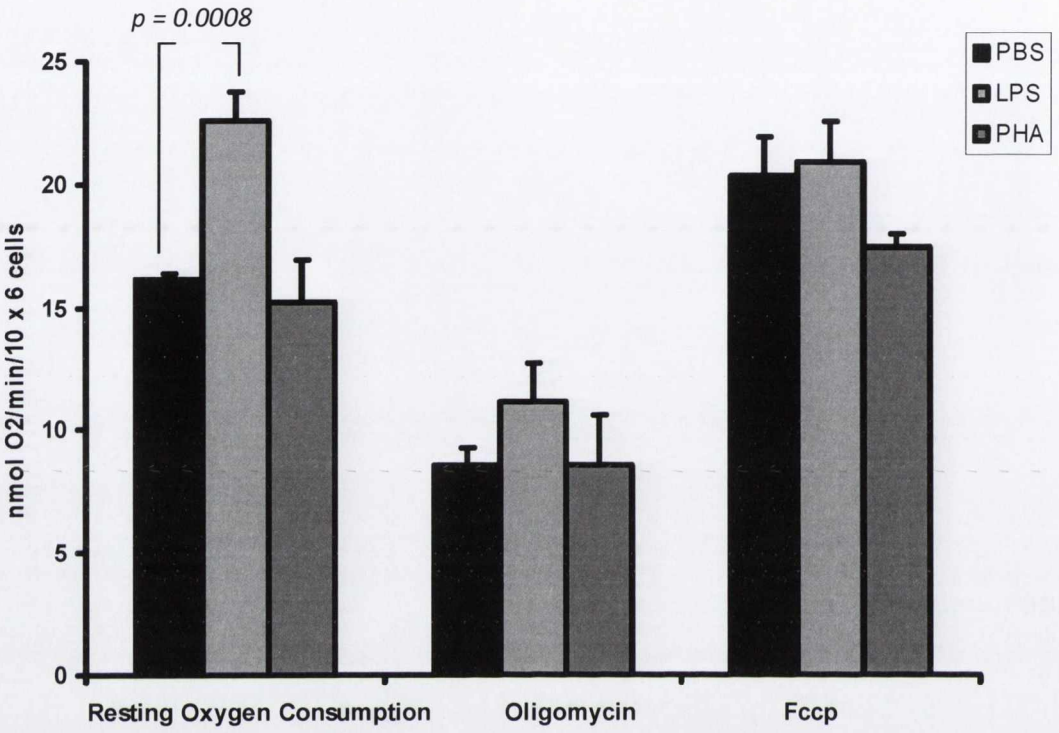

Figure 5.11. Resting oxygen consumption rates by thymocytes isolated from PBS , LPS and PHA treated 6-10 week old ♀ wildtype mice.

Thymocytes were isolated as described in section 2.3. Subsequent oxygen consumption rates by thymocytes ($5x10^6$/ml) were determined at 37°C in RPMI-1640 in a precalibrated Oroboros Oxygraph. Steady –state oxygen consumption rates were then obtained. 1 µg/ml oligomycin was added followed by titration with 0.25µM FCCP to achieve the state 4 uncoupled rate. Data are expressed as mean ± SEM of at least three independant experiments, each experiment performed in triplicate. Values of p less than < 0.05 were deemed significant

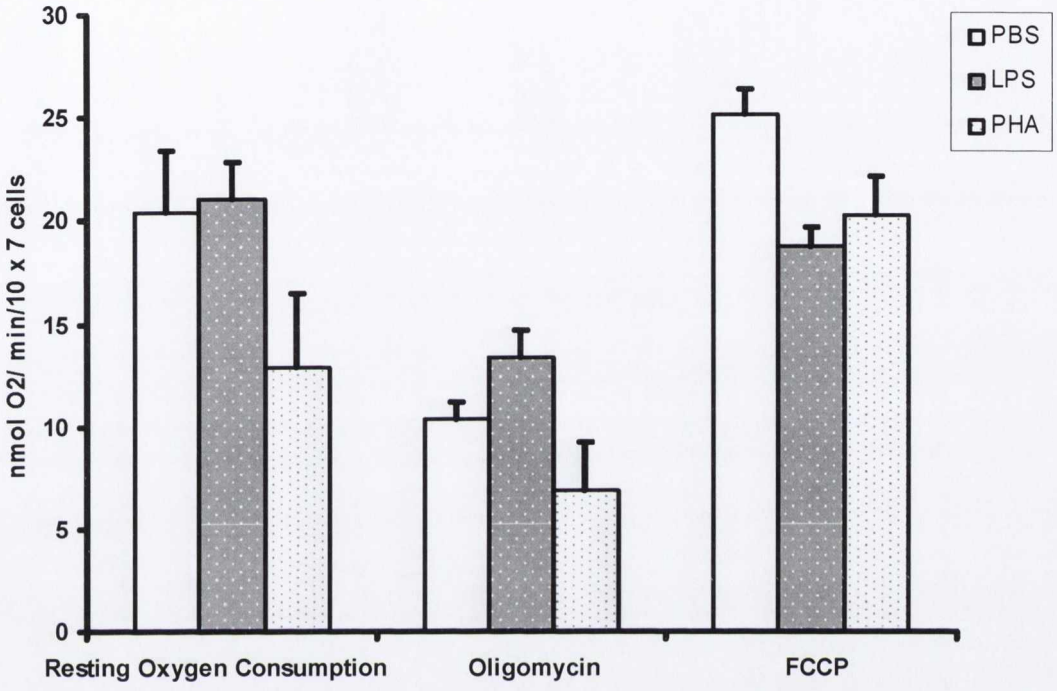

Figure 5.12 Resting oxygen consumption rates by thymocytes isolated from PBS, LPS and PHA treated 6-10 week old ♀ UCP 1 knock out mice.

Thymocytes were isolated as described in section 2.3. Subsequent oxygen consumption rates by thymocytes ($5x10^6$/ml) were determined at 37°C in RPMI-1640 in a precalibrated Oroboros Oxygraph. Steady –state oxygen consumption rates were then obtained. 1 µg/ml oligomycin was added followed by titration with 0.25µM FCCP to achieve the state 4 uncoupled rate. Data are expressed as mean ± SEM of at least three independant experiments, each experiment performed in triplicate. Values of p less than < 0.05 were deemed significant

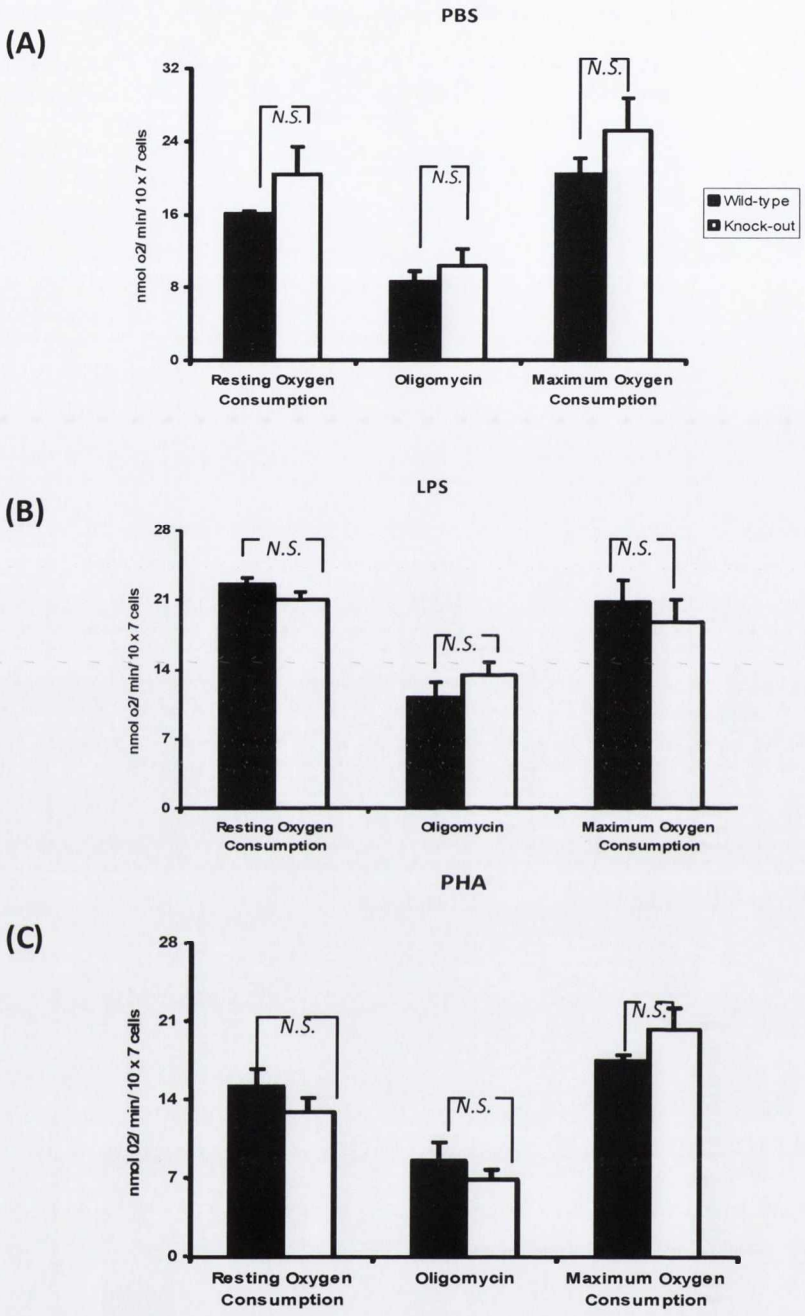

Figure 5.13 Resting oxygen consumption, state 4 and maximum oxygen consumption rates by thymocytes isolated from PBS, LPS and PHA treated 6-10 week old ♀ wildtype mice compared UCP 1 knock out mice.

Thymocytes were isolated as described in section 2.3. Subsequent oxygen consumption rates by thymocytes ($5x10^6$/ml) were determined at 37°C in RPMI-1640 in a precalibrated Oroboros Oxygraph. Steady –state oxygen consumption rates were then obtained. 1 µg/ml oligomycin was added followed by titration with 0.25µM FCCP to achieve the state 4 uncoupled rate. Data are expressed as mean ± SEM of at least three independant experiments, each experiment performed in triplicate. Values of p less than < 0.05 were deemed significant.

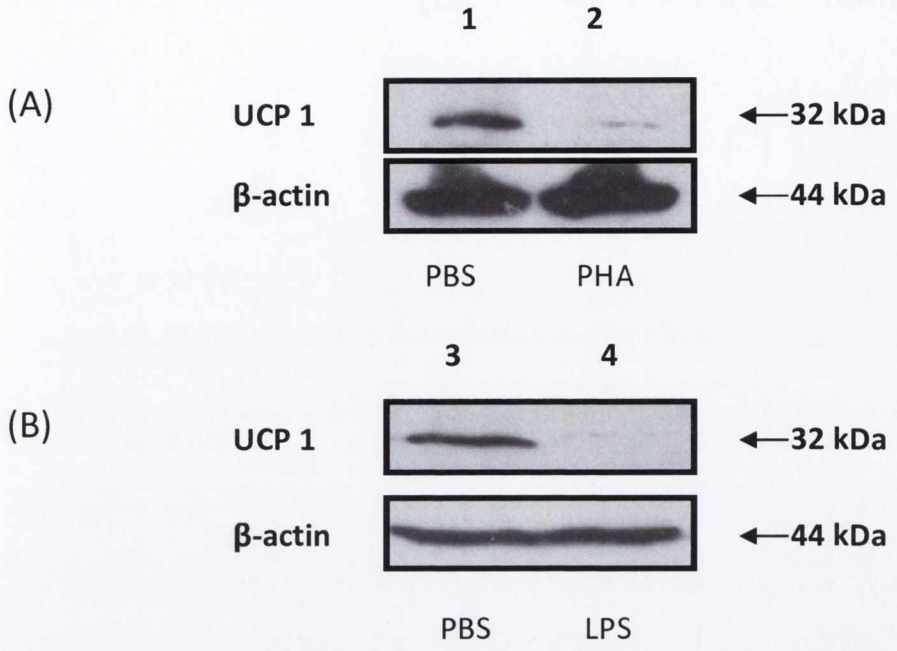

Figure 5.14 UCP 1 expression in naive and mitogen-activated thymocytes.

The expression of UCP 1 in naïve and PHA/LPS-activated thymocytes was determined by immunoblotting. Thymocytes from wild-type mice were cultured in the absence or presence of 10ug/ml PHA (A) or 1ug/ml LPS(B) for 24 hr. After 24 hr, cells were lysed and 100 ug cell lysate were subjected to SDS-PAGE (12% resolving gel) and transferred to PDVF membrane and immunoreactive proteins were detected using anti-UCP 1 peptide antibody (Sigma) and anti-β-actin (Millipore).

1.100μg thymocyte lysate (PBS treated)
2.100μg thymocyte lysate (PHA treated)
3.100μg thymocyte lysate (PBS treated)
4.100μg thymocyte lysate (LPS treated)

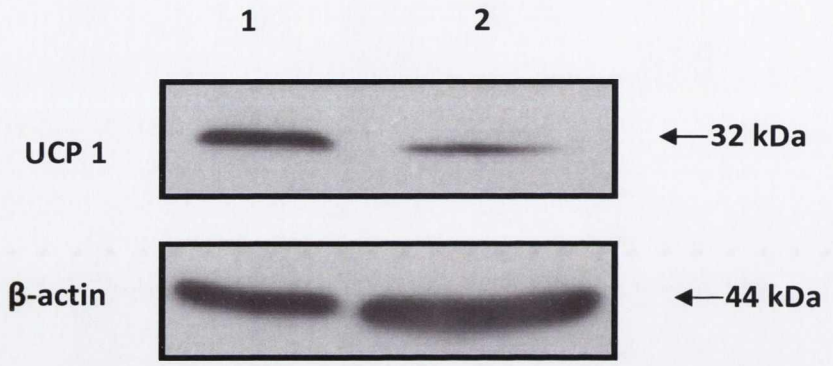

Figure 5.15 UCP 1 protein expression in activated murine peritoneal neutrophils.

Cells were lysed and 100 ug or 150ug cell lysate were subjected to SDS-PAGE (12% resolving gel) and transferred to PDVF membrane and immunoreactive proteins were detected using anti-UCP 1 peptide antibody (Sigma) and anti-β-actin (Millipore).

1.100μg thymocyte lysate wild-type mice

2.150μg lysate from activated murine peritoneal neutrophils

[5.3] Discussion

In light of the fact that UCP 1 activity correlates with apoptotic potential in quiescent thymocytes (Chapter 4), it was decided to investigate if UCP 1 expression in the thymus was affected by mitogenic stimulants in vivo by treatment with LPS or PHA. LPS, indirectly and PHA, directly, are both mitogens for T cells, leading to proliferation of T cells. LPS, through the activation of macrophages, stimulates the production of CD4 and CD8 T-cells (Gruver & Sempowski, 2008, Baroni *et al.*, 1976) and an ablation of DP thymocytes from the thymic cortex. In addition, mitogenic lectins, like PHA, stimulate production of thymus dependent lymphocytes (T-cells), but through direct interaction with the thymus, and induce their proliferation into the peripheral immune system (Zhang *et al.*, 2009)

We were able to demonstrate that UCP 1 expression in the thymus is significantly increased ~2 fold in LPS treated wild-type mice and ~3 fold in PHA treated wild-type mice compared to control PBS treated mice (Figure 5.1). UCP 1 protein expression was not affected in brown adipose tissue by in vivo treatment of mice with LPS or PHA (Figure 5.2). There have been some reports suggesting a stimulatory effect of LPS on BAT thermogenesis, as manifest through an increase in GDP binding to mitochondria and increased blood flow to this tissue (Rothwell, 1989 Gwosdow *et al.*, 1990). However, Okamatsu-Ogura *et al.* (2007) found that there was no effect of LPS on UCP 1 mRNA level in brown adipose tissue. Saito *et al.* (1991) also reported that IL-1β/LPS increases norepinephrine turnover in spleen and lung, but not in BAT, indicating the absence of activation of sympathetic nerve to BAT in fever. Taken together, our results and those in the literature suggest little or no stimulatory effect of LPS on BAT thermogenesis. Okamatsu-Ogura *et al.* (2007) also investigated whether the thermogenic effect of LPS was affected by the ablation of *ucp1* gene. They observed an increase in body temperature in UCP 1 knock-out mice, in the same way as wild-type mice, confirming similar febrile response in the two types of mice. In regard to PHA, no effect of PHA on UCP 1 expression in BAT would be expected as PHA is a specific mitogen for T cells (Zhang *et al.*, 2009), and subsequently in accordance with this prediction we saw no change in the level of UCP 1 expression in BAT following PHA treatment of WT mice as indicated in Figure 5.2.

Since all circulating T cells, are derived from the thymus, combined with the fact that LPS and PHA treatment increases UCP 1 expression in the thymus, we sought to investigate whether this increase in UCP 1 protein manifested itself as expression of UCP 1 in the T-cells in the spleen. However no UCP 1 could be detected in the spleen (Figure 5.3). This may reflect the fact that there is no UCP1 in the T-cells of the spleen or that UCP 1 expression in T-cells is at too low a level to be detected within the milieu of other cells in the spleen. Reassuringly, no UCP 1 expression was detected in liver mitochondria after LPS or PHA treatment (Figure 5.4) as the liver is frequently used as a negative control for UCP 1 expression. So in light of the observation that UCP 1 was only increased in the thymus mitochondria after LPS and PHA treatment of wild-type mice, and not in mitochondria from brown adipose tissue or spleen, we decided to focus investigations on the thymus.

Apart from its role, in the short-term, in promoting CD4 and CD8 production in the thymus, LPS is known to cause acute thymic atrophy leading to a dramatic decrease in thymus weight and thymus cell number (Baroni *et al.*, 1976, Rocha *et al.*, 2005), and in our study a reduction in thymus mass was observed following LPS treatment of wild-type mice compared to PBS treated controls (Figure 5.5). We observed a significant ~2.5 fold decrease in thymic weight and a significant 2.5-fold decrease in thymus cell number upon treatment of mice with LPS in a comparison with PBS treated wild-type mice. PHA induces the acquisition of T cell markers, an index of maturation, and depending on dosage, leads to a decrease in thymus weight and thymus cell number as naïve T-cells leave the thymus and enter the periphery (Wagener, 1973). In our study, PHA treatment of wild-type mice did not affect thymus cell number or thymus weight (Figure 5.5) which is in agreement with Wagener (1973) for the dose used.

We also investigated whether lack of UCP1 affected thymus mass and thymus cell number following PBS, LPS and PHA treatment. PBS, LPS and PHA treated UCP 1 knock out mice displayed the same trends as the wild-type mice in regard to thymus weight and thymus cell number (Figure 5.6 & B). In the LPS treated UCP 1 knock out mice there was a significant decrease in thymus weight ($p= 0.0007$) and a significant decrease in total thymus cell number ($p= 0.0001$) compared to PBS treated wild-type mice. No significant differences in thymus weight or total thymocyte number were

observed. The PBS treated wild-type and UCP 1 knock-out data, regarding thymus mass and cell number is consistent with Adams *et al.* (2010), in that lack of UCP 1 does not affect thymus mass or thymus cell number after LPS or PHA treatment (Figure 5.7)

Despite the fact that no significant differences were seen in thymus mass or total thymocyte number between PBS, LPS and PHA treated wild-type and UCP 1 knock-out mice, one might expect the proportion of thymocyte subsets to vary as a result of LPS and PHA treatment of mice, as in Adams *et al.*, (2010) we observed significant differences in thymocyte subset proportions, with more DP and CD8 thymocytes in three week old female UCP 1 knock out mice compared to three week old wild-type mice. This increase in CD8 and DP thymocytes was not observed in the thymus of the 6-10 week old PBS treated UCP 1 knock-out mice compared to 6-10 week old wild-type mice. However, there is a dramatic decrease in total thymocyte number between 3 week old mice (~ $250x10^6$ cells) to 6-10 week old mice (~ 150 $x10^6$ cells), consistent in both wild-type and UCP 1 knock-out mice, due to the reduced T cell output after puberty. The milieu of naïve T-lymphocytes is built up in early life, and they enter the peripheral immune system, ready to respond to any immune challenge it may come across. The differences in DP and CD8 frequencies are not observed in a comparison of PBS treated 6-10 week old female wild-type mice and PBS treated 6-10 week old female UCP 1 knock-out mice, perhaps since most of the mature lymphocytes have already exited the thymus.

In LPS treated wild-type mice there was a significant increase (~3 fold) in CD4 and CD8 T-cells [p=0.02 & p=0.01, respectively], and a significant (~25% decrease) decrease in DPs [p=0.005] (Figure 5.8). LPS has been demonstrated to selectively causes apoptosis of DP thymocytes (Rocha *et al.*, 2005), and increased selection of CD4 and CD8 positive cells, which is consistent with the known effects of LPS to stimulate T cell proliferation through macrophages (Baroni *et al.* 1974, Gruver & Sempowski, 2008). Our data are consistent with these observations in the literature. Since PHA stimulates maturation of T-lymphocytes in the thymic medulla, a significant increase in CD4 and CD8 T-cells was expected (Hallgren *et al.*, 1988), and after PHA treatment the proportion of CD4 and CD8 thymocytes was found to have

doubled significantly [p= 0.02 and p= 0.01, respectively] in the thymus (Figure 5.8 D & G).

Figure 5.9 shows the proportion of thymocyte subsets in UCP 1 knock-out mice after LPS and PHA treatment compared to PBS treated controls. PHA caused a significant ~4 fold increase in the amount of CD8 [p=0.008] and CD4 [p=0.007] single positives T-cells compared to PBS treated control mice (Figure 5.9 (D) & (G)). Correspondingly, there was a significant ~3 fold decrease ($p < 0.0001$) in the total % of DP cells (Figure 5.9(E)). LPS treated UCP 1 knockout mice also had a significant ~3 fold increase in CD4 [$p< 0.001$] and CD8 cells [p=0.0002] (Figure 5.9 (D) & (G)) and a significant halving of DP cells [$p<0.0001$] (Figure 5.9(E)) compared to PBS control UCP 1 knock out mice. The lack of UCP 1 in PHA and LPS treated mice seems to lead to greater proliferation of the CD4 and CD8 T cells, than in the wild-type treated mice.

The effect of the lack of UCP1 in thymus following LPS or PHA treatment of mice is presented in Figure 5.10. In PHA treated UCP 1 knock-out mice compared to PHA treated wild-type mice, there is a significant [(CD4, p=0.01)(CD8, p= 0.02)][p value]~ 3-fold increase in the % of CD4 and CD8 cells (Figure 5.10 (A) & (D)), and a significant [p= 0.008] halving in the % of DP cells (Figure 5.10 (C)) in PHA treated UCP 1 knock-out mice compared to PHA treated wild-type mice. In LPS treated UCP 1 knock-out mice there is a significant [p = 0.02] 25% increase in the frequency of CD4 cells and a significant ~ 20% decrease [p = 0.04] in DP thymocytes compared to LPS treated wild-type mice.

The differences in the proportion of thymocyte subsets following LPS and PHA treatment of wild-type and UCP1 knock-out mice are also reflected in the absolute numbers of cells within the thymocyte subsets measured (Table 5.1). From this table it can be seen that the lack of UCP 1 leads to a significant ~3 fold increase in the absolute number of CD4 [p=0.0007] and CD8 [p=0.0009] naïve T cells in a comparison with PHA treated wild-type mice. This aberrant proliferation of T cells, could lead to inefficient deletion of potentially auto reactive T cells in the thymus (negative selection) and their entry to the peripheral immune system (Chen *et al.*, 2005). These potentially pathogenic cells must be kept in check by the diverse mechanisms of peripheral tolerance induction (Sakaguchi *et al.*, 1995). One of these

mechanisms, dominant suppression by Tregs has become a major focus of research. Tregs are characterised by the transcription factor, FOXP3 (Hori *et al.*, 2003). UCP 1 knock out mice, after an immune challenge with LPS, have been observed to have more FOXP3 mRNA in there Tregs than wild type mice (unpublished observation, Porter & Fallon). The lack of UCP1 and the increased proliferation of T cells could lead to this up regulation of Treg cells to deal with potential autoreactive T cells.
So, combining our observation of a relative increase in the proportion of CD4 and CD8 cells following PHA and LPS treatment in UCP1 knock-out mice compared to wild-type mice [with a concomitant decrease in the proportion of DP cell] with our observations of a relative increase in the amount of CD4 and CD8 cells following PHA treatment in UCP1 knock-out mice compared to wild-type mice [with a concomitant decrease in the amount of DP cells], we conclude that UCP 1 is important for naïve T cell selection in the thymus.

Another interesting observation was that isolated thymocytes from LPS treated wild-type mice had significantly higher levels of oxygen consumption compared to those isolated from PBS treated wild-type mice (Figure 5.10). In light of the fact that UCP1 expression was increased in thymocytes following LPS treatment, we looked to determine whether the observed increase in oxygen consumption rates were due to proton leak. We observed no increase in proton leak in thymocytes isolated from LPS treated wild-type mice compared to PBS treated wild-type mice, as indicated by the absence of any difference in oxygen consumption rates after oligomycin administration to cells. There were no significant differences in oxygen consumption in thymocytes isolated from PHA treated wild-type mice compared with PBS treated wild-type mice (Figure 5.10). To determine if lack of UCP 1 had any effect on oxygen consumption, oxygen consumption rates and proton leak was also measured in thymocytes isolated from treated UCP 1 knock-out mice (Figure 5.11). No differences were observed in any rates. Figure 5.12 provides a direct comparison of oxygen consumption and proton leak for isolated thymocytes from LPS and PHA treated wild-type and UCP 1 knock-out mice mice. There are no significant differences in oxygen consumption or indices of proton leak rates between wild-type and UCP 1 knock-out mice, suggesting UCP 1 does not affect oxygen consumption in

thymocytes isolated from LPS treated mice compared to the PBS treated wild-type mice.

Since there is an increase in UCP 1 protein in thymus after LPS and PHA (Figure 5.1) a difference in oxygen consumption due to proton leak might have been expected, however this is not the case. An increase in UCP abundance in cells following LPS doesn't necessarily result in an increased in mitochondrial proton leak. Couplan *et al.* (2001) showed an increase in UCP 2 in lung mitochondria following LPS treatment but saw no differences in oxygen consumption or proton leak in isolated lung mitochondria. Also, Yu *et al.*, (2000) observed a five-fold increase in UCP 3 mRNA in skeletal muscle after intraperitional injection of LPS to female C57BL6/J mice, but observed no difference in mitochondrial leak between control and LPS treated mice. So if the increase in oxygen consumption in our thymocytes from wild-type mice is not due to increased proton leak, what could it be due to? Well it might be due to an increase in oxygen consumption due to non-oxidative phosphorylation processes, perhaps caused by increased oxygen requirement for cytosolic detoxification and repair purposes after LPS challenge, as shown by New *et al.* (2000). The increase in oxygen consumptions might also be due to a higher level of ATP turnover in the thymocytes following LPS treatment as has been observed for ConA stimulated thymocytes in rats (Buttergeit *et al.*, 1997). We also observed no differences in proton leak between thymocytes isolated from PHA treated mice and their PBS controls (Figure 5.11). So despite that fact that PHA increases UCP1 protein expression in thymocytes, there was no increase in oxygen consumption following PHA treatment (Figure 5.13(c)). This further suggests that UCP 1 does not have an uncoupling role under conditions of mitogenic proliferation in thymocytes.

So if UCP 1 does not have an uncoupling role following LPS and PHA treatment, what other role might it have? Replicative cell division is an energetically demanding process that can be carried out only if cells have sufficient metabolic resources to support a doubling of cell mass (Buttergeit *et al.*, 2000; Gray, 2004). The mitogenic stimulation of thymocytes or naïve T cells induces an almost 20-fold increase in glucose uptake within 1 hour (Grenier *et al.* 1994). In proliferating thymocytes the production of ROS is nearly abolished in comparison to non-stimulated resting thymocytes (Brand

& Hermfissue, 1997). It is believed that this reduction in ROS production in proliferating cells is due to a switch from mitochondrial oxidative phosphorylation to cytosolic glycolysis, thereby preventing ROS production by the respiratory chain due to the greater energy demands of the proliferating cell.

A by-product of all normally functioning mitochondria is a continual non-productive release of electrons from the electron transport chain resulting in the production of intracellular reactive oxygen containing species (ROS), such as superoxide. It is estimated that at least 0.2% of oxygen consumed by mitochondria is converted to ROS (Balaban *et al.*, 2005). The sites of ROS production from the electron transport chain are predominantly complexes I and III with in vitro evidence showing that oxidation through glycerol-3-phosphate dehyrogenase being a major source of ROS (Drahota *et al.*, 2002)(Muller *et al.*, 2004). Vulnerable targets of ROS include local sites such as the mitochondrial inner membrane lipids, like cardiolipin (Nomura *et al.*, 2000) and polyunsaturated fatty acids in membrane lipids in particular (Ernster, 1993). Oxidation of polyunsaturated fatty acids results in highly reactive aldehydes such as 4-hydroxy-2-nonenals which covalently modify and interfere with protein/enzyme function (Sayre, 2006).

However, all cells have antioxidants and antioxidation mechanisms which counteract ROS production by mitochondria to differing extents (Jezek & Hlvata, 2005), such as ubiquinol (Forsmark-Andree *et al.*, 1995). A further potential physiological mechanism to alleviate ROS production by mitochondria is termed mild-uncoupling (Skulachev, 1996). Mild-uncoupling is based on the observations that uncoupling lowers Δp, decreases the degree of reduction in the electron transport chain and thus will reduce ROS from the electron transport chain.

The mitochondrial uncoupling proteins, UCP 2 and UCP 3 have been shown to be efficacious in alleviating ROS production in cells/tissue (McLeod *et al.*, 2005) Dlaskova *et al.*, (2010) have shown that UCP 1 has the potential to alleviate ROS production in brown adipose tissue mitochondria. Mitochondrial uncoupling proteins are known to be activated by reactive oxygen species (Echtay *et al.*, 2002). Clarke & Porter (in preparation) have shown that UCP 1 has the potential to regulate ROS production in isolated thymocyte mitochondria. UCP 2 knock-out mice have

been shown to have an increased proinflammatory response in immune cells triggered by an increased ROS production (Arsenijivic *et al.*, 2000) (Bai *et al*, 2005).).

Although there is a switch to a greater level of glycolysis in the proliferating T cells, there is also an increase in the global rate of oxidative phosphorylation (Krauss *et al.*, 2001). An increase in oxidative phosphorylation activity could potentially increase ROS through glycerol-3-phosphate dehydrogenase. We have shown in this chapter that UCP 1 expression is significantly increased (~2 fold in LPS treated mice (Figure 5.1)) (~3 fold in PHA treated mice (Figure 5.1)) in thymus mitochondria of proliferating cells. This increase in UCP 1 expression may attenuate any putative increase in ROS production which may occur due to the increase in glycerol-3-phosphate dehydrogenase activity. [An increase in oxidative phosphorylation flux usually reduces ROS production by the electron transport chain but an increase in glycerol-3-phosphate dehydrogenase activity would increase ROS production.]

In UCP 1 knock out mice, we see greater proliferation of T cells as discussed earlier and shown in Table 5.1. It has been shown that low levels of ROS stimulate proliferation and enhance cell survival in different cell types (Burdon *et al.*, 1990) (Burdon, 1995) (Burdon *et al.*, 1996). If UCP 1 in thymus mitochondria can attenuate ROS production in a similar manner to UCP 1 in BAT mitochondria (Dlaskova *et al.*, 2010) then thymus mitochondria from UCP 1 knock out mice would have an increased rate of ROS production which could induce the rate of proliferation of T cells in UCP 1 knock out mice.

Another possibility for the increased UCP1 expression following LPS and PHA treatment of mice is that UCP 1 is a pyruvate transporter; Pecqueur *et al.* (2008) have suggested that UCP 2 functions as a pyruvate transporter from the mitochondria to the cytosol in proliferating cells, by promoting fatty acid oxidation and limiting glycolysis-derived utilization, as proliferating cells require the unrestricted availability of glucose. The proliferative phenotype observed in murine embryonic fibroblasts cells lacking UCP 2 could play a role in the alteration of the

immune system obtained in UCP 2 knock-out mice (Arsenijevic *et al.*, 2000)(Vogler *et al.*, 2006). UCP1 may play a similar role in thymocytes.

Having observed an increase in UCP1 in thymocytes of LPS and PHA treated animals, we looked to see whether direct addition of LPS and PHA to isolated thymocytes had an effect on UCP1 expression therein. Isolated thymocytes were treated in vitro with LPS and PHA for 24 hrs. Contrary to what we saw in vivo, UCP 1 expression in thymocytes appears to be reduced by both direct LPS and direct PHA addition to thymocytes (Figure 5.14). Thymocytes should not be able to respond to LPS directly as no TLR4 receptors have ever been detected on their cell surface (Poltorak, 1998), but a decrease in UCP 1 expression was observed. In regard to PHA, thymosin enhances the response of thymic cells of mice to PHA (Rotter *et al.*, 1976). Proliferation of cells induced by mitogens under in vitro conditions is dependant on serum or plasma components such as thymosin (Walker & Lucas, 1971) (Yachin and Raymond, 1975), therefore the lack of serum or plasma components in our in vitro investigation, may explain the differential UCP1 expression results in vitro compared to in vivo. It could however be due to the artificial in vitro system, and the decrease in UCP 1 protein could be due to a secondary effect of the LPS or PHA stimulation (at high levels both can act as toxins).

Another possibility is that UCP 1 may also be present in the mitochondria of the thymic epithelium, perhaps it is increased in these cells after LPS or PHA treatment of wild type mice. Recent evidence for the expression of TLR4 on thymic epithelial cells (TECs) in the medulla has been reported (Bernasconi *et al.*, 2005). Normal thymic development is dependant on the interaction between the thymic epithelium and the haematopoietic thymocytes. Thymocytes that reach the medulla have successfully undergone TCR rearrangement and positive selection in the thymic cortex. In the medulla, upon hormonal and proliferative signals from the medullary TECs thymocytes undergo additional rounds of negative selection to remove the autoreactive T cells (through interaction of TCR with epithelial MHC antigens) from the mature repertoire (Sleckman, 2005). Interestingly it has recently been shown that ROS can act as a cell death inducer and proliferative factor in a cell-

type-specific and concentration-dependant manner within the same tissue (Kim et al., 2010). Kim et al. (2010) observed that ROS induced cell death in the epithelial cells of the kidney through apoptosis while ROS induced proliferation of interstitial cells within the kidney after ischemia and reperfusion injury.

Figure 5.15 shows the detection of UCP 1 in the innate immune system. Neutrophils are the most abundant white blood cells in mammals and are an essential part of the innate immune system. They are the first cells to migrate to the site of inflammation where they engulf bacteria, through phagocytosis, and by production of reactive oxygen species. UCP 2 is thought to control immune cell activation by modulating MAPK pathways and the production of mitochondrial ROS. Inflammation is stronger in Ucp2-KO mice and can lead to exacerbated inflammatory diseases e.g. Type 1 diabetes (Emre *et al.*, 2007) Activated neutrophils have a similar function to macrophages in that they kill phagocytosed microbes by ROS production. Neutrophils are already known to express UCP2 (Rousset et al., 2006; Tagen et al., 2009). The presence of UCP1 in neutrophils may indicate that UCP 1 plays a role in controlling ROS production in naïve neutrophils.

[5.4] Conclusion

The study presented has shown the novel finding of an increase in UCP 1 protein expression after activation and proliferation of T cells in the thymus using LPS and PHA. We have also shown that LPS or PHA treatment of mice has no effect on UCP 1 expression in brown adipose tissue. Lack of UCP1 results in (a) a doubling of the proportion of CD4 & CD8 cells concomitant with a halving of the proportion of DP cells following PHA treatment, and (b) an increase in the proportion of CD4 and a reduction in the proportion of DP cells following LPS treatment. We have shown that lack of UCP 1 leads to a tripling of the absolute cell numbers of CD4 and CD8 cells after PHA treatment. We have also shown that lack of UCP 1 has no effect on oxygen consumption or proton leak after LPS or PHA treatment, despite the increase in UCP 1 protein. This suggests UCP 1 may play a non-thermogenic role in the thymus. We also show the novel finding of UCP 1 in activated murine neutrophils.

Chapter 6

General Discussion

[6.1] General Discussion

The uncoupling proteins 1, 2 and 3 (UCP1, UCP2, and UCP3) are members of the super family of anion carrier proteins located in the inner membrane of mitochondria. UCP1 is found only in brown fat mitochondria of mammals. Studies, beginning in the 1960s, identified the function of UCP1 in providing heat and decreasing energy efficiency through dissipation of the proton electrochemical gradient across the inner mitochondrial membrane of brown adipose tissue without the generation of ATP (Nicholls, 2001). Thus, the function of UCP1 in brown adipose tissue was known before the gene was cloned. On the other hand, UCP2 (Fleury *et al.*, 1997) and UCP3 (Boss *et al.*, 1997;Vidal-Puig *et al.*, 1997), were identified in 1997 by reverse cloning, i.e. by 'mining' databases of expressed sequence tags or from similarity to UCP1 in cDNA libraries (reviewed in Nedergaard & Cannon, 2003). UCP2 and UCP3 have 59% and 57% identity, respectively, with UCP1, and 73% identity with each other (Krauss *et al.*, 2005).

The primary function of UCP1 is to allow a leak of protons through the inner mitochondrial membrane of brown fat thereby, uncoupling substrate oxidation from phosphorylation of ADP to ATP resulting in rapid oxygen consumption, heat production, and energy wastage. This function of UCP1 is mediated by the sympathetic nervous system and norepinephrine in brown adipose tissue and is stimulated by fatty acids and inhibited by purine nucleotides.

Up until recently, UCP 1 was only ever associated with BAT mitochondria (Cannon *et al.,* 1982). UCP 1 has been reported to be found in white fat, however, in such cases it was always related to the presence of brown adipocytes dispersed in white fat depots (Cinti *et al.,* 2002). UCP 1 expression in other tissues has occasionally been reported; For instance UCP 1 has been shown to be expressed in skeletal muscle of mice chronically treated with a ß-adrenoreceptor agonist and in the longitudinal muscle layer of peristalic organs such as the intestine (Yoshhida *et al.,* 1998) and uterus (Nibblelink *et al.,* 2001). However, the former data have never been confirmed, whereas the presence of UCP 1 in the longitudinal muscle layer of uterus has been conclusively disproved (Rousset *et al.,* 2003).

Carroll *et al.*, (2005) detected UCP 1 protein in thymus and thymocyte mitochondria. The evidence they provided was multilayered and extremely convincing. Carroll *et al* (2005) firstly detected (i) UCP 1 transcripts in whole thymus and thymocytes by using RT-PCR, (ii) UCP 1 protein by using immunoblotting in mitochondria isolated from whole thymus and thymocytes. They also purified and identified UCP 1 from thymus mitochondria by using mass spectrometry. They also showed that mitochondria isolated from thymus bind GDP with kinetics consistent with the presence of UCP 1 and have a GDP-sensitive and fatty acid-dependent proton leak indicative of the presence of UCP 1. This work was recently challenged by Frontini *et al.,* (2007), who argued that any UCP 1 present in the thymus is due to brown adipose tissue contamination.

To finally resolve this issue it was decided to isolate the thymocytes from thymus and using laser scanning confocal microscopy probe for UCP 1 reactivity (Chapter 3). This way it overcame the possibility of contamination from surrounding BAT. Our study has clearly shown that UCP 1 is associated with mitochondria from isolated thymocytes in wild-type mice but not with thymocytes from UCP 1 knock out mice. The detection of UCP 1 in mitochondria from isolated thymocytes from mice was also confirmed using rats (Chapter 3).

In an attempt to resolve the discrepancy between our confocal microscopy data reported by us, (Adams *et al.,* 2007), and data reported in studies by others (Frontini *et al.,* 2007), the specificity of the respective UCP 1 antibodies used in these studies was compared.

We predicted that the discrepancy could be due to the relative specificity of the peptide antibody used by us and the full length antibody used by Frontini *et al.,* (2007) Confocal analysis shows that using the full-length UCP 1 antibody, a protein is detected (figure 3.5) in Thy 1 positive thymocytes from wild-type mice and also UCP 1 knock out mice. The full-length UCP 1 antibody detects a ~32 k Da band in mitochondria from BAT, spleen, liver and also BAT mitochondria from mice deficient in UCP 1 (Adams *et al.*, 2008). Clearly, the antibody to full-length UCP 1 is detecting other proteins at ~32kDa and possibly at other masses. We have also demonstrated that the full-length antibody to UCP1 used by Frontini *et al.* (2007) clearly detects protein in mitochondria of UCP1 knock-out mice. Also interestingly there are recent

reports of the detection of UCP 1 in human skin and skin derived cells at an mRNA and protein level (Mori *et al.*, 2008) which shows that UCP 1 is not an exclusive marker to BAT.

Under acute starvation it has been shown that UCP 1 protein expression in BAT decreases (Rothwell *et al.*, 1984; Nedergaard *et al.*, 2001). Carroll et al. (2004) observed that under the same conditions of acute starvation, there was no difference in abundance of UCP 1 protein in thymocyte or thymus mitochondria. The fact that starvation decreases UCP 1 expression in BAT, whilst having no effect on UCP 1 expression in thymus, implies that UCP 1 functions differently in BAT than in thymus. There is already circumstantial evidence that UCP 1 does not play a thermogenic role in the thymus in that oxygen consumption by thymocytes isolated from cold-acclimated animals have decreased oxygen consumption rates (Brennan *et al.*, 2006).

UCP 1 also has an interesting time-dependant profile in the thymus (Chapter 3). From this it appears UCP 1 is expressed at a higher level immediately after birth and in the first few weeks of life, while mice are forming their own fully functioning immune system. During this time most of the T cells that are required through out life are formed, and enter the circulation until needed.

The thymus provides an inductive environment for development of T-lymphocytes from haematopoietic progenitor cells, after which the mature T-cells migrate to the tissues of the peripheral immune system. As UCP 1 appears to be expressed in all thymocyte subsets, and not in progenitor cells or the spleen (Chapter 3; Figure 3.6) one may postulate a role for UCP 1 in the maturation of early T-lymphocytes.

We observed that the half-life of UCP 1 in thymocytes was approximately 3 hours, which is significantly less than the 30h half life of UCP 1 in brown adipocytes (Puigserver *et al.*, 1992). Cold-induced thermogenesis due to UCP 1 activity in brown adipocytes is generally not transient, and, therefore it is important for UCP 1 to be expressed at a high level over a long period of time. UCP 2 has been shown to have a half-life of about 1 hour (Azzu *et al.*, 2008, Rousset *et al.*, 2007). UCP 1 is transcriptionally regulated whereas UCP 2 protein level can change without any

alteration in mRNA level, highlighting different physiological functions (Pecqueur *et al.*, 2001; Azzu *et al.*, 2008). This makes it completely plausible that UCP 1 plays a different function in the thymus than in BAT.

Using flow cytometry, we have shown that the lack of UCP 1 in the thymus affects the % of thymocyte subsets in the thymus. We observed a significant increase in DPs cells and a halving of CD8 cells in the thymus (Chapter 4). These trends were also apparent in the T cells from spleens of UCP 1 knock-out mice. We conclude from this data that the process of determining SP cell type after negative selection is affected by the absence of UCP 1. We observed that thymocytes from UCP 1 knock-out mice had a reduced spontaneous apoptotic potential (Chapter 4), perhaps leading to the selection of autoreactive T cells. We observed a significantly higher level of ATP in thymocytes isolated from UCP 1 knock-out mice (Chapter 4), and we expected to see a decrease in proton leak in quiescent thymocytes from UCP 1 knock-out mice, manifesting itself as a decrease in oxygen consumption at the whole cell (thymocyte level) oxygen consumption level. We observed no significant difference in the whole cell oxygen consumption of thymocytes from UCP 1 knock-out mice and from wild-type mice (Chapter 4). However an equivalent observation was made by Krauss *et al.*, (2002) who observed no significant difference in the rate of thymocyte oxygen consumption rates in a comparison of UCP 2 knock-out and wild-type mice, yet they did manage to detect a difference in in situ proton leak. It has been shown that the thymus is innervated by adrenergic receptors, like in BAT (Ritter & Crispe, 1992). Thermogenesis in BAT results from the sympathetic simulation of β-adrenergic receptors on the surface of BAT cells and is stimulated by fatty acids and inhibited by purine nucleotides. So perhaps UCP 1 in thymocytes requires activation to increase leak. Further work will establish if UCP 1 plays a role in adaptive leak in thymocytes.

In light of the fact that UCP 1 activity correlates with apoptotic potential in quiescent thymocytes (Chapter 4), it was decided to investigate if UCP 1 expression in the thymus was affected by mitogenic stimulants in vivo by treatment with LPS or PHA. After LPS or PHA treatment of wild-type mice we observed a significant increase in UCP 1 protein in isolated mitochondria from thymus, but no change in UCP 1 expression in BAT (Chapter 5). This agrees with the findings of Okamatsu-

Ogura *et al.* (2007) who found that there was no effect of LPS on UCP 1 mRNA level in brown adipose tissue. This also adds to the evidence that UCP 1 plays a unique role in the thymus. We observed no significant difference in thymus masses and total cell number in thymus after LPS and PHA treatment in a comparison of UCP 1 knock-out and wild-type mice (Chapter 5). After LPS treatment of UCP 1 knock-out mice, we observed a significant increase in CD4 T cells and a significant decrease in DP thymocytes, compared to the wild-type mice. After PHA treatment of UCP 1 knock-out mice, we observed a more significant increase in CD4 and CD8 T cells and a significant decrease in the DP thymocytes. From the absolute cell numbers of each subset after PHA treatment of UCP 1 knock-out mice, it can be seen there is significantly greater proliferation of CD4 and CD8 T cells in the thymus compared to wild type mice (Chapter 5).

We observed no significant differences in oxygen consumption or indices of proton leak rates between wild-type and UCP 1 knock-out mice, suggesting UCP 1 does not affect oxygen consumption in thymocytes isolated from LPS or PHA treated mice compared to the PBS treated wild-type mice. Since there is an increase in UCP 1 protein in thymus after LPS and PHA (Chapter 5) a difference in oxygen consumption due to proton leak might have been expected, however this was not the case. An increase in UCP abundance in cells following LPS doesn't necessarily result in an increased in mitochondrial proton leak. Couplan *et al.* (2001) showed an increase in UCP 2 in lung mitochondria following LPS treatment but saw no differences in oxygen consumption or proton leak in isolated lung mitochondria. This suggests that UCP 1 does not have an uncoupling role under conditions of mitogenic proliferation in thymocytes.

UCP2 knockout mice have elevated ROS production in macrophages (Arsenijevic *et al.*, 2000) and pancreatic islet cells (Krauss *et al.*, 2003) and UCP3 knockout mice have elevated ROS in muscle (Vidal-Puig *et al.*, 2000) further supporting the role of these UCPs in protecting against ROS production and tissue oxidative damage. Dlaskova *et al.*, (2010) observed that UCP 1 has the potential to alleviate ROS production in brown adipose tissue mitochondria. Mitochondrial uncoupling proteins are known to be activated by reactive oxygen species (Echtay *et al.*, 2002). Clarke & Porter (unpublished) have shown that UCP 1 has the potential to

regulate ROS production in isolated thymus mitochondria. So perhaps UCP 1 plays a role in the regulation of ROS production in thymus mitochondria.

It is now well established that UCP 2 plays an important role in regulation of insulin secretion. Pancreatic β-cells secrete insulin in response to a meal by sensing the ATP/ADP ratio resulting from glucose metabolism in the cell. UCP 2, by mildly increasing proton leak, decreases the ATP/ADP ratio of the cell thus reducing the effect of glucose on insulin secretion (Brand & Esteves, 2005). Pecqueur *et al.* (2008) have suggested that UCP 2 functions as a pyruvate transporter from the mitochondria to the cytosol in proliferating cells, by promoting fatty acid oxidation and limiting glycolysis-derived utilization, as proliferating cells require the unrestricted availability of glucose. The fact that UCP 2 can play many different roles, in different tissues means that UCP 1 could play a role in the thymus and that further investigations into the role of UCP 1 in the thymus are worthy.

The proliferation of T cells after mitogenic stimulation is greater after LPS and PHA treatment of UCP 1 knock-out mice compared to wild type mice, perhaps leading to increased ROS production. It has been shown that low levels of ROS stimulate proliferation and enhance cell survival in different cell types (Burdon *et al.*, 1990) (Burdon, 1995; Burdon *et al.*, 1996). This increased proliferation of CD4 and CD8 T cells may lead an increased number of auto-reactive T cells leaving the thymus and entering the circulation. Normally additional mechanisms of tolerance active in the periphery exist to silence these cells such as anergy, deletion, and regulatory T cells. If these peripheral tolerance mechanisms also fail, autoimmunity may arise. Perhaps in mice lacking UCP 1 too many autoreactive T cells enter the circulation, for the body to deal with normally. Myasthenia gravis (MG) is an autoimmune neuromuscular disease leading to fluctuating muscle weakness and fatigability. It is an autoimmune disorder, in which weakness is caused by circulating antibodies that block acetylcholine receptors at the post-synaptic neuromuscular junction (Conti-Fine *et al.*, 2006) inhibiting the stimulative effect of the neurotransmitter acetylcholine. Myasthenia is treated medically with cholinesterase inhibitors or immunosuppressants, and, in selected cases, thymectomy. The antibodies are produced by plasma cells, derived from B-cells. B-cells convert into plasma cells by T-

helper cell stimulation. In order to carry out this activation, T-helpers must first be activated themselves, which is done by binding of the T-cell receptor (TCR) to the acetylcholine receptor antigenic peptide fragment (epitope) resting within the major histocompatibility complex of an antigen presenting cells. Bernasconi *et al*, (2005) have suggested that autoreactive T cells that are not deleted during normal T cell maturation in MG patients are the crucial step in iniating the autoimmune disease, due to the activation or penetration into the thymus of pre-existing autoreactive T cells, rather than the generation of new ones. Myasthenia Gravis is associated with various autoimmune diseases, including thyroid diseases, including Hashimoto's thyroiditis and Graves' disease, diabetes mellitus type 1,rheumatoid arthritis, lupus, and demyelinating CNS diseases. Interestingly spleens of UCP 1 knock out mice, after LPS injection, have an increased level of FOXP3 (a transcription factor and marker of Treg cells) (unpublished observation, Porter & Fallon). Regulatory T cells are a specialized subpopulation of T cells that act to suppress activation of the immune system and thereby maintain immune system homeostasis and tolerance to self-antigens (Sakaguchi, 2000).

Clearly, UCP 1 plays an important role in the development of functional T cells and their proliferation and has uncovered a new avenue for research into thymus bioenergetics, metabolism, development and function.

Chapter 7

References

Abbas, A.K., Lichtman, A.H., Pober, J.S. (1994) *Cellular and Molecular Immunology*, 2ND Edition

Adams, A.E, Hanrahan, O., Nolan, D.N., Voorheis, H.P., Fallon, P., Porter, R.K. (2007) Images of mitochondrial UCP 1 in mouse thymocytes using confocal microscopy. *Biochim. Biophys. Acta.* ;**1777**, 115-117

Adams, A.E., Carroll, A.M., Fallon, P.G., Porter, R.K., (2008). Mitochondrial uncoupling protein 1 expression in thymocytes, *Biochim. Biophys. Acta.* **1777** 772–776.

Adams, A.E., Kelly, O.M., Porter, R.K. (2010) Absence of mitochondrial uncoupling protein 1 affects apoptosis in thymocytes, thymocyte/T-cell profile and peripheral T-cell number. *Biochim. Biophys Acta.*; **1797(6-7)**:807-16

Adams, J.M., Cory, S. (2001). Life-or-death decisions by the Bcl-2 protein family. *Trends Biochem. Sci.* **26,** 61–66.

Aquila, H., Link, T.A., Klingenberg, M. (1985) The uncoupling protein from brown fat mitochondria is related to the mitochondrial ADP/ATP carrier. Analysis of sequence homologies and of folding of the protein in the membrane. *EMBO J.* **9,** 2369-76

Arsenijevic, D., Onuma, H., Pecqueur, C., Raimbault, S., Manning, B.S., Miroux, B., Couplan, E., Alves-Guerra, M.C., Goubern, M., Surwit, R., Bouillaud, F., Richard, D., Collins, S. and Ricquier, D. (2000) Disruption of the uncoupling protein-2 gene in mice reveals a role in immunity and reactive oxygen species production. *Nat. Genet.* **26**, 435-439

Azzu, V., Affourtit, C., Breen, E.P., Parker, N., Brand, M.D. (2008) Dynamic regulation of uncoupling protein 2 content in INS-1E insulinoma cells. Biochim Biophys Acta. 2008; **1777(10):** 1378–1383.

Bai, Y., Onuma, H., Bai, X., Madvedev, A.V., Misukonis, M., Weinberg, J.B., Cao, W., Robidoux, J., Floering, L.M., Daniel, K.W., Collins, S., (2005) Persistent nuclear factor-κB activation in UCP2−/− mice leads to enhanced nitric oxide and inflammatory cytokine production, *J. Biol. Chem* **19** , pp. 19062–19069.

Balaban, R.S., Nemoto, S., Finkel, T., (2005) Mitochondria, oxidants, and aging. *Cell*.**120(4)**:483-95.

Baldwin, T.A., Hogquist, K.A., Jameson, S.C. (2004) The fourth way? Harnessing aggressive tendencies in the thymus. *J Immunol*. **173**, 6515-20

Baroni, C.D., De Franceschi, G.S., Uccini, S., Adorini, L., Cnen, G.D., Ruco, L. (1976) Biological effects of Escherichia coli lipopolysaccharide (LPS) in vivo. I. Selection in the mouse thymus of killer and helper cells. *Immunology* **31**, 217-24.

Bernasconi, P., Barberis, M., Baggi, F., Passerini, L., Cannone, M., Arnoldi, E., Novellino, L., Cornelio, F., Mantegazza, R. (2005) Increased toll-like receptor 4 expression in thymus of myasthenic patients with thymitis and thymic involution. *Am J Pathol*. **167**(1):129-39.

Bienengraeber M, Echtay KS, Klingenberg M. (1998) H+ transport by uncoupling protein (UCP-1) is dependent on a histidine pair, absent in UCP-2 and UCP-3. Biochemistry, **37(1)**:3-8.

Bonet, M., Serra, F., Matamala, J.C., Garcia-Palmer, F.J., Palou, A. (1995) Selective loss of the uncoupling protein of light versus heavy mitochondria of brown adipocytes after a decrease in noradrenergic stimulation *in vivo* and *in vitro*. *Biochem.J.* **311,** 327-331

Boss, O., Samac, S., Paolini-Giacobino, A., Rossier, C., Dulloo, A., Seydoux, J., Muzzin, P., Giacobino, J.P. (1997) Uncoupling protein 3: a new member of the mitochondrial carrier family with tissue specific expression. *FEBS Lett* **408,** 39-42

Boss, O., Samac, S., Dulloo, A., Seydoux, J., Muzzin, P., Paolini-Giacobino, A., (1997) Tissue-dependant up-regulation of rat uncoupling protein 2 expression in response to fasting or cold *FEBS Lett* **412,** 111-114

Bouillaud, F., Ricquier. D., Thibault. J., Weissenbach. J. (1985) Molecular approach to thermogenesis in brown adipose tissue: cDNA cloning of the mitochondrial uncoupling protein. *Proc. Natl. Acad. Sci. USA.*, **82**, 445-8

Bouillet, P., Purton, J.F., Godfrey, D.I., Zhang, L.C., Coultas, L., Puthalakath, H., Pellegrini, M., Cory, S., Adams, J.M., Strasser, A., (2002) BH3-only Bcl-2 family member Bim is required for apoptosis of autoreactive thymocytes, *Nature* **415,** 922–926.

Brand, K.A., Hermfisse, U., (1997) Aerobic glycolysis by proliferating cells: a protective stragegy against reactive species. *FASEB J* **11** 388-395

Brand MD, Esteves TC. (2005) Physiological functions of the mitochondrial uncoupling proteins UCP2 and UCP3. *Cell Metab.* **2(2)**:85-93. Review.

Brand, M.D. (2000). Uncoupling to survive? The role of mitochondrial efficiency in aging. *Experimental Gerontology.* **35**, 811-820

Brand MD, Pamplona R, Portero-Otín M, Requena JR, Roebuck SJ, Buckingham JA, Clapham JC, Cadenas S. (2002). Oxidative damage and phospholipid fatty acyl composition in skeletal muscle mitochondria from mice underexpressing or overexpressing uncoupling protein 3.Biochem J.; **368(2)**:597-603.

Brand, M.D., Affourtit, C., Esteves, T.C., Green, K., Lambert, A.J., Miwa, S., Pakay, J.L., Parker, N. (2004). Mitochondrial superoxide: production, biological effects, and activation of uncoupling proteins. *Free Radic Biol Med.*;**37(6)**:755-67. Review.

Brand, M.D., Buckingham, J.A., Esteves, T.C., Green, K., Lambert, A.J., Miwa, S., Murphy, M.P., Pakay, J.L., Talbot, D.A., Echtay, K.S. (2004) Mitochondrial superoxide and aging: uncoupling-protein activity and superoxide production.*Biochem Soc Symp*;**(71)**:203-13. Review.

Breen, E.P., Gouin, S., Brennan, C.M., Murphy, A.F., Haines, L.R., Pearson, A.M. Jackson, T.W., Murphy, P.V. and Porter, R.K. (2006) On the mechanism of mitochondrial uncoupling protein 1 function. *J. Biol. Chem*. **281**, 2114-2119

Brennan, C.M., Breen, E.P., Porter, R.K. (2006) Cold acclimation and oxygen consumption in the thymus, *Biochim. Biophys. Acta* **1757** 1463–1468.

Burdon, R.H. (1995) Superoxide and hydrogen peroxide in relation to mammalian cell proliferation. *Free Radic. Biol. Med.* **18**,775-794

Burdon, R.H., Gill, V., Alliangana, D. (1996) Hydrogen peroxide in relation to proliferation and apoptosis in BHK-21 hamster fibroblasts. *Free Radic. Res.* **24**, 81-93

Burdon, R.H., Gill, V., Rice-Evans, C. (1990) Oxidative stress and tumour cell proliferation *Free Radic. Res. Commun.* **11**, 65-76

Buttgereit, F., Brand, M.D. (1995) A hierarchy of ATP-consuming processes in mammalian cells, *Biochem. J.* **312**, 163–167.

Buttgereit, F., Burmester, G.R., Brand, M.D. (2000). Bioenergetics of immune functions: fundamental and therapeutic aspects. *Immunol. Today* **21**, 192–199

Buttgereit, F., Grant, A., Muller, M., Brand, M.D. (1994). The effects of methylprednisolone on oxidative phosphorylation in Concanavalin-A-stimulated thymocytes. Top-down elasticity analysis and control analysis. *Eur. J. Biochem.* **15**, 513-519

Buttgereit, F., Krauss, S., Brand, M.D. (1997) Methylprednisolone inhibits uptake of Ca2+ and Na+ ions into concanavalin A-stimulated thymocytes. *Biochem J.*; **326**:329-32

Cadenas, S., Echtay, K.S., Harper, J.A, Jekabsons, M.B., Buckingham, J.A., Grau, E., Abuin, A., Chapman, H., Clapham, J.C., Brand, M.D. (2002).The basal proton conductance of skeletal muscle mitochondria from transgenic mice overexpressing or lacking uncouplingprotein-3. *J Biol Chem.* **277**, 2773–2778.

Cannon, B., Jacobsson, A., Rehnmark, S., Nedergaard, J. (1996) Signal transduction in brown adipose tissue recruitment: noradrenaline and beyond. *Int. J. Obesity.* **20**, S36-42

Cannon, B., Nedergaard, J., (2004) Brown adipose tissue: function and physiological significance, *Physiol. Rev.* **84** 277–359.

Cannon. B., Hedin. A., Nedergaard. J. (1982) Exclusive occurrence of thermogenin antigen in brown adipose tissue. *FEBS Lett.* **150**, 129-32

Carroll, A.M., Haines, L.R., Pearson, T.W., Brennan, C.M., Breen, E.P., Porter, R.K., (2004) Immunodetection of UCP 1 in rat thymus, *Biochem. Soc. Trans.* **32** 1066–1067.

Carroll, A.M., Haines, L.R., Pearson, T.W., Fallon, P.G., Walsh, C.M., Brennan, C.M., Breen, E.P. , Porter, R.K. (2005) Identification of a functioning mitochondrial uncoupling protein 1 in thymus. *J. Biol. Chem.* **280,** 15534-15543

Carroll, A.M., Porter, K., (2004) Starvation-sensitive UCP 3 protein expression in thymus and spleen mitochondria, *Biochim Biophys Acta.* **1700,** 145–150.

Casteilla L, Rigoulet M, Pénicaud L. (2001) Mitochondrial ROS metabolism: modulation by uncoupling proteins. *IUBMB Life*; **52(3-5)**:181-8. Review.

Chappell, J.B. and Hansford, R.G. (1972) in: Subcellular Components: Preparation and Fractionation (Birnie, G.D., Ed.), pp. 77-91, Butterworths, London.

Chen, Z., Benoist, C., Mathis, D., (2005) How defects in central tolerance impinge on a deficiency in regulatory T cells. *Proc Natl Acad Sci U S A* ;**102(41)**, 14735-40.

Cinti, S., Cancello, R., Zingaretti, M., Ceresi, E., Matteis, R., Giordano, A., Himms–Hagen, J., Ricquier, D. (2002) CL316, 243 and Cold Stress Induce Heterogeneous Expression of UCP1 mRNA and Protein in Rodent Brown Adipocytes *Journal of Histochemistry and Cytochemistry,* **50**, 21-32

Cinti, S., Frederich, R.C., Zingaretti, M.C., De Matteis, R., Flier, J.S., Lowell, B.B., (1997) Immunohistochemical localization of leptin and uncoupling protein in white and brown adipose tissue. *Endocrinol;* **138**, 797-804

Considine, M.J., Goodman, M., Echtay, K.S., Laloi, M., Whelan, J., Brand, M.D., Sweetlove, L.J. (2003) Superoxide stimulates a proton leak in potato mitochondria that is related to the activity of uncoupling protein.*J Biol Chem*. **278(25):**22298-302.

Conti-Fine, B.M., Milani, M., Kaminski, H.J (2006). "Myasthenia gravis: past, present, and future". *J. Clin. Invest.* **116 (11)**: 2843–54.

Couplan, E., Gonzalez-Barroso, M., Alves-Guerra, M.C., Ricquier, D., Goubern, M., Bouillaud, F., (2002) No Evidence for a Basal, Retinoic, or Superoxide-induced Uncoupling Activity of the Uncoupling Protein 2 Present in Spleen or Lung Mitochondria *J. Biol. Chem.* **277**, 26268–26275

Cunningham, O., McElligott, A.M., Carroll, A.M., Breen, E.P., Reguenga, C., Oliveira, M.E.M., Azevedo, J.E., Porter, R.K. (2003). Selective detection of UCP 3 expression in skeletal muscle: effect of thyroid status and temperature acclimation, *Biochim. Biophys. Acta;* **1604**, 170–179.

Dlasková, A., Clarke, K.J., Porter, R.K., (2010) The role of UCP 1 in production of reactive oxygen species by mitochondria isolated from brown adipose tissue. *Biochim Biophys Acta.*; **1797**(8),1470-6.

Drahota, Z., Chowdhury, S.K., Floryk, D., Mráček, T., Wihelm, J., Rauchová, H., Lenaz, G., Houštěk, J., (2002) Glycerophosphate-dependent hydrogen peroxide production by brown adipose tissue mitochondria and its activation by ferricyanide, *J. Bioenerg. Biomembr.* **34**, 105–113.

Echtay, K.S., Brand, M.D. (2001) Coenzyme Q induces GDP-sensitive proton conductance in kidney mitochondria, *Biochem. Soc. Trans.;* **29,** 763-768

Echtay, K.S., Roussel, D., St-Pierre, J., Jekabsons, M.B., Cadenas, S., Stuart, J.A., Harper, J.A., Roebuck, S.J., Morrison, A., Pickering, S., Clapham, J.C., Brand, M.D. (2002) Superoxide activates mitochondrial uncoupling proteins, *Nature;* **415**, 96–99

Ellmeier, W., Sunshine, M. J., Losos, K., Hatam, F., Littman, D. R. (1997) An enhancer that directs lineage-specific expression of CD8 in positively selected thymocytes and mature T cells. *Immunity;* **7**, 537–547.

Emre, Y., Hurtaud, C., Ricquier, D., Bouillaud, F., Hughes J., Criscuolo, F. (2007) Avian UCP: the killjoy in the evolution of the mitochondrial uncoupling proteins. *J. Mol. Evol.* **65**, pp. 392–402

Ernster, L., (1993) Lipid peroxidation in biological membranes: mechanism and implications. In: K. Yagi, Editor, *Active Oxygen, Lipid Peroxides, and Antioxidants*, Japan Science Society Press, Tokyo, pp. 1–38.

Fleury, C., Neverova, M., Collins, S., Raimbault, S., Champigny, O., Levi-Meyruesis, C., Bouillaud, F., Seldin, M.F., Surwit, R.S., Ricquier, D., Warden, C.H. (1997) Uncoupling preotein-2: a novel gene linked to obesity and hyperinsulinemia. *Nature Genetics*. **15,** 269-272

Forsmark-Andrée, P., Dallner, G., Ernster, L., (1995) Endogenous ubiquinol prevents protein modification accompanying lipid peroxidation in beef heart submitochondrial particles, *Free Radic. Biol. Med.* **19**, pp. 749–757

Foster, D.O. (1986) Quantitive role of brown adipose tissue in thermogenesis. In: Brown Adipose Tissue, pp31-52 (Paul Trayhurn and David G. Nicholls eds.)(Edward Arnold Publishers, London).

Frontini, A., Rousset, S., Cassard-Doulcier. A.M., Zingaretti. C., Ricquier, D., Cinti, S. (2007) Thymus Uncoupling Protein 1 Is Exclusive to Typical Brown Adipocytes and Is Not Found in Thymocytes. *Journal of Hist. and Cytochem.* **55**, 183-189

Garlid, K.D., Jaborek, M., Jezek, P. (1998) The mechanism of proton transport mediated by mitochondrial uncoupling proteins. *FEBS Letts*. **438**, 10-14

Garlid, K.D., Orosz, D.E., Modriansky, M., Vassanelli, S., Jezek, P. (1996) On the mechanism of fatty acid-induced proton transport by mitochondrial uncoupling protein. *J. Biol. Chem.* **271,** 2615-20

Gimeno, R.E., Dembski, M., Weng, X., Deng, N., Shyjan, A.W., Gimeno, C.J., Iris, F., Ellis, S.J., Woolf, E.A, Tartaglia, L.A. (1997). Cloning and characterization of an uncoupling protein homolog: a potential molecular mediator of human thermogenesis. *Diabetes* **46**, 900-906

Gong, D.W., He, Y., Karas, M., Reitman, M., (1997) Uncoupling protein 3 is a mediator of thermogenesis regulated by thyroid hormone, β-adrenergic agonists and leptin. *J. Biol. Chem* **272,** 24129-24132

Gong, D.W., Monemdjou, S., Gavrilova, O., Leon, L.R., Marcus-Samuels,B., Chou, C.J., Everett, C., Kozak, L..P., Li, C., Deng, C., Harper, M.E., Reitman, M.L. (2000). Lack of obesity and normal response to fasting and thyroid hormone in mice lacking uncoupling protein-3. *J Biol Chem* **275**, 16251–16257.

Gray, J. V. (2004) 'Sleeping beauty': quiescence in *Saccharomyces cerevisiae*. *Microbiol. Mol. Biol. Rev.* **68**, 187–206

Greiner, E.F., Guppy, M., Brand, K. (1994). Glucose is essential for proliferation and the glycolytic enzyme induction that provokes a transition to glycolytic energy production. *J. Biol. Chem.* **269**, 31484–31490.

Gruver, A.L., Sempowski, G.D. (2008) Cytokines, leptin, and stress-induced thymic atrophy.*J Leukoc Biol.*; **84**(4):915-23.

Gwosdow, A.R., Kumar, M.S., Bode, H.H., (1990) Interleukin 1 stimulation of the hypothalami-pituitary-adrenal axis *Am J Physiol Endocrinol Metab* **258**, 65-70

Hallgren, H.M., Bergh, N., Rodysill, K.J., O'Leary, J.J.(1988) Lymphocyte proliferative response to PHA and anti-CD3/Ti monoclonal antibodies, T cell surface marker expression, and serum IL-2 receptor levels as biomarkers of age and health. *Mech Ageing Dev*. **43(2)**, 175-85.

Hanson, E.S., Knudson, J. (1986) Parallel measurements of heat production and thermogenin content in brown fat cells during cold acclimation of rats. *Biosci Rep.*, **1,** 31-8

Harper, J.A., Stuart, J.A., Jekabsons, M.B., Roussel, D., Brindle, K.M., Dickinson, K., Jones, R.B., Brand, M.D. (2002). Artifactual uncoupling by uncoupling protein 3 in yeast mitochondria at the concentrations found in mouse and rat skeletal-muscle mitochondria. *Biochem J* **361**, 49–56.

Hayday, A.C., Pennington, D.J., (2007) Key factors in the organized chaos of early T-cell development. *Nat. Immunol.* **8** 137–144.

Heaton, G.M., Wagenvoord, R.J., Kemp, A., Nicholls, D.G. (1978) Brown-adipose-tissue mitochondria: photoaffinity labelling of the regulatory site of energy dissipation. *Eur J Biochem.*, **82**, 515-521

Henze, K., Martin, W. (2003) Evolutionary biology: Essence of mitochondria *Nature* **426**, 127 – 128

Hettmann, T., DiDonoto, J., Karin, M., Leiden, J.M. (1999) An essential role for nuclear factor kappa β in promoting double positive thymocyte apoptosis. *J Exp Med* **189**; 145-158

Hofmann, W.E., Liu, X., Bearden, C.M., Harper, M-E., Kozak, L.P., (2001) Effects of genetic background on thermoregulation and fatty acid-induced uncoupling of mito-chondria in UCP1-deficient mice, *J. Biol. Chem.* **276** 12460–12465.

Honda, K., Kato, K., Dairaku, N., Iijima, K., Koike, T., Imatani, S., Sekine, H., Ohara, S., Matsui, H., Shimosegawa, T. (2003) High levels of intracellular ATP prevent nitric oxide-induced apoptosis in rat gastric mucosal cell, *Int. J. Exp. Path.* **84** 281–288.

Hori, S., Nomura, T., Sakaguchi, S. (2003) Control of regulatory T cell development by the transcription factor Foxp3. *Science,* **299**(5609), 1030-1.

Huang, S.G., Klingenberg, M. (1995) Fluorescent nucleotide derivatives as specific probes for the uncoupling proteins: thermodynamics and kinetics of binding and the control by pH. *Biochemistry* **34**, 349-360

Huang, S.G., Klingenberg, M. (1996) Two-stage nucleotide binding mechanism and its implications to H+ transport inhibition of the uncoupling protein from brown adipose tissue mitochondria. *Biochemistry.* **35**, 7846-54

Izon, D. J. *et al.* (2001) Notch1 regulates maturation of $CD4^+$ and $CD8^+$ thymocytes by modulating TCR signal strength. *Immunity* **14**, 253–264.

J.B. Chappell, R.G. Hansford, in: G.D. Birnie (Ed.), Subcellular Components: Preparation and Fractionation, Butterworths, London, 1972, pp. 77–91.

Jankovic, B.D., (2006) Brown adipose tissue: its in vivo immunology and involvement in neuroimmunomodulation, *Ann. N.Y. Acad. Sci.* **496** 3–26.

Jezek P, Zácková M, Reháková Z, Růzicka M, Borecký J, Skobisová E, Brucknerová J, Garlid KD, Gimeno RE, Tartaglia LA. (1999) Existence of uncoupling protein-2 antigen in isolated mitochondria from various tissues.*FEBS Lett.* **455(1-2):**79-82.

Ježek, P., Hlvatá, L. (2005) Mitochondria in homeostasis of reactive oxygen species in cell, tissues, and organism, *Int. J. Biochem. Cell Biol.* **37**, pp. 2478–2503.

Kim, J., Jung, K-J., Park. K.M. (2010) Reactive oxygen species differently regulate renal tubular epithelial and interstitial cell proliferation after ischemia and reperfusion injury *AJP - Renal Physiol* **298(5)**, F1118-F1129

Klaus, S., Casteilla, L., Bouillaud, F., Ricquier, D. (1991) The uncoupling protein UCP: a membraneous mitochondrial ion carrier exclusively expressed in brown adipose tissue. *Int J Biochem.* **23**,791-801

Klingenberg, M. (1988) Nucleotide binding to uncoupling protein. Mechanism of control by protonation. *Biochemistry* **27**, 781-791

Klingenberg, M., Echtay, K.S. (2001) Uncoupling proteins: the issues from a biochemist point of view. *Biochim. Biophys. Acta* **1504,** 128-143

Klingenberg, M., Huang, S.G. (1999) Structure and function of the uncoupling protein of brown adipose tissue. *Biochim. Biophys. Acta* **1415,** 271-296

Klingenberg. M., Echtay. K.S., Bienengraeber. M., Winkler. E., Huang, S.G. (1999) Structure-function relationship in UCP1. *Int J Obes Relat Metab Disord.* **23** Suppl 6:S24-9

Krauss, S., Brand, M.D., Buttgereit, F. (2001) Signaling takes a breath--new quantitative perspectives on bioenergetics and signal transduction. *Immunity*. **15**(4):497-502.

Krauss, S., Zhang, C.Y., Lowell, B.B., (2002) A significant portion of mitochondrial proton leak in intact thymocytes depends on expression of UCP2, *Proc. Natl. Acad. Sci. U. S. A.* **99**, 118–122.

Krauss, S., Zhang, C.Y., Scorrano, L., Dalgaard, L.T., St-Pierre, J., Grey, S.T., Lowell, B.B. (2003) Superoxide-mediated activation of uncoupling protein 2 causes pancreatic beta cell dysfunction. *J. Clin. Invest.* **112**, 1831–1842.

Krauss, S., Zhang, C.Y., Lowell, B.B. (2005) The mitochondrial uncoupling-protein homologues, *Nat. Rev. Mol. Cell Biol.* **6**, 248–261.

Laemmli, U.K. (1970) Cleavage of structural proteins during the assembly of the head of bacteriophage T4. *Nature*, **227**, 680-685

Lagresle, C, Gardie, B., Eyquem, S., Fasseu, M., Vieville, J-C., Pla, M., Sigaux, F., Bories, J-C. (2002) Transgenic expression of the p16 (INK4a) cyclin-dependent kinase inhibitor leads to enhanced apoptosis and differentiation arrest of CD4-CD8-immature thymocytes. *J. Immunol.* **168:**2325-2331.

Larose, M., Cassard-Doulcier, A.M., Fluery, C., Serra, F., Champigney, O., Bouillaud, F., Ricquier, D. (1996) Essential *cis*-acting elements in rat uncoupling protein gene are in an enhancer element containing a complex retinoic acid domain response. *J. Biol. Chem.* **271,** 31533-31542

Larrouy D, Laharrague P, Carrera G, Viguerie-Bascands N, Levi-Meyrueis C, Fleury C, Pecqueur C, Nibbelink M, Andre M,Casteilla L & Ricquier D (1997). Kupffer cells are a dominant site of uncoupling protein 2 expression in rat liver. *Biochem BiophysRes Commun* **235**, 760–764.

Lebien, T.W., Tedder, T.F., (2008) B lymphocytes: How they develop and function, *Blood* **112**(5) 1570-1580

Leung, R. K. (2001) Deletion of the CD4 silencer element supports a stochastic mechanism of thymocyte lineage commitment. *Nature Immunol.* **2**, 1167–117.

Liblau, R., Tournier-Lasserve, E., Maciazek, J., Dumas, G., Siffert, O., Hashim, G. & Bach, M. A. (1991) T cell response to myelin basic protein epitopes in multiple sclerosis patients and healthy subjects. *Eur. J. Immunol.* **21**, 1391-1395

Lin, C.S., Klingenberg, M. (1980) Isolation of the uncoupling protein from brown adipose tissue mitochondria. *FEBS Lett.* **,113,** 299-303

McLeod, C.J., Abdulhameed, C.A., Hoyt, R.F., McCoy, J.P., Sack, M.N., (2005) Uncoupling proteins 2 and 3 function in concert to augment tolerance to cardiac ischaemia. *J. Biol. Chem.* **280**, 33470–33476.

Mebius, R.E., Kraal, G., (2005) Structure and function of the spleen. *Nat. Rev. Immunol.* **5** 606–616.

Migita, K., Tanaka, F., Abiru, S., Ida, H., Izumi, Y., Kawakami, A., Eguvhi, K., (2003) The role of mitochondria in nitric oxide-mediated thymocyte apoptosis, *Immunol. Lett.* **90,** 87–91.

Miller, J.F. (2002) The discovery of thymus function and of thymus-derived lymphocytes. *Immunol Rev.* **185**, 7-14

Miller, J.F. (2004) Events that led to the discovery of T-cell development and function--a personal recollection. *Tissue Antigens* **63**, 509-17

Mills, K.H.G. (1996) in: Methods in Molecular Medicine-Vaccine Protocols. (A. Robinson, G. Farrar & C. Wilbin eds) pp. 197-221, Humana Press, New Jersey.

Minter, L.M. & Osbourne, B.A., (2003) Cell death in the thymus-it's all a matter of contacts. *Seminars in Immunology* **15**, 134-144,

Monemdjou, S., Hofmann, W.E., Kozak, L.P., (2000) Harper, M-E., Increased mitochondrial proton leak in skeletal muscle mitochondria of UCP1-de.cient mice, *Am. J. Physiol. Endocrinol. Metab.* **279** E941–E946.

Montecino-Rodrigez, E., Dorshkind, K., (2002) Idenfitication of B/macrophages progenitors in adult bone marrow. *Seminars in Immunology* **14** (6) 371-376

Mori, S., Yoshizuka, N., Takizawa, M., Takema, Y., Murase, T., Tokimitsu, I., Saito, M., (2008) Expression of uncoupling proteins in human skin and skin-dervived cells *J Invest Dermatol.* **128**(8):1894-900.

Muller, F.L., Liu, Y., Van Remmen, H., (2004) Complex III releases superoxide to both sides of the inner mitochondrial membrane, *J. Biol. Chem.* **279** , pp. 49064–49073

Nascimbeni, M., Shin, E.C., Chiriboga, L., Kleiner, D.E., Rehermann, B.,(2004) Peripheral CD4 (+)CD8(+) T cells are differentiated effector memory cells with antiviral functions, *Blood* **104**, 478–486.

Néchad, M. (1986) Structure and development of brown adipose tissue. In: Brown Adipose Tissue, pp86-104 (Paul Trayhurn and David G. Nicholls eds.)(Edward Arnold Publishers. London).

Nedergaard, J., Cannon, B., The 'novel' 'uncoupling' proteins UCP2 and UCP3: what do they really do? Pros and cons for suggested functions, *Exp. Physiol.* **88**,65–84.

Nedergaard, J., Bengtsson, T., Cannon, B., (2007) Unexpected evidence for active brown adipose tissue in adult human. *Am. J. Phys. Endocrinol. Metab.* **293,** 444-452

Nedergaard, J., Golozoubova, V., Matthias, A., Asadi, A., Jacobsson, A., Cannon, B. (2001) UCP 1: the only protein able to mediate adapyive non-shivering thermogenesis and metabolic inefficiency. *Biochim. Biophys. Acta* **1504,** 82-106

New, K.J., Eaton, S., Elliot, K.R.F., Spitz, L., Quant., (2001) Effect of lipopolysaccharide and cytokines on oxidative metabolism in neonatal rat hepatocytes *Journal of Pediatric Surgery,* **36** 338-340

Nibbelink, M., Moulin, K., Arnaud, E., Duval, C., Pénicaud, L., Casteilla, L. (2001) Brown fat UCP 1 is specifically expressed in uterine longitudinal smooth muscle cells. *J Biol Chem*. **276**, 47291-47295

Nicholls, D.G., (2006) The physiological regulation of uncoupling proteins, *Biochim. Biophys. Acta* **1757** 459–466.

Nicholls, D.G., Locke, R.M. (1984) Thermogenic Mechanism in Brown Fat. *Physiol Rev*. **64,** 1-64

Nicholls, D.G., Rial, E. (1974) Measurement of proton leakage across mitochondrial inner membranes and its relation to proton motive force. *Methods in Enzymology* **174**, 85-94

Nicholls, D.G., Rial, E. (1999) A history of the uncoupling protein, UCP 1. *J. Bioenerg. Biomembr.* **31**, 399-406

Nicholls, D.G. (2001) A history of UCP1. *Biochem. Soc. Trans*. **29**, 751–755

Nomura, K., Imai, H., Koumura, T., Kobayashi, T., Nakagawa, Y., (2000) Mitochondrial phospholipid hydroperoxide glutathione peroxidase inhibits the release of cytochrome c from mitochondria by suppressing the peroxidation of cardiolipin in hypoglycaemia induced apoptosis, *Biochem. J.* **351**, pp. 183–193.

Okamatsu-Ogura, Y., Kitao, N., Kimura, K., Saito, M., (2007) Brown fat UCP1 is not involved in the febrile and thermogenic responses to IL-1beta in mice. *Am J Physiol Endocrinol Metab*. **292**, 1135-9

Page, D.M., Kane, L.P., Onami, T.M., Hedrick, M. (1996) Cellular and biochemical requirements for thymocyte negative selection. *Semin. Immunol.* **8**, 69–82

Palou, A., Picó, C., Bonet, M.L., Oliver, P. (1998) The uncoupling protein, thermogenin. *Int.J.Biochem & Cell Biol*. **30,** 7-11

Parascandola, J. (1974) Dinitrophenol and Bioenergetics: An Historical Perspective *Mol. Cell. Biochem* .**5,** 69-77

Pecqueur, C., Alves-Guerra, MC., Gelly, C., Levi-Meyrueis, C., Couplan, E., Collins, S., Ricquier, D., Bouillaud, F., Miroux, B. (2001) Uncoupling protein 2 , *in vivo* distribution, induction upon oxidative stress, and evidence for translational regulation. *J. Biol. Chem.* **276**, 8705-8712

Pecqueur, C., Bui, T., Gelly, C., Hauchard, J., Barbot, C., Bouillaud, F., Ricquier, D., Miroux, B., Thompson, C.B. (2008) Uncoupling protein-2 controls proliferation by promoting fatty acid oxidation and limiting glycolysis-derived pyruvate utilization. *FASEB J.* **22**(1):9-18.

Poltorak, A., He, X., Smirnova, I., Liu, M.Y., Van Huffel, C., Du, X., Birdwell, D., Alejos, E., Silva, M., Galanos, C., Freudenberg, M., Ricciardi-Castagnoli, P., Layton, B., Beutler, B. (1998) Defective LPS signaling in C3H/HeJ and C57BL/10ScCr mice: mutations in Tlr4 gene. *Science.* ;**282** (5396):2085-8

Porter, R.K. (2001) Mitochondrial proton leak: a role for uncoupling protein 2 and 3 *Biochim. Biophys. Acta* **1504,** 120-127

Porter, R.K., (2006) A new look at mitochondrial uncoupling protein 1, *Biochim. Biophys. Acta* **1757,** 446-448

Porter, R.K., Brand, M.D., (1995) Causes of differences in respiration rate of hepatocytes from mammals of different body mass, *Am. J. Physiol.* **269** R1213–R1224.

Puigserver, P., Herron, D., Gianotti, M., Palou, A., Cannon, B., Nedergaard, J. (1992) Induction and degradation of the uncoupling protein thermogenin in brown adipocytes in *vitro* and *in vivo. Biochem.J.* **284**, 393-398

Rial, E., Gonzalez-Barroso, M., Fleury, C., Iturrizaga, S., Sanchis, D., Jimenez-Jimenez, J., Ricquier, D., Goubern, M., Bouillaud, F. (1999) Retinoids activate proton transport by the uncoupling proteins UCP1 and UCP2. *EMBO J.* **18,** 101-108

Ricquier, D., Bouillaud, F. (1986) Brown adipose tissue mitochondrial uncoupling protein . In: Brown Adipose Tissue, pp86-104, (Paul Trayhurn and David G. Nicholls eds.)(Edward Arnold Publishers. London).

Ricquier, D., Barlet, J.P., Garel, J.M., Combes-George, M., Dubois, M.P. (1983) An immunological study of the uncoupling protein of brown adipose tissue mitochondria. *Biochem. J.* **210**, 859-866.

Ricquier, D., Bouillaud, F., (2000) The uncoupling protein homologues: UCP1, UCP2, UCP3, stUCP and atUCP, *Biochem. J.* **345** 161–179.

Ricquier, D., Bouillaud, F., (2000a) Mitochondrial uncoupling proteins: from mitochondria to the regulation of energy balance. *J. Physiol.* **529,** 3-10

Ritter, M.A., Crispe, I.N. (1992) Structure and development. In: The Thymus, pp 9-26, (David Rickwood and David Male eds.) (IRL press at Oxford University Press)

Rocha, P.N., Plumb, T.J., Robinson, L.A., Spurney, R., Pisetsky, D., Koller, B.H., Coffman, T.M., (2005) Role of thromboxane A2 in the induction of apoptosis of immature thymocytes by lipopolysaccharide. *Clin Diagn Lab Immunol.* **8,** 896-903.

Rodriguez-Pinto, D. (2005) B cells as antigen presenting cells. *Cellular Immunology* **238** (2) 67-75

Rothwell, N.F., (1989) CRF is involved in the pyrogenic and thermogenic effects of interleukin 1β in the rat. *Am J Physiol Endocrinol Metab* **256**, 111-115

Rothwell, N.J., Stock, M.J, (1979) A role for brown adipose tissue in diet-induced thermogenesis. *Nature*, **281**, 31-33

Rothwell, N.J., Saville, M.E., Stock, M.J (1984) Brown fat activity in fasted and refed rats. *Biosci.Rep*. **4** 351-357

Rotter, V., Schlesinger, M., Kalderon, R., Trainin, N. (1976) Response of human lymphocytes to PHA and Con A, dependant on and regulated by THF, a thymic hormone J. Immunol. **117**(5) 1927-1932

Rousset, S., Alves-Guerra, M.C., Ouadghiri-Bencherif, S., Kozak, L.P., Miro, B., Richard, D., Bouillaud, F., Ricquier, D., Cassard-Doulcier, A.M. (2003) Uncoupling protein 2, but not

uncoupling protein 1 , is expressed in the female mouse reproductive tract. . *J Biol Chem*. **278**, 45843-45847

Rousset, S., Emre, Y., Join-Lambert, O., Hurtaud, C., Ricquier, D., Cassard-Doulcier, A.M. (2006) The uncoupling protein 2 modulates the cytokine balance in innate immunity, *Cytokine* **35**, pp. 135–142

Rousset, S., Mozo, J., Dujardin, G., Emre, Y., Masscheleyn, S., Ricquier, D., Cassard-Doulcier, A.M. (2007) UCP2 is a mitochondrial transporter with an unusual very short half-life. *FEBS Letters* **581,** 479-482

Rutter GA. (2001) Nutrient-secretion coupling in the pancreatic islet beta-cell: recent advances. *Mol Aspects Med.*; **22(6)**:247-84. Review.

Saito, M., Akiyoshi, M., Shimizu, Y., (1991) Possible role of the sympathetic nervous system in responses to interleukin-1. *Brain Res Bull.* **(3-4)**, 305-8.

Sakaguchi, S. (2000) Regulatory T cells: Key controllers of immunological self tolerance *Cell* **101**, 455-458

Sakaguchi, S., Sakaguchi, N., Asano, M., Itoh, M., Toda, M., (1995) Immunologic self-tolerance maintained by activated T cells expressing IL-2 receptor alpha-chains (CD25). Breakdown of a single mechanism of self-tolerance causes various autoimmune diseases. *J Immunol.* **155**(3):1151-64.

Sawada, S., Littman, D. R. (1991) Identification and characterization of a T-cell-specific enhancer adjacent to the murine CD4 gene. *Mol. Cell. Biol;.* **11**, 5506–5515.

Sawada, S., Scarborough, J. D., Killeen, N. & Littman, D. R. (1994) A lineage-specific transcriptional silencer regulates CD4 gene expression during T-lymphocyte development. *Cell* **77**, 917–929

Sayre, L.M., Lin, D., Yuan, Q., Zhu, X., Tang, X., (2006) Protein adducts generated from products of lipid oxidation: focus on HNE and ONE, *Drug Metab. Rev.* **38**, pp. 651–675.

Scarpace, P.J., Bender, B.S., Borst, S.E. (1991) *Escherichia coli* peritonitis activates thermogenesis in brown adipose tissue: relationship to fever. *Can. J. Physiol. Pharmacol.* **69**, 761-766

Schwarz, B.A., Bhandoola, A., (2006) Trafficking from the bone marrow to the thymus: a prerequisite for thymopoiesis. *Immunol Rev* **209**, 47-57

Sears, I.B., Mac Ginnitie, M.A., Kovacs, L.G., Graves, R.A. (1996) Differentiation-dependant expression of the brown adipocyte uncoupling protein gene: regulation by peroxisome proliferators-activated receptor gamma. *Mol. Cell. Biol.* **16,** 3410-3419

Shimosato,Y., & Mukai, K. (1997) Tumors of the thymus and related lesions. In: Shimosato Y, Mukai K, eds. Atlas of tumor pathology: tumors of the mediastinum, Washington, DC: Armed Forces Institute of Pathology, 158–168.

Silva, J.J. and Rabelo, R. (1997) Regulation of the uncoupling protein gene expression. *Eur. J. Endocrinology.* **136,** 251-264

Skulachev, V.P., (1996) Role of uncoupled and non-coupled oxidations in maintenance of safely low levels of oxygen and its one-electron reductants, *Q. Rev. Biophys.* **29**, pp. 169–202.

Sleckman, B.P. (2005) Lymphocyte antigen receptor gene assembly: multiple layers of regulation.*Immunol Res.*; **32(**1-3):253-8. Review.

Smith,P.K.,, Krohn, R.I., Hermanson,G.T., Mallia, A.K., Gartner, F.H., Provenzano, M.D., Fujimoto, E.K., Goeke, N.M., Olson, B.J., Klenk, D.C. (1985) Measurement of protein using bicinchoninic acid *Anal Biochem.*; **150(1):**76-85.

Starr, T.K., Jameson, S.C., Hogquist, K.A. (2003) Positive and negative selection of T cells. *Annu. Rev. Imunol.* **21,** 139–176.

Stefanelli, C., Bonavita, F., Stanic', I., Farruggia, G., Falcieri, E., Robuffo, I.,Pignatti, C. Muscari, C., Rossoni, C., Guarnieri, C., Caldarera, C.M., (1997) ATP depletion inhibits glucocorticoid-induced thymocyte apoptosis, *Biochem. J.* **322** 909–917.

Sutherland, J.S. (2005) Activation of thymic regeneration in mice and humans following androgen blockade. *J Immunol* **15;**175(4):2741-53.

Sun, J. B., Olsson, T., Wang, W. Z., Xiao, B. G., Kostulas, V., Fredrikson, S., Ekre, H. P. & Link, H. (1991) Autoreactive T and B cells responding to myelin proteolipid protein in multiple sclerosis and controls. *Eur. J. Immunol.* **21**, 1461-1468.

Tagen, M., Elorza, A., Kempuraj, D., Boucher, W., Kepley, C.L., Shirihai, O.S., Theoharides, T.C., (2009) Mitochondrial uncoupling protein 2 inhibits mast cell activation and reduces histamine content, *J. Immunol.* **183**, pp. 6313–6319.

Talbot, D.A., Duchamp, C., Rey, B., Hanuise, N., Rouanet, J.L., Sibille, B., Brand, M.D. (2004) Uncoupling protein and ATP/ADP carrier increase mitochondrial proton conductance after cold adaptation of king penguins *J. Physiology* **558,** 123-135

Terszowski, G., Muller, S.M., Bleul, C.C., Blum, C., Schirmbeck, R., Reimann, J., Pasquier, L.D., Amagai. T., Boehm, T., Rodewald, H.R. (2006) Evidence for a Functional Second Thymus in Mice. *Science.* **312**, 284-287

Ushiki, T. (1986) A scanning electron-microscopic study of the rat thymus with special reference to cell types and migration of lymphocytes into the general circulation : *Cell Tissue Res.* **244**, 285-98

von Boehmer, H., Teh, H. S. & Kisielow, P. (1989) The thymus selects the useful, neglects the useless and destroys the harmful. *Immunol. Today* **10**, 57–61.

Vidal-Puig, A., Solanes, G., Grujic, D., Flier, J.S., Lowell, B.B., (1997) UCP 3: an Uncoupling protein homologue expressed preferentially and abundantly in skeletal muscle and brown adipose tissue *Biochem Biophys Res Commun* **235,** 79-82

Vidal-Puig AJ, Grujic D, Zhang CY, Hagen T, Boss O, Ido Y,Szczepanik A, Wade J, Mootha V, Cortright R, Muoio DM &Lowell BB (2000). Energy metabolism in uncoupling protein 3 gene knockout mice. *J Biol Chem* **275**, 16258–16266.

Voet, D., Voet, J.G., Pratt, C. (2006) Fundamentals of Biochemistry (2nd Edition) John Wiley and Son.

Vogler, S., Pahnke, J., Rousset, S., Ricquier, D., Moch, H., Miroux, B., Ibrahim, S. M. (2006) Uncoupling protein 2 has protective function during experimental autoimmune encephalomyelitis. *Am. J. Pathol.* **168**, 1570-1575

Wagener, D.J., (1973) Enhanced Growth of Fibrosarcoma in Mice Treated with Phytohemagglutinin *Cancer Research* **33**, 1295-1300

Walker, S., Lucas, Z. (1971) Mitogen-serum relationships in transformation of lympbocytes *in vitro.* Proceedings of the 4th Leucocyte Culture Conference. Edited by O. Ross McIntyre. Appleton-Century-Crofts, New York. P. 49.

Williams, A.F. (2005) Many cells in rat bone marrow have cell-surface Thy-1 antigen. *Eur. Jour. Immunol* **6 (7)**, 526–528

Winkler, E., Klingenberg, M. (1994) Effect of fatty acids on H^+ transport activity of the reconstituted uncoupling protein. *J Biol Chem*. **269**, 2508-2515

Wolfer, A. (2001) Inactivation of Notch 1 in immature thymocytes does not perturb $CD4^+$ or $CD8^+$ T-cell development. *Nature Immunol.* **2**, 235–241.

Yachnin, S., Raymond, J. (1975). An absolute requirement for serum macromolecules in phytohaemagglutinin-induced human lymphocytes DNA synthesis. *Clin. Exp. Immunol.* **22:**153.

Yoshida, T., Umekawa, T., Kumamoto, K., Sakane, N., Kogure, A., Kondo, M., Wakabayashi, Y., Kawada, T., Nagase, I., Saito, M. (1998) $_{B3}$-Adrenergic agonist induces a functionally active uncoupling protein in fat and slow-twitch muscle fibers *Am J Physiol Endocrinol Metab* ***274,*** 469-475

Yu, X.X., Barger, J.L., Boyer, B, B., Brand, M.D., Pan, G., Adams, S.H., (2000) Impact of endotoxin on UCP homolog mRNA abundance, thermoregulation, and mitochondrial proton leak kinetics. *Am J Physiol Endocrinol Metab* **279,** 433-446

Zacharchuk, C.M., Mercep, M., Ashwell, J.D. (1991) Thymocyte activation and death: a mechanism for molding the T cell repertoire. *Ann. N.Y. Acad. Sci.* **636**, 52–70

Zhou,Y.T., Shimabukuro, M., Koyama, K., Lee, Y., Wang, M.Y., Trieu, F., Newgard, C.B., Unger, R.H. (1997) Induction by leptin of uncoupling protein-2 and enzymes of fatty acid oxidation.*Proc Natl Acad Sci U S A.* **94(12)**:6386-90.

Zhou, M., Lin, B.Z., Coughlin, S., Vallega, G., Pilch, P.F.(2000) UCP-3 expression in skeletal muscle: effects of exercise, hypoxia, and AMP-activated protein kinase. *Am J Physiol Endocrinol Metab.* **279(3):**E622-9.

Zhang, C.Y., Baffy, G., Perret, P., Krauss, S., Peroni,O., Grujic, D., Hagen, T., Vidal-Puig, A.J., Boss, O., Kim, Y.B., Zheng, X.X., Wheeler, M.B., Shulman, G.I., Chan, C.B., Lowell, B.B. (2001). Uncoupling protein-2 negatively regulates insulin secretion and is a major link between obesity, beta cell dysfunction, and type 2 diabetes. *Cell* **105**, 745–755.

Zhang, J., Shi, J., Ilic, S., Xue, S.J., Kakuda, Y., (2009) Biological Properties and Characterisation of Lectin from Red Kidney Bean (*Phaseolus Vulgaris*) *Food Reviews International* **25**, 12-27

Zhou, Z., Yon Toh, S., Chen, Z., Guo, K., Ng, C.P., Panniah, S., Lin, S.C., Hong, W., Li, P., (2003) Cidea-deficient mice have lean phenotype and are resistant to obesity, *Nat. Genet.* **35** 49–56.

Zúñiga-P.ücker, J., (2004) T-cell development made easy. *Nat. Rev., Immunol.* **4** 67–72.

Chapter 8

Publications